THESIS

RISK-REWARD TRADEOFFS IN THE FORAGING STRATEGY OF COUGAR (*PUMA CONCOLOR*): PREY DISTRIBUTION, ANTHROPOGENIC DEVELOPMENT, AND PATCH SELECTION

Submitted by

Kevin A. Blecha

Graduate Degree Program in Ecology

In partial fulfillment of the requirements

For the Degree of Master of Science

Colorado State University

Fort Collins, Colorado

Spring 2015

Master's Committee:

Advisor: Randall B. Boone

Mat W. Alldredge
Mevin B. Hooten
Lisa M. Angeloni

ABSTRACT

RISK-REWARD TRADEOFFS IN THE FORAGING STRATEGY OF COUGAR (*PUMA CONCOLOR*): PREY DISTRIBUTION, ANTHROPOGENIC DEVELOPMENT, AND PATCH SELECTION

Empirical efforts to understand the space utilization patterns of large elusive carnivores that forage on highly mobile prey are sparse. Investigating the patch choices made by a large carnivore while engaged in foraging behaviors is of particular importance to understanding their conflicts with humans. The over-arching goal of this thesis is to test whether the foraging strategies carried out by a large carnivore inhabiting an area marked by human housing development can be explained by classic optimal foraging theory (OFT). My research takes place in a portion of the Colorado Front Range, which is a foothill-montane system characterized by the urban-wildland interface of the greater Denver metropolitan area and surrounding cities (Boulder, Golden, Evergreen). A matrix of varying levels of rural, exurban, and suburban development are expected to drive the patch choices made by the cougar, a large obligate carnivore that can conflict with human interests when engaged in foraging behavior.

Before answering questions involving patch choice, several pieces of information must be acquired. Specifically, Chapter 1 and Chapter 2 take an Eulerian approach to understanding the space utilization patterns of wild prey commonly sought by cougars in this area. Predicted utilization by these prey species is mapped for the study area on a fine (30 m) scale, with the premise that cougars may be attracted to localities where the opportunity of encountering a potential prey item is greater. Appendix 2 provides details on methods used to determine the

distribution of housing development, a patch characteristic that cougars may fear. This appendix also provides background discussion of anthropogenic development in the study area. Appendix 4 provides details on the construction of various "natural" landscape variables from readily available data sources.

A focus of many studies employing camera traps is to describe spatial and temporal utilization patterns of animals, often with a goal to obtain a population level response. In Chapter 1, I conducted an experiment using agent based modeling (ABM) simulations to demonstrate how encounter rate (count of triggering events) is influenced by abundance, movement rate, home range size, and dimensions of the camera's field-of-view. I demonstrate which sampling frequency scenarios, either by using a camera trigger delay period or with data post-processing steps, may result in non-linear and interacting effects between these four predictor variables and encounter rate. Results of the experiment generally supported previous simulation studies. However, intentionally imposing delay periods in sampling frequency produced biased inferences of habitat usage, and weakened the relationship between relative abundance and encounter rates; simple linear responses between biological properties (abundance and movement) and the underlying encounter rates were unobtainable. With a habitat explicit ABM, I compared camera trap encounter rates to a true measure of utilization using a perfect GPS telemetry system. The model demonstrated that raw encounter rates are a property of localized abundance and habitat utilization behaviors of all individuals, and that camera encounter rates measured between treatment groupings can be used to produce habitat utilization inferences at the population level assuming certain study design characteristics.

In Chapter 2 I applied the methods developed in Chapter 1 to model the utilization of a set of six medium to large mammalian species inhabiting the Front Range study area. This was

done using a measure of the amount of time spent by animals within the field-of-view of 131 camera trap sites monitored over a one-year period. The purpose of this chapter was multi-part. First, I assess the probability of detection within the camera trap's field-of-view using distance sampling technique. Adding to previous studies, I demonstrate that false-absences are a function of distance to the camera codependent on site and observation level variables. A secondary focus was to understand the associations between animal utilization and housing development. Using compound-Poisson generalized linear models, I show that the utilization patterns of the six species with respect to housing development were generally supportive of those found in published studies using habitat selection, occupancy, and abundance as response variables. Some of the species modeled were also species commonly preyed on by cougar in the Front Range. Thus, for a third objective, I develop utilization distribution maps for each species using predictions of the compound-Poisson models. This utilization map was then used as an input data source for models created in Chapter 3.

Finally in Chapter 3, using cougar as a model species, I tested whether a large carnivore's foraging strategy can be explained by optimal foraging theory. Understanding how large carnivore foraging strategies influence space utilization decisions is important for explaining human-large carnivore conflicts. Seminal optimal foraging papers proposed that an animal will be less cautious in avoiding risks when energetically stressed. I demonstrated that cougars make a tradeoff between choosing locations that would yield a higher prey encounter rate with choosing safer patches. Cougars avoided higher housing densities, but were attracted to higher primary prey (mule deer) availability. Support for this tradeoff was evident in the increase in hunting success in higher housing densities. Inter-individual differences in foraging behavior existed, with some variation explainable by cougar sex and age classes. As for intra-individual

differences, energetic stressors mediated the foraging strategy at two temporal scales. During periods associated with decreased availability of and accessibility to primary prey, cougars became less cautious of higher housing densities. On a shorter time scale, avoidance of housing declined as cougar hunger levels (time since last feeding event) increased. Cougars normally avoided higher housing densities when conducting hunting activities. However, in the event where a kill was not made soon enough, the risk avoidance response dwindled until cougars showed no avoidance to higher housing densities when hunting. This study provides a mechanistic understanding of the space utilization patterns of a large carnivore in landscapes where human and carnivore utilizations overlap. Furthermore, it explains a carnivore's occasional utilization of risky landscapes and thus potentially the occasional conflicts between large carnivores and humans.

ACKNOWLEDGEMENTS

I would like to thank my advisor Dr. Randall Boone for always having his door open and administering my graduate research assistantship with the Natural Resources Ecology Laboratory during my time at Colorado State University. I especially appreciate what he has taught me regarding agent-based modeling and programming in general, as it will continue to serve me in the future. I give special thanks to Dr. Mat Alldredge for initially hiring me on as a field technician with the Front Range Cougar research study at Colorado Parks and Wildlife (CPW). I am grateful he saw my potential for being a graduate student and the advice given as a committee member. I also appreciate the help of my other committee members, Dr. Mevin Hooten and Dr. Lisa Angeloni. Dr. Hooten lent some great statistical methodological advice. Dr. Angeloni gave the right amount of encouragement for me to aim my research questions high. I hope that this thesis is a reflection of my ambition to do so.

I was fortunate to have help in the field from staff at CPW. Especially that of the hard work of Tasha Blecha (Eyk), Joe Halseth, Darlene Kilpatrick, Gabrielle Coulombe, Rebecca Mowry, Ryan Platte, Eric Newkirk, Wynne Moss, Elizabeth Joyce, Duggins Wroe, Matt Strauser, Laura Nold, Fred Quarterone, and Natalie Flowers put forth either conducting kill site investigations or checking camera traps. In the office, Chris Woodward and Erik Newkirk not only provided database support, but got me off on the right foot when it came to building my own data storage solutions.

As for providing advice on project design, methodologies, and interpretation, I am indebted to Dr. Jake Ivan, Dr. Heather Johnson, Dr. Ken Logan, Dr. Eric Bergman, and Mark

Vieira, all of CPW. I also thank lab-mate Jared Stabach for providing feedback on my papers and in various coursework.

Field components of this thesis would not have been possible without the land access provided from various entities, which includes: U.S. Forest Service, Rocky Mountain National Park, Golden Gate Canyon State Park, Eldorado Springs State Park, various state wildlife areas under CPW, Boulder County Parks and Open Space and Mountain Parks, Jefferson County Open Space, City of Boulder Open Space and Mountain Parks, Denver Mountain Parks, Button Rock Preserve (City of Longmont), City of Boulder Public Works, City of Black Hawk, Colorado School of Mines, Rilliett park Association, Genessee Open Space, Ken-Caryl Ranch Masters Association, Cal-wood Education Center, Mt. Evans Outdoor Lab School, Denver Water Board. Several hundred private landowners that granted permission for me and my crews to conduct kill site investigations deserve more acknowledgement than I have room for here. Especially that of the 75 private landowners that allowed me to monitor a wedge of their property with camera traps for an entire year.

Funding for my graduate research assistantship and the acquisition of data utilized for generating Chapters 2 and 3, were provided by CPW. Cougar GPS location data and kill-site ground-truthing data was provided by the Front Range Cougar Project, a parent research study aimed at understanding cougar ecology in the urban-wildland interface, led by Dr. Mat Alldredge. Jefferson County Open Space provided the additional financial support needed for carrying out the objectives of Chapter 2.

DEDICATION

I dedicate this thesis to Tasha. I am fortunate to have been initially trained by her on the Front Range Cougar Study and even more fortunate to be married to her later. In her off-seasons while not working directly for the cougar study, the months she accumulated helping me process data made all the difference. All the jokes ever made (e.g., "they should grant Tasha an M.S. too") are somewhat substantiated.

TABLE OF CONTENTS

CHAPTER 1 - INFERRING POPULATION LEVEL HABITAT UTILIZATION FROM CAMERA TRAP ENCOUNTER RATES

INTRODUCTION

Camera traps are increasingly used as tools for studying animal population size, occupancy/distribution, and habitat use. Compared to conventional survey techniques, camera traps are non-invasive (Cutler and Swann 1999), cost-efficient (Silveira et al. 2003), and reduce human observation error as a photo record can always be referenced (Swann et al. 2011). Remote photography of animals is not a new concept (Shiras 1906), but recent technological advances have overcome many logistical challenges regarding battery life, triggering mechanisms, image storage, and processing. These advances have allowed acquisition efforts to move from anecdotal collections to intensive large scale surveys. With its increased accessibility, camera trapping has become a staple in species distribution modeling.

An objective of many camera trap studies is to make ecological inferences by testing for differences in a state variable (e.g., abundance, occupancy) between spatial or temporal treatment groups. These population-level state variables are often used as currencies to infer some measure of importance of a particular landscape to animals (Buskirk and Millspaugh 2006) or to map the distribution of animals across the landscape. Despite the array of published studies that give direct or indirect inference to habitat usage with camera traps, habitat usage definitions are inconsistent; it is not certain what currency should be used to infer habitat importance. Rather than acquiring habitat utilization measures, camera trap platforms thus far are mainly used in conjunction with mark resight techniques to produce abundance estimates (Karanth 1995) or with occupancy modeling analysis to produce probability of occurrence (MacKenzie et al. 2006).

These methods may not be the most appropriate for some study objectives (e.g., habitat utilization study), or have some shortcomings in certain systems (e.g., animals without insufficient markings for a mark-resight study). Some researchers have thus turned to relative abundance indices (RAIs) (Carbone et al. 2001, O'Brien et al. 2003, Rovero and Marshall 2009). Occasionally RAIs are used to infer habitat utilization (Bowkett et al. 2007).

RAIs are an abundance proxy that attempts to characterize directions and magnitudes of change in population abundances between treatment groups (i.e., habitats, seasons, years, or species) rather than actual abundance values. Camera trap RAIs, in their generic form, are counts of animals triggering the camera per camera trap location, standardized by the effort (i.e., number of survey days), essentially a raw encounter rate. RAIs are often justified by arguing that a measure of the absolute number of unique animals is unnecessary and that abundance differences are reflected in encounter rate. It assumes that all potentially confounding variables that may influence the encounter rate are standardized in the design process. Some empirical studies have successfully correlated RAI with actual density estimates (Carbone et al. 2001, Rovero and Marshall 2009), but these methods likely have unmentioned shortcomings (Jennelle et al. 2002) or fail in some systems (Mathews et al. 2011, Sollmann et al. 2013). Rather than a pure abundance effect as assumed in inferences stemming from RAI studies, what researchers observe with camera trap encounter rates might be a reflection of overall habitat specific utilization patterns of the population, or an emergent property combining the processes of movement and localized aggregations of individuals.

Lagrangian habitat use and selection studies are now implementing methods that take advantage of the high temporal resolution that GPS telemetry can provide for individual animals, giving a better understanding of how long an individual uses a particular location and the choices

available. To gain a population level understanding, habitat selection data from many individuals are aggregated in analysis. Whereas telemetry studies give insight at the individual level, the utilization pattern for what the population does as a whole is sometimes the most important inference. Popescu et al. (2014) did give empirical evidence for a radio-telemetered meso-carnivore that a camera trap's encounter rate measure was associated with telemetered animals' utilization distributions. However, telemetry studies have their own biases (Reynolds and Laundre 1990, Johnson and Ganskopp 2008), thus comparing camera trap encounter rate measures to a true utilization measure would be useful.

One of the earliest works using camera platforms simply aimed at comparing habitat units by the utilization of waterfowl (using counts of individuals) in defined plots bounded by the camera's field-of-view (FOV) (Cowardin and Ashe 1965). Several studies have since used encounter rate data to do similar habitat use assessments (Di Bitetti et al. 2006), with some assuming their currency for measurement is relative abundance (Bowkett et al. 2007). Whereas some work has demonstrated that photographic encounter rates do have a relationship with abundance (Carbone et al. 2001, Rowcliffe et al. 2008, Sollman et al. 2013), other factors like movement rates (Carbone et al. 2001, Rowcliffe et al. 2008, Rowcliffe et al. 2011, Glen et al. 2013), home range size (Sollman et al. 2013), and FOV dimensions (Rowcliffe et al. 2008, Rowcliffe et al. 2011) are also important. Thus, disentangling the influence of any one factor from the others is difficult, but an important step for understanding which basic variables influence encounter rate.

An important component to most modern passive infrared camera studies is that sampling frequency or photo collection rate can be determined by programming the camera's trigger delay period to record pictures nearly continuously (i.e., 1 second delay) or at other user-specified

intervals (i.e., 30 seconds, 5 minutes, 1 hour). Alternatively, temporal re-sampling can be carried out in post-processing. In the case of RAI and habitat comparison studies, many rarify the series of photos to some arbitrary level of independence, so that the same individual animal is less likely to be captured repeatedly in a short amount of time (Kinnaird et al. 2003, O'Brien et al. 2003, George and Crooks 2006, Bowkett et al. 2007, Gessner et al. 2013). Passive camera studies sometimes implement a time-lapse trigger to allow detections to be made at standardized intervals (Cowardin and Ashe 1965, Temple 1972, Hamel et al. 2013). No study has examined how this delay period or rarefication may influence inferences of habitat utilization. Both movement rate and camera delay period incorporate a time element, while movement rate incorporates an additional spatial element; thus, I hypothesize that interactions between movement rate and delay period will confound utilization comparisons between habitats. A simulation that manipulates camera delay period, along with abundance, home range size, movement rate, and camera FOV size factors in a single environment may elucidate whether population level habitat utilization patterns can be inferred from camera traps.

My overarching goal is to help researchers understand the capabilities and limitations of passive infrared camera traps to infer habitat utilization measures at a population level. Using agent-based model (ABM) simulations I demonstrate how biological factors (home range, movement rate, abundance) and design factors (camera maximum FOV detection distance and camera delay period) influence encounter rate, and how these variables may have interacting effects. I then use a similar ABM to simulate a population of agents selectively using certain habitats to test if habitat specific encounter rates measured by camera traps match measurements of habitat usage derived from a perfect telemetry study.

METHODS

ABM Description

Using Netlogo 5.1.0 (Wilensky 1999) a simple temporally and spatially explicit ABM (CamEncounter) was created to simulate the contact between animals and camera agents. The spatial environment of the Netlogo "world" consisted of a plane of pixels, each one being a square meter. The landscape (a 200 x 200 m landscape) was overlaid by a grid of four camera traps with 100 m spacing (Figure 1.1). A sector radiates from the camera agent to form the FOV with a fixed 42° angle and a user defined FOV distance. The temporal component of the model was governed by time steps representing one second of true time.

A user defined number of animal agents were generated randomly on the landscape in response to the parameter ABUND. Each animal was restricted to a circular home range area (HOME) with a user defined radius and home range center (Figure 1.1). Within each home range, each agent carried out a correlated random walk with an adjustable movement rate (MOVE) and a turning angle that was chosen from a normal distribution (mean: 0°, stdev: 5°). For each tick of the simulation, agents chose a turning angle, and then moved forward the distance specified in the MOVE parameter. When an animal reached its home range edge, the heading was temporarily reset to face the home range center. This effectively resulted in an approximate bivariate normal distribution of home range utilization intensity (Figure 1.1). The "world-wrap" feature of NetLogo allowed agents to move out of the world from one side and enter into the other side (Figure 1.1). Therefore, even with only four cameras, animals had the ability to come into contact with cameras as if a larger landscape and camera grid were examined. This also negated any study area edge effects on movement characteristics or inferences, while maintaining a constant animal density throughout a model run. Stochasticity

was introduced into the model by the random positioning of home range centers and the random turning angle of the correlated random walk.

Upon initiation of the simulation, animal agents moved freely about the home range while the camera agents remained in an armed state. Once an animal passed within the FOV, the encounter was recorded, and the camera went into a delay mode in which the camera was unable to record any encounters. After the user specified delay period (DELAY) had passed, the camera agent was armed and ready to record the next contact of an animal within the FOV. If the delay was set to 1 second, then the camera triggered continuously given that time-steps themselves were one second. Camera agents tallied all animals within the FOV if multiple animals happened to co-occur. Counts of triggering events were tracked for each camera individually.

Experimental Test of Factors Influencing Photographic Counts

An experimental design was used to test how an encounter rate response variable could be influenced by four independent variables: ABUND, HOME (ha), FOV (m^2), and MOVE (m/s) in an orthogonal parameter space (Table 1.1) resulting in 1,512 combinations. To examine how temporal sampling design could influence the response of encounter rate to those four variables, scenarios were run using a trigger delay period of 1 second (DELAY1), 30 seconds (DELAY30), and 300 seconds (DELAY300). The model was allowed to simulate 1 day (86,400 ticks). For each combination of the parameters, 15 iterations were simulated in which new home range centers were generated, producing 22,680 sets of results. ABUND represented a range of 2-22 animals (density of 0.5 – 5.5 animals/ha). HOME represented an aerial home range extent of 0.28 – 5.31 ha. MOVE spanned 0.2 to 2.0 meters/second, which may represent a potential speed of a foraging animal to one at a fast gait. FOV represented an aerial measure of 3.3-61.9 m^2 (FOV distances: 3-13 m). The small world size (4 ha) and small home range sizes are most

representative of smaller mammals (e.g., lagomorphs) and less representative of mega-fauna, but also reduced computational requirements given the fine 1 m^2 resolution used.

For each model run, the mean number of encounters (i.e., trigger counts) across the four cameras was calculated. Because the duration of each model run was constant, this was a sufficient response variable to measure rather than encounters per unit time. The resulting encounter response was a non-negative continuous variable with zeros occurring in some iterations of the model. Therefore, a generalized linear model using a Tweedie compound Poisson error distribution (R package 'cplm') (Zhang 2013) (R Development Core Team 2013) was used to model the encounter rate response as a function of covariates. A separate analysis was conducted for each of the three delay period scenarios, as a goal was to examine which combination of variables explained the process observed under each scenario. Candidate models were created with combinations of main effects, quadratic terms, and all possible interactions between pairs of main covariates. Best fitting models were selected using Akaike's Information Criterion adjusted for small samples size (AICc, Burnham and Anderson 2002). To help protect against spurious inclusion of variables, models were examined for potential "pretender variables" (Anderson 2008, Arnold 2010). Models in the top set (those with $\Delta AICc < 7$) were inspected by assessing changes in log likelihood with the addition of potential pretending variables, along with 95% bootstrap confidence intervals of coefficient estimates. Coefficient estimates of pretender variables are near zero, have confidence intervals overlapping zero, and do not contribute to improving model fit; thus models with pretenders were removed. Across the three trigger delay scenarios, the best models were compared based on the selected set of coefficients, standardized coefficient estimates (covariates standardized and centered), and response plots of predicted values.

Habitat Utilization Experiment

To assess whether habitat-specific encounter rates could track relative habitat usage, I constructed a second model (CamHabitat) using a separate world (height and width: 800, 1 m x 1 m cells) consisting of a checkerboard of two habitat types (GRASS and FOREST: each 200 x 200 m) (Figure 1.2). Behavior of the animal agents was extended to include a "seeking" behavior where grassland habitats were used during the night and forest habitats during the day. A directed walk was made by dividing a 259,200 tick (3 day) simulation period into single days, in which habitat selection behaviors of animals followed user specified diel proportions for each day. A diel proportion of 0.25 would indicate forest habitat was sought for a 6 hour period, while a proportion of 0.5 and 0.75 would indicate that forest habitat was sought for a 12 and 18 hour period of the day respectively. Programmatically, ticks were assigned to certain behavior states and animals would target a certain habitat type based on the behavior state. By matching the mean of the distribution of potential turning angles to point toward the nearest targeted habitat, a basic habitat selection behavior was generated. Once an animal was inside the targeted habitat it would carry out a non-directed correlated random walk, unless a series of randomly selected turning angles happened to let it meander into the non-favored habitat, in which case the directed walk was re-engaged.

A pair of camera agents was placed systematically in each of the 8 grassland and 8 forested habitats (Figure 1.2). Placements were adjusted so that camera agents' FOVs were completely contained within the targeted habitat. Fixing home range size, FOV area, and animal abundance (Table 1.1), animal agents were programmed to behave under three habitat utilization scenarios corresponding to diel-proportions of 0.25 ("FOREST<GRASS"), 0.5 ("FOREST=GRASS"), and 0.75 ("FOREST>GRASS"). Furthermore, I programmed animals to behave under two movement rate scenarios, in which animals would either have a constant

movement rate (0.2 m/s) throughout both habitats, or a 2 m/s movement rate while occupying GRASS habitats and a 0.2 m/s while occupying FOREST habitats.

For each of the three habitat utilization scenarios and the two movement rate scenarios, three measurement methods were tested: TRUETIME, CAMDELAY1, and CAMDELAY30. TRUETIME was the measure of an animal agent's true usage of habitat, based on the amount of time an agent spent in each of the habitat types accumulated on an individual basis (Buskirk and Millspaugh 2006). In a field setting this would be analogous to measuring resource utilization with a GPS telemetry system continuously (i.e., 1 second GPS acquisition interval) for every animal of the population (a.ka., the "perfect" telemetry study). The proportion of total time spent in the forested habitat was then averaged among all members of the population. Because the landscape was composed of only two habitat types, grassland habitat usage was simply the compliment of forested habitat usage. CAMDELAY1 and CAMDELAY30, assuming a trigger delay period of 1 and 30 seconds respectively, are also proportion measures, but were derived from the number of photos tracked for each camera individually and then aggregated by mean trigger count for a given habitat type. This proportion was calculated with forested mean trigger count as the numerator and mean total trigger count (regardless of habitat) as the denominator. Analysis consisted of comparing the distribution of counts derived from the three measurement methods for each of the three habitat utilization scenarios and the two movement rate scenarios. This resulted in 18 unique combinations for each simulation, which was then replicated 100 times. Parameter space for the input values tested is shown in Table 1.1.

The code used in the Netlogo environment for CamEncounter and CamHabitat is provided in Appendix I. Digital copies of the full models' Netlogo file and animations of the

models can be obtained at: < https://sites.google.com/site/wildlifecamerastudy/camera-trapping-theory/agent-based-model-simulations >.

RESULTS

Experimental Test of Factors Influencing Photographic Counts

True trigger counts generated by the ABM resulted in a mean (95% C.I.) of 714.7 (704.9 – 724.5), 154.8 (152.9 – 156.8), and 82.4 (81.6 – 83.1) for the DELAY1, DELAY30, and DELAY300 trigger delay scenarios respectively. For DELAY1, an initial set of 94 models had ΔAICc <7. After removing models with pretending variables, the top model held >99% AICc weight. All coefficients estimates of the single best models were statistically significant (<0.001). For DELAY30, the two competing models held 54 and 45% of the AICc weight, with the first model being nested within the second. A single model could be distinguished as the best fitting (>99% AICc weight) in DELAY300 scenario. Confidence intervals for the parameter estimates of the additional variable in the second model overlapped zero, and thus it was removed from consideration, leaving the first model to hold >99% AICc weight. With predicted 95% confidence intervals being nearly invisible in the response plots, variation estimates receive no further discussion. Coefficient estimates were reflective of log transformed predictor values, as this improved model fit in all model sets.

The most parsimonious model for the DELAY1 scenario resulted in a simpler model (fewer terms) than the most parsimonious models selected for the DELAY30 and DELAY300 scenarios (Table 1.2). For the three scenarios, ABUND, FOV, and HOME generally had a positive influence on photographic counts (Table 1.2, Figure 1.3). Counts increased linearly with FOV and ABUND in the DELAY1 scenario, but showed a non-linear response when delay periods were increased in the DELAY30 and DELAY300 scenarios (Figure 1.3). HOME (in

units of area) showed a small threshold relationship, with the steepest positive slope occurring when the home range diameter appeared to be less than the 100 m spacing of the cameras (HOME = 0.283 or 0.503 ha) (Figure 1.3), especially when movement rate increased (Figure 1.4). Although weak, the ABUND*HOME interaction indicated this relationship was most apparent when animal density was relatively high (Table 1.2).

The best model for each trigger delay scenario differed mostly as a result of the MOVE effect. In the DELAY1 scenario, trigger counts showed no response to MOVE as indicated in the best model (Table 1.2), but showed a slight curvilinear response in the DELAY30 scenario and a stronger curvilinear concave relationship in the DELAY300 scenario (Figure 1.3). The strongest interactions of variables appeared to be in the terms: ABUND*MOVE, HOME*MOVE, ABUND*FOV, and FOV*MOVE (Table 1.2, Figure 1.4). The degree of non-linearity for the interactions appeared greater in the DELAY300 than in the DELAY30 scenario (Figure 1.4). For DELAY30, the effect of ABUND was strongest when MOVE was faster (Figure 1.4). This same general relationship was observed in the DELAY300 scenario, but was less predictable as a stronger threshold relationship between ABUND was observed as MOVE increased. A similar relationship was observed in the HOME*MOVE interaction and ABUND*FOV interaction (Figure 1.4). Although not explicitly tested, higher order interactions were likely present for the DELAY30 and DELAY300 scenarios. Evidence for this existed in the ABUND*FOV interaction term, in which the influence of ABUND was greater as FOV area increased (Figure 1.4), an indirect relationship likely resulting from the FOV*MOVE interaction.

Habitat Utilization Experiment

For the CamHabitat model, the distribution of the observed proportions of each method, scenario, and behavior are depicted in the boxplots (median, interquartile range, 1.5*interquartile

range, outliers) of Figure 1.5. Forest utilization as measured by the TRUETIME method followed the expectations of the habitat selection scenario imposed when movement rates were equal (forest < grass: 0.261, forest = grass: 0.508, forest > grass: 0.754) and deviated only slightly when movement rates were habitat specific (forest < grass: 0.313, forest = grass: 0.535, forest > grass: 0.758). With movement rates held constant, CAMDELAY1 and CAMDELAY30 methods approximated the TRUETIME method in the three habitat selection scenarios, with the mean differing by less than 0.02 for any scenario (Figure 1.5: left pane). However, when movement rate was slower in the forest than in the grassland, the CAMDELAY30 method caused an underestimation of the true forest utilization in all three habitat selection scenarios (forest < grass: 0.123, forest = grass: 0.215, forest > grass: 0.4) (Figure 1.5: right pane). The negative bias exhibited in the "forest > grass" scenario was strong enough to change the overall direction of the inferred relationship; forest utilization should have dominated the proportion of time, while cameras using a 30 second delay period indicated grassland utilization dominated. Implementing a 1 second delay period when movement rates were habitat specific only caused underestimation by less than 0.027 in any habitat selection scenario (Figure 1.5, right panel).

DISCUSSION

Factors Influencing Encounter Rate

The CamEncounter ABM behaved as expected for mobile objects interacting with fixed passive sampling devices (Gurarie and Ovaskainen 2012), and my findings expand on work of other camera trapping studies (Carbone et al. 2001, Rowcliffe et al. 2008, Sollmann et al. 2013) to show that abundance, home range, FOV dimensions, and movement rate all influence encounter rate when manipulated in a rigorous experiment. Specifically I demonstrated that trigger delay settings, or even sub-sampling images in post-processing (i.e., DELAY30 or

DELAY300 scenarios) can mediate the relationship between trigger counts and relative abundance, FOV dimensions, and movement rate. By including a trigger delay period, trigger counts will be influenced by complex interactions between the biological processes (abundance, home range size, movement rate) with further non-additive or non-linear responses occurring if FOV dimensions change from site to site. Allowing the camera to trigger continuously defined the encounter rate as an actual measure of the amount of time an animal spent within the FOV, thus negating the movement rate effect. This is based on the idea that as movement rate decreases, the number of potential passes across the home range (and thus the potential number of unique encounters with the FOV) decreases, but is balanced by the increase in residence time inside the FOV. Matching the camera agent's delay period to the smallest unit of time measureable by the ABM (1 tick = 1 sec) in DELAY1, essentially allowed a continuous representation rather than a discrete one.

I showed a weak non-linear threshold relationship between trigger counts and home range size. Interestingly, simulations of Sollmann et al. (2013) showed a positive relationship between home range and trigger count, which likely stems from their assumption that home range size and movement rate are positively correlated. My simulations indicated that the effect of home range area on trigger counts was negligible compared to the strength of other variables tested (i.e., ABUND, FOV). However, the home range effect was most pronounced at the lower home range sizes examined, particularly when the minimum spacing of cameras (100 m) exceeded animal home range diameters. In the case of small home range sizes (diameter less than camera spacing), any increase in home range size would allow more unique individuals to come into contact with any camera. As home range sizes grow sufficiently large (diameter greater than camera spacing), modeled encounters exhibit two counteracting behaviors; repeat utilization by a

particular animal of any particular location within the home range decreases, while the probability of that individual encountering more cameras increases (i.e., each camera picks up encounters from more unique individual animals). The ABUND*HOME interaction indicated that this was less identifiable when fewer animals were present; which was likely due to animals being more dispersed.

My simulation showed that increases in FOV area had a positive effect on encounter rate. Given a triangular-shaped FOV, this response to FOV distance from the camera would be positive convex or exponential. However, the process of detecting an animal within the FOV of a camera trap is not as error free as advertised; the probability of detection declines as distance from the camera sensor increases (Rowcliffe et al. 2011) thus making the FOV dimensions difficult to define. Although accounting for imperfect detection may be done in some cases by implementing time-lapse triggers (Hamel et al. 2013) or standardizing the maximum FOV with physical barriers (Glen et al. 2013), applying a distance sampling methods (Rowcliffe et al. 2011) would be a better solution.

The habitat utilization experiment (CamHabitat) revealed that relative encounter rates between habitat types can approximate relative habitat utilization patterns derived from a "perfect" telemetry study in which location acquisition is done at a fine temporal scale (1 second) for every member of the population. Essentially, the utilization metric measured by cameras can be considered a true measure of the amount of time spent by any member of the population in any particular given aerial unit. However, as observed in the CamEncounter simulations, biases will likely occur if a delay period is implemented. The bias uncovered in these simulations is similar to the type of bias occurring with respect to location acquisition intervals in telemetry studies (Reynolds and Laundre 1990, Johnson and Ganskopp 2008). While

it may seem that delay period is strictly a temporal issue related to camera study design, it can interact with movement rates because they both share a time component. Considering movement rate (m/s) has an element of time and space, any purely spatial factor (i.e., FOV area) can in turn be influenced indirectly, as a non-linear (less predictable) influence on encounter rate was observed. Given the increasing complexities in relationships as delay period increased from 1 to 30 to 300 seconds in the CamEncounter simulation, bias would likely increase as some function of delay period in addition to biological characteristics of targeted species or population.

Guidance for Future Studies

Many past studies attempting to understand animal utilization with respect to treatment groups (habitat types or seasons) have made efforts to program camera delay periods or rarify data to assumed "independent" events of individual usage or activity (George and Crooks 2006, Bowkett et al. 2007, Gessner et al. 2013). Given sampling units are based on spatial (the camera location) or temporal (i.e., diel periods, seasons) units of effort, where an encounter rate is derived by pooling observations across a sampling unit, it is uncertain why independence within a site is deemed necessary. If localized abundance is the habitat utilization currency, then perhaps distinct events of individual animals are important. However, the simulations show that relative abundance can be difficult to infer when faced with delay periods and dynamic movement rates. Future study designs should abandon the common practice of arbitrarily defined delay periods and allow cameras to trigger nearly continuously or employ video recording (Scheibe et al. 2008) to track the amount of time spent within the FOV. Technological advances in data storage, battery capacity, and data processing techniques are making this more achievable than ever before.

The influence of movement rate and habitat selection heterogeneity found in the simulations has implications toward the importance of placing cameras probabilistically (i.e., random sampling or stratified random sampling) throughout a study area. Placing cameras on micro-habitat features such as "game trails" or bait sites is commonly done in camera trap studies when occupancy modeling is an objective (Thornton et al. 2011, Rovero et al. 2013, Bender et al. 2014) or near baits (O'Connell et al. 2006, Hamel et al. 2013, Robinson et al. 2014). Placing cameras only on trails would be akin to placing cameras on only the grassland habitats (habitat with higher movement rate) in my habitat utilization experiment (CamHabitat). Given the effects of movement rate and habitat selection found in the utilization measure, there is no reason to believe a habitat feature like game trails would give a representative utilization for the non-game trail micro-habitats available to animals. This is supported by several studies examining the probabilistic camera placement of versus the placement of cameras on game trails or bait sites (Harmsen et al 2010, McCoy et al. 2011, Wearn et al. 2013, Sollmann et al. 2013).

Restrictions on inferences may be required for species that can escape from the camera's view (e.g., animals resting in cavities or underground). Conducting surveys using camera traps that are triggered using infrared may be biased because movement within the FOV is needed for an encounter to be counted; which is a requirement shared with recent studies using camera traps to assess animal activity patterns (Bridges and Noss 2011, Oliveira-Santos et al. 2013, Rowcliffe et al. 2014). The habitat utilization measure discussed here is more concerned with residency time, while the activity pattern treatments only consider initial contact with the FOV. Residency time is important for making spatial utilization inferences on the intensity of usage. Tracking FOV residency time capitalizes on the fact that camera trap survey platforms are capable of operating continuously. Animals more often at rest within the FOV may not trigger the camera

frequently enough to ensure an accurate count of time spent. While time lapse methods would free the dependency of a trigger on the animal's behavior, it essentially introduces a trigger delay period, which I showed to be problematic. Technological advances, such as improved triggering systems, video recording (Scheibe et al. 2008) and automated image recognition (Yu et al. 2013, Swinnen et al. 2014), may help solve some of these issues.

Conclusion

From a research methods standpoint, population level encounter rates can have various utilities. For instance, a grazing impact study, assessing the influence of a particular ungulate species on stream bank erosion, aims at assessing the combined effect of local ungulate abundances and the average utilization pattern made by the constituent individuals. Retrieving a similar measure with telemetry would require monitoring every individual (or a representative sample of individuals) relative to the underlying distribution pattern of individuals on the landscape. Collecting an abundance measure alone to make habitat usage inferences on the stream would be of little use for inference at larger scales (i.e., km^2) typically employed in ungulate studies. Another example is when assessing predation risk of a rare species, where the combined effect of predator numbers and individual selection behaviors of hunting sites are of importance.

Raw encounter rate measures can be a fruitful alternative to occupancy modeling inferences (Thornton et al. 2011, Bender et al. 2014, Robinson et al. 2014) or abundance inferences (Bowkett et al. 2007) for judging habitat utilization with passive camera trap designs. Assuming probabilistic placement of survey stations, continuous monitoring of animal residency within the FOV, and detection probability within the FOV is known or constant, a population level measure of habitat utilization can be inferred. Continuously monitoring plots allows for the

animal residency time to be accounted for. Future studies should take advantage of the continuous temporal data provided by camera platforms, an attribute unmatched in most human based surveys and even current GPS telemetry studies.

TABLES AND FIGURES

Table 1.1. Input parameter space for the encounter rate model for multivariate tests and the habitat utilization model. Results were simulated using all combinations of the given values in the CamEncounter ABM model and then for the CamHabitat ABM model.

Parameter	CamEncounter Model	CamHabitat Model
ABUND (animals)	2, 6, 10, 14, 18, 22	20
HOME (ha)*	0.283, 0.503, 1.131, 2.011, 3.146, 4.155, 5.310	-
FOV (m^2)†	3.299, 9.163, 17.959, 29.688, 44.348, 61.942	93.829
MOVE (m/s)	0.200, 0.56, 0.92, 1.28, 1.64, 2.00	-
MOVE (GRASS) (m/s)	-	0.2, 2
MOVE (FOREST) (m/s)	-	0.2
Turning Angle (°)	5	5
Forest Seeking Proportion	-	0.25, 0.5, 0.75

*HOME area measures correspond to home range diameter of 60, 80, 120, 160, 200, 230, and 260 m respectively.

†FOV area measures correspond to maximum FOV distances of 3, 5, 7, 9, 11, and 13 m respectively.

Table 1.2. Beta coefficient estimates (95% confidence intervals in parenthesis) for variables of the best fitting model developed under the scenarios using a 1 second (DELAY1), 30 second (DELAY30), and 300 second (DELAY300) trigger delay.

Coefficient	DELAY1	DELAY30	DELAY300
β_0	5.931 (5.914, 5.948)	4.519 (4.503, 4.534)	4.078 (4.064, 4.090)
β_{ABUND}	0.812 (0.804, 0.821)	0.848 (0.819, 0.876)	0.952 (0.930, 0.973)
β_{FOV}	0.992 (0.983, 0.999)	0.672 (0.651, 0.692)	0.636 (0.622, 0.651)
β_{HOME}	0.134 (0.026, 0.224)	0.196 (0.106, 0.284)	0.714 (0.644, 0.784)
β_{MOVE}	NA	0.626 (0.619, 0.632)	0.444 (0.439, 0.450)
β_{FOV^2}	NA	-0.116 (-0.136, -0.096)	-0.242 (-0.256, -0.229)
β_{ABUND^2}	NA	-0.060 (-0.083, -0.036)	-0.297 (-0.313, -0.281)
β_{MOVE^2}	NA	NA	-0.104 (-0.108, -0.101)
β_{HOME^2}	-0.122 (-0.213, -0.021)	-0.158 (-0.240, -0.073)	-0.609 (-0.674, -0.544)
$\beta_{ABUND*FOV}$	NA	-0.012 (-0.018, -0.007)	-0.068 (-0.072, -0.065)
$\beta_{ABUND*HOME}$	-0.008 (-0.016, 0.000)	-0.009 (-0.017, -0.001)	-0.048 (-0.054, -0.041)
$\beta_{ABUND*MOVE}$	NA	-0.023 (-0.028, -0.018)	-0.087 (-0.091, -0.082)
$\beta_{FOV*HOME}$	NA	0.008 (0.002, 0.013)	0.015 (0.011, 0.018)
$\beta_{FOV*MOVE}$	NA	-0.024 (-0.028, -0.020)	-0.045 (-0.048, -0.043)
$\beta_{HOME*MOVE}$	NA	0.022 (0.017, 0.027)	0.021 (0.018, 0.025)

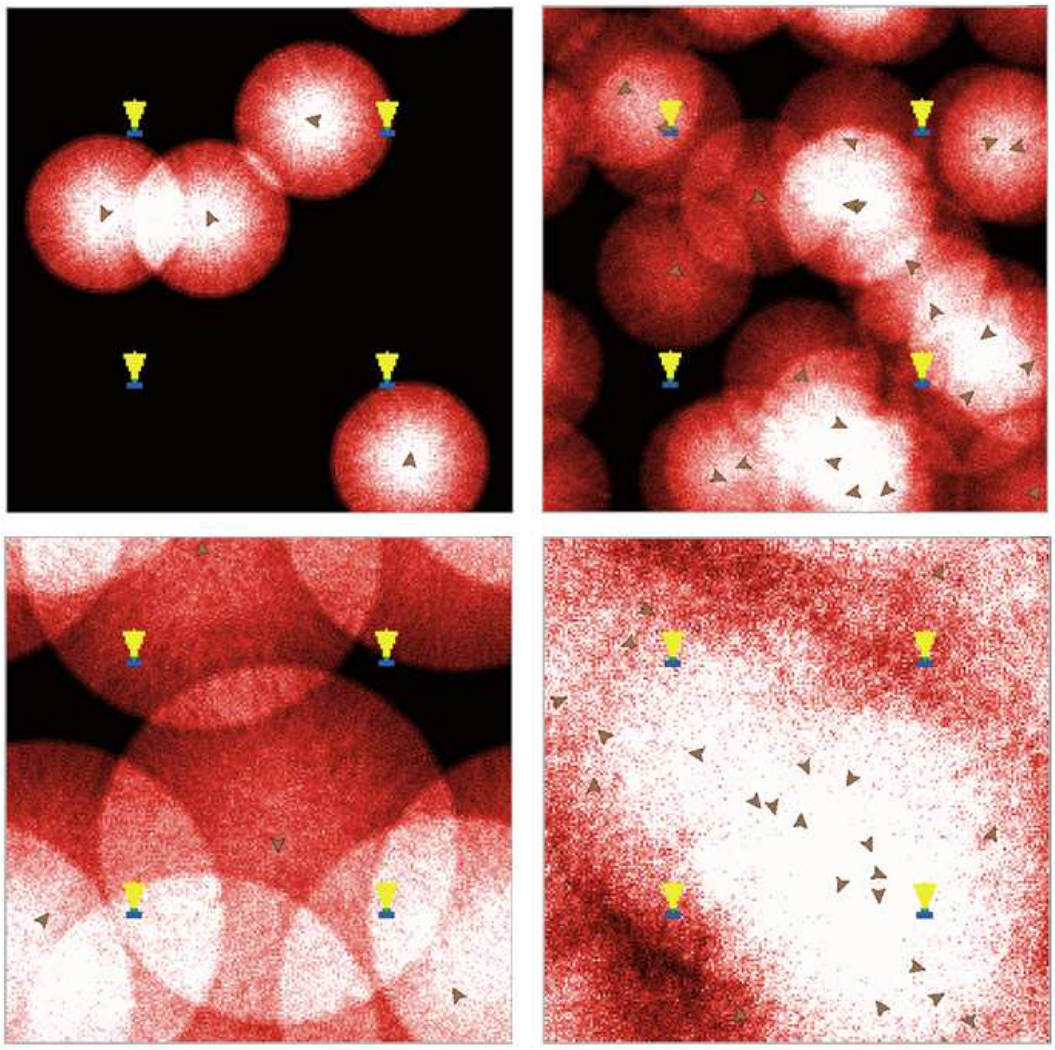

Figure 1.1. CamEncounter world depictions of four scenarios with camera FOV agents (yellow cones) and animal agents (brown arrowheads). Animal agents are shown at their home range centers superimposed over the observed joint utilization pattern tracked for pixel "patch" agents (display purposes only). Home ranges spanning the edges continue onto the opposite side of the world ("world wrapping"). Top and bottom panes represent a home range diameter of 60 and 140 m (HOME: 1 and 1.53 ha) respectively. Left and right panes represent an ABUND of 4 and 22 animals (density: 1 and 5.5/ha) respectively.

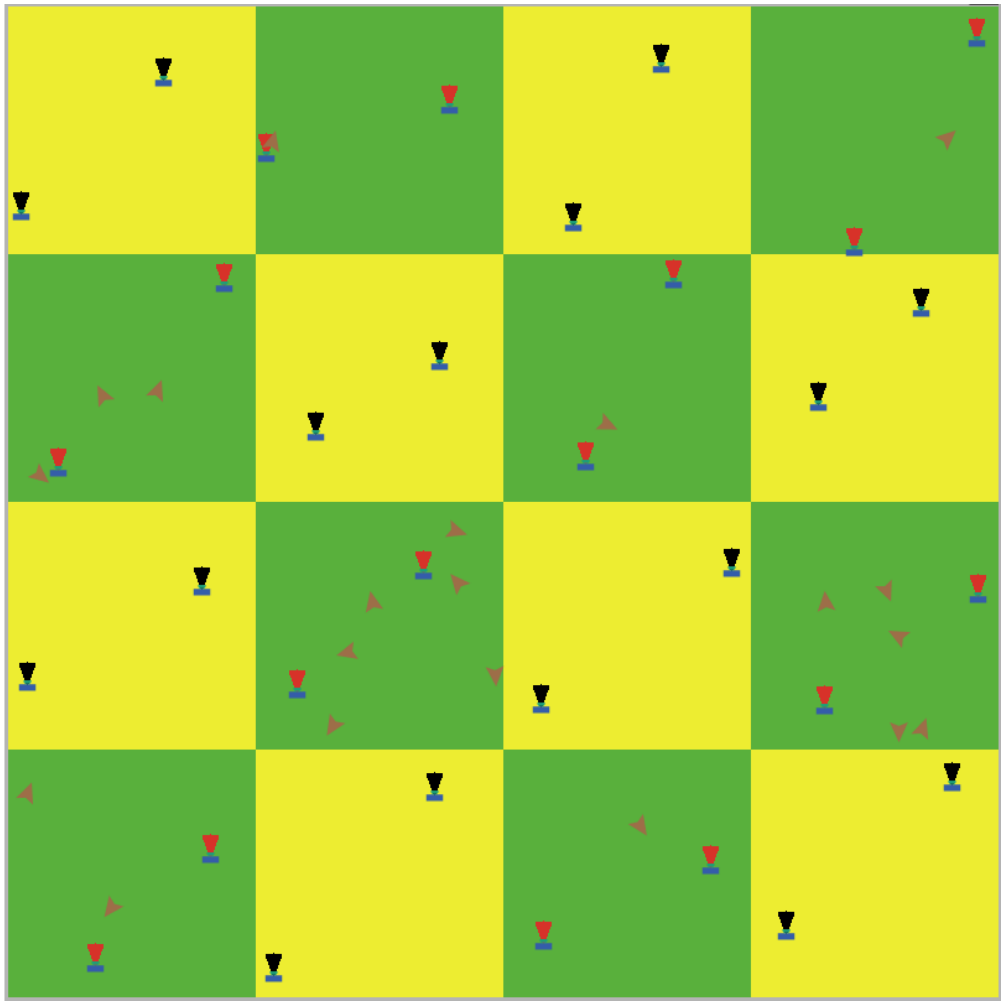

Figure 1.2. CamHabitat world depiction (800m x800 m) with camera FOV agents (red cones in FOREST and black cones in GRASS) and animal agents (brown arrowheads). Animal agent movements are able to respond to FOREST (green) and GRASS (yellow) patch agents.

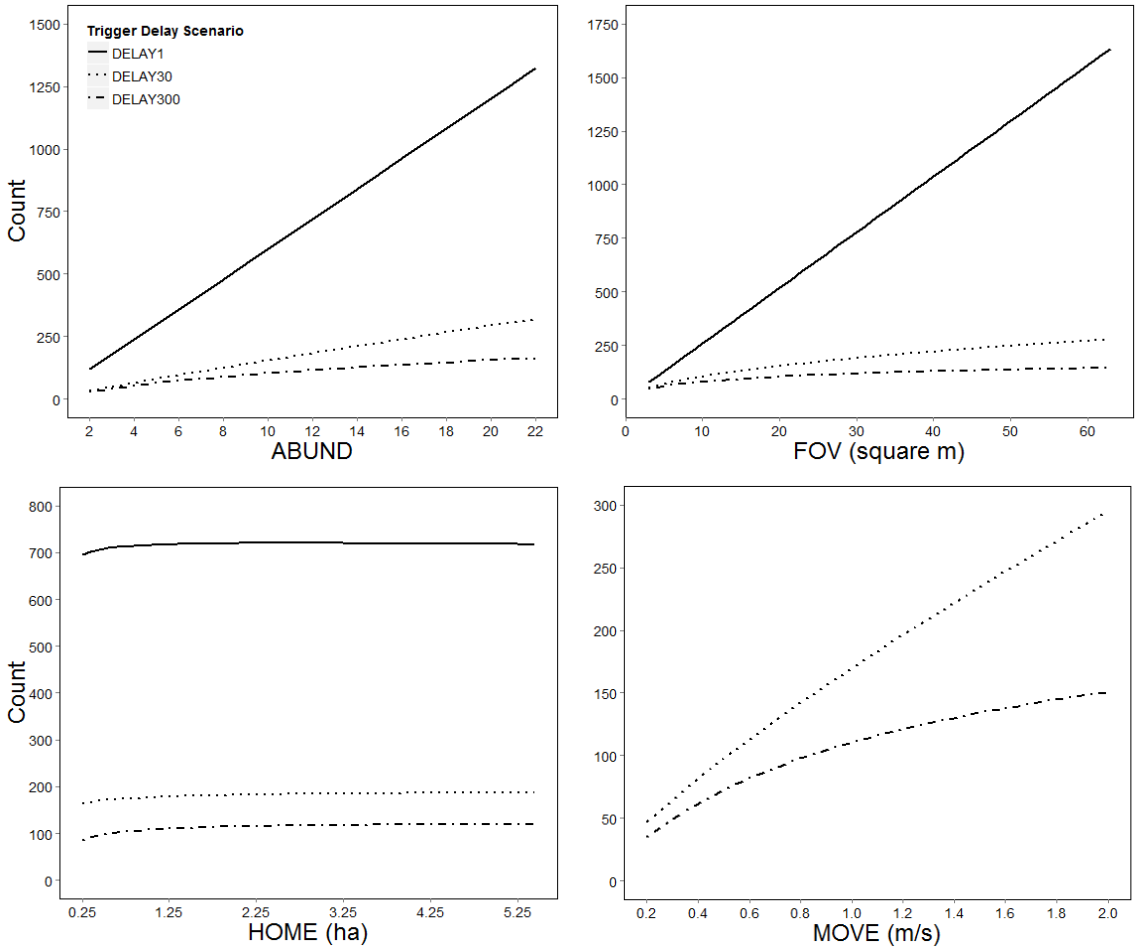

Figure 1.3. Trigger count response plots as a function of animal abundance (ABUND), field of view area (FOV), home range area (HOME), and movement rate (MOVE) for scenarios when the camera is programmed with 1 (DELAY1), 30 (DELAY30), and 300 (DELAY300) second trigger delay periods.

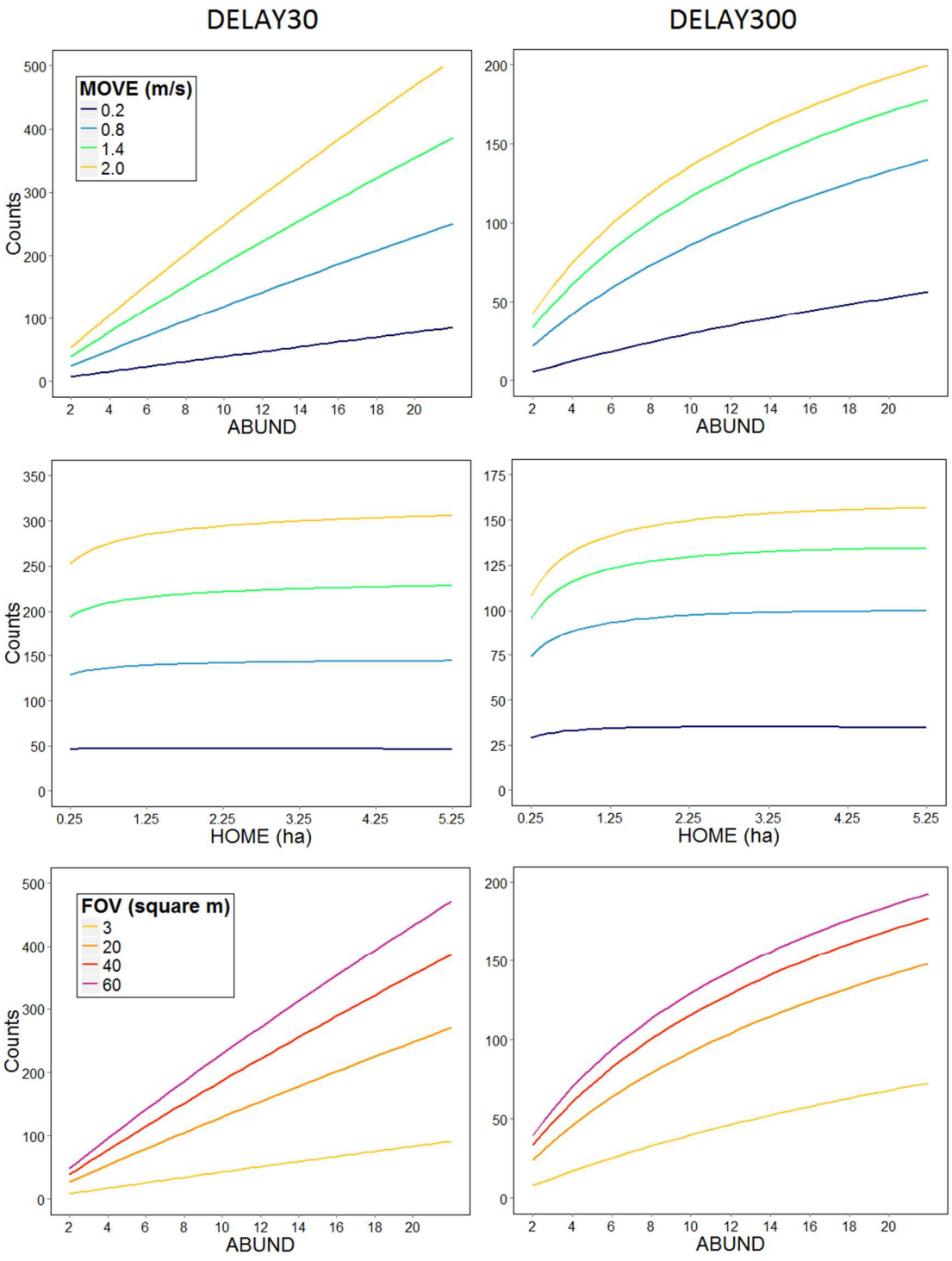

Figure 1.4. Trigger count responses to ABUND and HOME for the four MOVE rates and trigger count responses to ABUND for the four FOV areas for scenarios when camera is programmed with 30 (DELAY30) and 300 (DELAY300) second trigger delay periods.

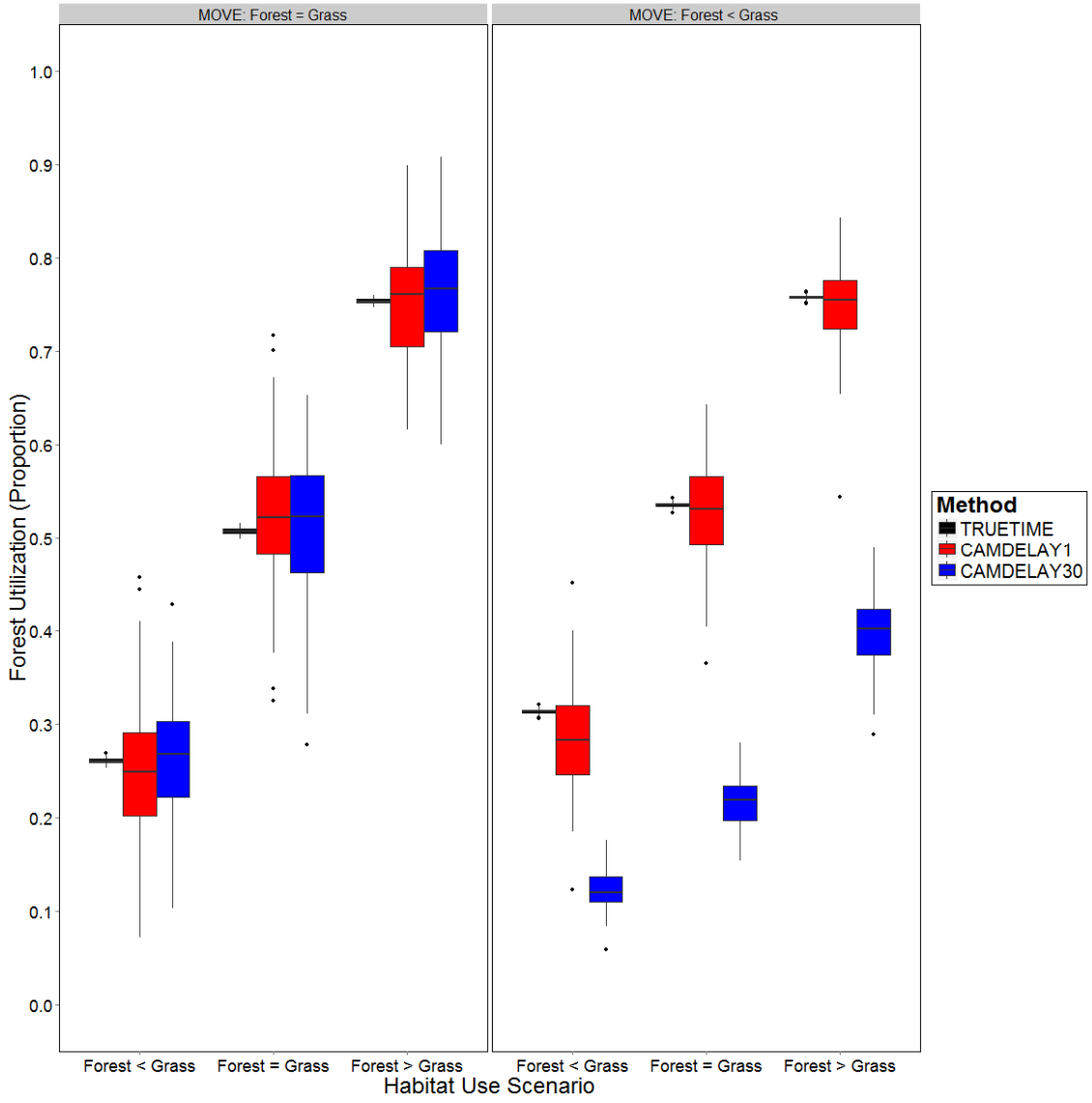

Figure 1.5. Box-whisker plots of distributions comparing three measures (TRUETIME, CAMDELAY1, CAMDELAY30) of the relative forest utilization (y-axis) for three scenarios in which animal agents were programmed to carry out three behaviors (x-axis) which included seeking forests 25% of the time (FOREST < GRASS), 50% of the time (FOREST = GRASS), and 75% of the time (FOREST > GRASS), with an additional factor specifying whether animal movement rates were equal between habitats (left pane) or greater in the grasslands than in the forests (right pane).

LITERATURE CITED

Anderson, D. R. 2008. Model Based Inferences in the Life Sciences: A Primer on Evidence. Springer Science & Business Media, New York, NY, USA.

Arnold, T. W. 2010. Uninformative parameters and model selection using Akaike's Information Criterion. Journal of Wildlife Management 74:1175-1178.

Bender, L. C., M. E. Weisenberger, and O. C. Rosas-Rosas. 2014. Occupancy and habitat correlates of javelinas in the southern San Andres Mountains, New Mexico. Journal of Mammalogy 95:1-8.

Bowkett, A. E., F. Rovero, and A. R. Marshall. 2007. The use of camera-trap data to model habitat use by antelope species in the Udzungwa Mountain forests, Tanzania. African Journal of Ecology 46:479-487.

Bridges, A. S., and A. J. Noss. 2011. Behavior and Activity Patterns. Pages 57-69 *in* A. F. O'Connell, J. D. Nichols, andK. U. Karanth, editors. Camera Traps in Animal Ecology: Methods and Analysis. Springer, New York, NY, USA.

Burnham, K. P., and D. R. Anderson. 2002. Model selection and model inference: a practical information-theoretic approach. 2nd edition edition. Springer-Verlag, New York, NY, USA.

Buskirk, S. W., and J. J. Millspaugh. 2006. Metrics for studies of resource selection. Journal of Wildlife Management 70:358-366.

Carbone, C., S. Christie, K. Conforti, T. Coulson, N. Franklin, J. R. Ginsberg, M. Griffiths, J. Holden, K. Kawanishi, M. Kinnaird, R. Laidlaw, A. Lynam, D. W. Macdonald, D. Martyr, C. McDougal, L. Nath, T. O'Brien, J. Seidensticker, D. J. L. Smith, M. Sunquist,

R. Tilson, and W. N. Wan Shhruddin. 2001. The use of photographic rates to estimate densities of tigers and other cryptic mammals. Animal Conservation 4:75-79.

Cowardin, L., M., and J. E. Ashe. 1965. An automatic camera device for measuring waterfowl use. Journal of Wildlife Management 29:636-640.

Cutler, T. L., and D. E. Swann. 1999. Using remote photography in wildlife ecology: a review. Wildlife Society Bulletin 27:571-581.

Di Bitetti, M. S., A. Paviolo, and C. De Angelo. 2006. Density, habitat use and activity patterns of ocelots (Leopardus pardalis) in the Atlantic Forest of Misiones, Argentina. Journal of Zoology 270:153-163.

George, S. L., and K. R. Crooks. 2006. Recreation and large mammal activity in an urban nature reserve. Biological Conservation 133:107-117.

Gessner, J., R. Buchwald, and G. Wittemyer. 2013. Assessing species occurrence and species-specific use patterns of bias in Central Africa with camera traps. African Journal of Ecology 52:59-68.

Glen, A. S., S. Cockburn, M. Nichols, J. Ekanayake, and B. Warburton. 2013. Optimising camera traps for monitoring small mammals. PLoS One 8:e67940.

Gurarie, E., and O. Ovaskainen. 2012. Towards a general formalization of encounter rates in ecology. Theoretical Ecology 6:189-202.

Hamel, S., S. T. Killengreen, J.-A. Henden, N. E. Eide, L. Roed-Eriksen, R. A. Ims, N. G. Yoccoz, and R. B. O'Hara. 2013. Towards good practice guidance in using camera-traps in ecology: influence of sampling design on validity of ecological inferences. Methods in Ecology and Evolution 4:105-113.

Harmsen, B. J., R. J. Foster, S. C. Silver, L. Ostro, and C. P. Doncaster. 2010. Differential use of trails by forest mammals and implications for camera-trap studies: a case study from Belize. Biotropica 42:126-133.

Jennelle, C. S., M. C. Runge, and D. I. MacKenzie. 2002. The use of photographic rates to estimate densities of tigers and other cryptic mammals: a comment on misleading conclusions. Animal Conservation 5:119-120.

Johnson, D. D., and D. C. Ganskopp. 2008. GPS Collar Sampling Frequency: Effects on Measures of Resource Use. Rangeland Ecology & Management 61:226-231.

Johnson, D. H. 1980. The comparison of usage and availability measurements for evaluating resource preference. Ecology 61:65-71.

Karanth, K. U. 1995. Estimating tiger (*Panthera tigris*) populations from camera trap data using capture-recapture models. Biological Conservation 71:333-338.

Kinnaird, M. F., E. W. Sanderson, G. O'Brien T, H. T. Wibisono, and G. Woolmer. 2003. Deforestation trends in a tropical landscape and implications for endangered large mammals. Conservation Biology 17:245-257.

MacKenzie, D. I., J. D. Nichols, J. A. Royle, K. H. Pollock, L. L. Bailey, and J. E. Hines. 2006. Occupancy Estimation and Modeling: Inferring Patterns and Dynamics of Species Occurrence. Elsevier, San Diego, CA, USA.

Mathews, S. M., J. M. Higley, J. S. Yaeger, and T. K. Fuller. 2011. Densities of fishers and the efficacy of relative abundance indices and small-scale occupancy estimation to detect a population decline on the Hoopa Valley Indian Reservation, California. Wildlife Society Bulletin 35:69-75.

McCoy, J. C., S. S. Ditchkoff, T. D. Steury. 2011. Bias associated with baited camera sties for assessing population characteristics of deer. Journal of Wildlife Management 75:472-477.

O'Brien, T. G., M. F. Kinnaird, and H. T. Wibisono. 2003. Crouching tigers, hidden prey: Sumatran tiger and prey populations in a tropical forest landscape. Animal Conservation 6:131-139.

O'Connell, A. F., N. W. Talancy, L. L. Bailey, J. R. Sauer, R. Cook, and A. T. Gilbert. 2006. Estimating site occupancy and detection probability parameters for meso- and large mammals in coastal ecosystem. Journal of Wildlife Management 70:1625-1633.

Oliveira-Santos, L. G. R., C. A. Zucco, and C. Agostinelli. 2013. Using conditional circular kernel density functions to test hypotheses on animal circadian activity. Animal Behaviour 85:269-280.

Popescu, V. D., P. Valpine, and R. A. Sweitzer. 2014. Testing the consistency of wildlife data types before combining them: the case of camera traps and telemetry. Ecology and Evolution 4:933-943.

Reynolds, T. D., and J. W. Laundre. 1990. Time intervals for estimating pronghorn and coyote home ranges and daily movements. Journal of Wildlife Management 54:316-322.

Robinson, Q. H., D. Bustos, and G. W. Roemer. 2014. The application of occupancy modeling to evaluate intraguild predation in a model carnivore system. Ecology http://dx.doi.org/10.1890/13-1546.1.

Rovero, F., L. Collett, S. Ricci, E. Martin, and D. Spitale. 2013. Distribution, occupancy, and habitat associations of the gray-faced sengi (Rhynchocyon udzungwensis) as revealed by camera traps. Journal of Mammalogy 94:792-800.

Rovero, F., and A. R. Marshall. 2009. Camera trapping photographic rate as an index of density in forest ungulates. Journal of Applied Ecology 46:1011-1017.

Rowcliffe, J. M., J. Field, S. T. Turvey, and C. Carbone. 2008. Estimating animal density using camera traps without the need for individual recognition. Journal of Applied Ecology 45:1228-1236.

Rowcliffe, J.M., C. Carbone, P. A. Jansen, R. Kays, and B. Kranstauber. 2011. Quantifying the sensitivity of camera traps: an adapted distance sampling approach. Methods in Ecology and Evolution 2:464-476.

Rowcliffe, J. M., R. Kays, B. Kranstauber, C. Carbone, P. A. Jansen, and D. Fisher. 2014. Quantifying levels of animal activity using camera trap data. Methods in Ecology and Evolution 5:1170-1179.

Scheibe, K. M., K. Eichhorn, M. Wiesmayr, B. Schonert, and O. Krone. 2008. Long-term automatic video recording as a tool for analysing the time patterns of utilisation of predefined locations by wildlife. European Journal of Wildlife Research 54:53-59.

Shiras, G. 1906. Photographing wild game with a flash-light and camera. National Geographic Magazine 17:366-423.

Silveira, L., A. T. A. Jacomo, and J. A. Diniz-Filho. 2003. Camera trap, line transect census and track surveys: a comparative evaluation. Biological Conservation 114:351-355.

Sollmann, R., A. Mohamed, H. Samejima, and A. Wilting. 2013. Risky business or simple solution – Relative abundance indices from camera-trapping. Biological Conservation 159:405-412.

Swann, D. E., K. Kawanishi, and J. Palmer. 2011. Evaluating Types and Features of Camera Traps in Ecological Studies: A Guide for Researchers. Pages 27-43 *in*.

Swinnen, K. R., J. Reijniers, M. Breno, and H. Leirs. 2014. A novel method to reduce time investment when processing videos from camera trap studies. PLoS One 9:e98881.

Temple, S. A. 1972. A portable time-lapse camera for recording wildlife activity. Journal of Wildlife Management 36:944-947.

Thornton, D. H., L. C. Branch, and M. E. Sunquist. 2011. The relative influence of habitat loss and fragmentation: do tropical mammals meet the temperate paradigm? Ecological Applications 21:2324-2333.

Wearn, O. R., J. M. Rowcliffe, C. Carbone, H. Bernard, R. M. Ewers. 2013. Assessing the status of wild felids in a highly disturbed commercial forest reserve in Borneo and the implications for camera trap survey design. PLoS One 8:e77598. doi:10.1371/journal.pone.0077598

Wilensky, U. 1999. NetLogo V.5.1.0. Center for Connected Learning and Computer Based Modeling, Northwestern University. Evanston, IL.

Yu, X., J. Wang, R. Kays, P. A. Jansen, and T. Wang. 2013. Automated recognition of species in camera traps. EURASIP Journal of Image and Video Processing 2013:(doi: 10.1186/1687-5281-2013-1152).

Zhang, Y. 2013. Likelihood-based and bayesian methods for Tweedie compound poisson linear mixed models. Statistics and Computing 23:743-757.

CHAPTER 2 - MODELING ANIMAL UTILIZATION WITH CAMERA TRAP SENSORS: URBAN-WILDLAND CASE STUDY

INTRODUCTION

A primary goal in many ecological studies is to assess interactions determining the distribution of organisms (Krebs 1994). Animal distribution modeling often requires discerning the response of an animal state variable (i.e., occupancy, abundance, resource selection) to fixed spatial variables, such as topography, flora communities, or anthropogenic development. An underlying thread to these state variables is the rate of encounter between animals and the fixed landscape feature. Two parameters essential to understanding encounter rate with landscape features are animal population size and movement/utilization patterns of the individuals comprising a population (Gurarie and Ovaskainen 2012, Chapter 1).

It can be argued that raw encounter rate measures are a useful response in animal utilization distribution modeling at fine spatial scales. Generally, field and analytical methods, such as GPS telemetry (Cagnacci et al. 2010) and mark-recapture statistics (Williams et al. 2002), have allowed detailed inferences on animal abundance and animal movement/utilization to be obtained as two separate components. However, in broader ecological studies focused on understanding all the interactions between flora, fauna, abiotic, and anthropogenic components, resources are not always available to conduct sophisticated telemetry and mark-recapture techniques on the animal component. In some instances, disentangling the influence of animal abundance and individual animal utilization patterns are not required for assessing the interactions between animals and spatial features (e.g., vegetation communities). For a study of plant-animal interactions, it may not matter whether the animals occur at high density if very few

animals use the focal plant community. For a soil erosion study, it may not matter if a large number of animals use a stream bank for a short period of time or if few animals used it for a long period of time.

Remote camera trapping is a method for measuring animal utilization of landscape features (Chapter 1). Camera encounter rate studies have been primarily focused on relative abundance (O'Brien et al. 2003, Bowkett et al. 2007, Gessner et al. 2013) or activity measures (George and Crooks 2006, Rowcliffe et al. 2014) to infer importance or utilization of discrete habitat features. Encounter rates may be better inferred as a product of the amount of discrete temporal units spent by animals within the camera's field-of-view (FOV: the area visible by a camera's lens and triggering system) and the number of animals within some large area around the camera (Chapter 1). Two requirements are that plots be monitored continuously, if animal movement rates are habitat specific, and that FOV size is accounted for (Chapter 1). Camera traps are a natural platform for fulfilling the first requirement as infrared systems (Cutler and Swann 1999) with continuous triggering capabilities or continuous video monitoring (Scheibe et al. 2008) are becoming more accessible. To gather the same inference with conventional animal utilization measurement techniques, individual animal locations of all members of the population would need to be monitored continuously (i.e., with GPS telemetry). If all animals cannot be monitored, then a sample of animals, representative of the population's density distribution on the landscape must be available. Depending on the system and species, executing either GPS telemetry and abundance estimation methods can be difficult and costly.

One limitation with infrared triggered platforms is that detectability within the field of view is imperfect (Kelly and Holub 2008, Swann et al. 2010, Hamel et al. 2013). Rowcliffe et al. (2011) showed with distance sampling methods that the probability of detecting an animal

decreases with increasing distance and angle from the camera's sensor; a relationship influenced by biological and environmental covariates. Integration of the probability density function for distance (Burnham et al. 1980) and angle can be used to define effective dimensions of the survey plot for a sampling location (Rowcliffe et al. 2011). An alternative parameterization of the problem may be to use coefficients from a modeled probability density function that provides detection probability estimates given an observed detection distance, site or observation level covariates, and a suitable truncation distance. Detection probability can then be used to directly correct count data (Marques and Buckland 2003, Marques et al. 2007) for a fixed plot size.

The overarching goal of this chapter is to give an empirical demonstration on inferring habitat utilization with raw encounter rate measures produced by camera traps. The methodology demonstrated here is two-part: detection probability modeling and utilization modeling. First, I use the distance sampling techniques of Rowcliffe et al. (2011) to correct encounter rate measures on a site level and encounter specific (observation level) basis. I shed additional light on variables thought to influence detection probability in camera trapping studies. Second, using the corrected encounter rate measures, I used a generalized linear model (GLM), to examine habitat features that influence the utilization of a set of six medium – large terrestrial mammal species (mule deer [*Odocoileus hemionus*], raccoon [*Procyon lotor*], elk [*Cervus elaphus*], red fox [*Vulpes vulpes*], domestic cat *[Felis catus*]), and coyote [*Canis latrans*]), inhabiting a foothill-montane system. The effects of human housing development is emphasized, which is well studied for some species (i.e., coyote), but less for others (i.e., mule deer and elk) (Table 2.1). Although this chapter is primarily focused on serving as a methodological case study, a desired side product of this study is to develop utilization distribution maps at the population level for the six species, which are potential prey species of cougar (*Puma concolor*). Other

studies ongoing in the same study area are interested in understanding whether cougars select for certain locations characterized by a higher likelihood of encountering a potential prey item (Chapter 3). A higher likelihood of encountering a prey item is dependent on the combined effect of the time spent by a prey animal and the number of prey individuals potentially using a location. Thus, camera trapping encounter rates (Chapter 1) are an ideal measure.

METHODS

Study Area

Methods were approved by IACUC protocol of Colorado Parks and Wildlife (84-R0045 #09-2011). Camera traps were placed within a 2700 km^2 study area in the Colorado Front Range adjacent to the Denver metropolitan area (Figure 2.1). This area spans west-east from the continental divide to the foothills and the urban-wildland interfaces (i.e., of Boulder, Golden, and Denver), and south-north from the South Platte to the Big Thompson Rivers. A patchwork of private and public land makes up 43% and 57% of the study area respectively. Private land is characterized by a gradient of rural-exurban-suburban development, interspersed with small towns. Rural areas have a few smaller developments related to mining, hobby ranching, and tourism based industries. Public land is managed by federal, state, and municipal governments primarily for consumptive and non-consumptive recreational activities or purely as open space. A full discussion of anthropogenic development present in this Front Range region can be found in Appendix 2.

Camera Deployment

A sample of 131 camera traps (Reconyx HyperFire PC800; Holmen, WI, USA) were deployed following a stratified random sampling design in which the study area was gridded into 25 m cells, each classified into one of seven major vegetation strata as determined by digital land

cover data (Table 2.2). Additional strata were defined by three levels of housing density and three levels of structure proximity (Table 2.2). Upon visitation to a sampled cell by a field technician, the camera was only installed if the vegetation appeared to fit the respective *a-priori* defined strata level.

Placement of the camera unit within the 25 m site was chosen by randomly generating a point location and azimuth (1-360º). Cameras were mounted on a steel post driven into the ground at the point, or on the closest tree or permanent structure within 5 m of the generated point. FOV angle for this particular camera trap model was 40.5°. If the camera's FOV was severely limited by boulders or micro-terrain features, it was adjusted to a new randomly chosen azimuth. If no alternative azimuth was available because of complete 360º obstruction, then the camera was moved to an alternative random location within the 25 m cell. Cameras were placed without regard to the presence of any apparent game trails or wildlife sign. No baits or attractants were deployed. Small handheld pruning shears were used to remove some shrubbery/branches within the first 1-3 m inside the FOV, but carried out in a way to minimize alterations to the site, by only removing specific "stray" pieces that may trigger the camera if blown in the wind. Cameras were elevated 0.5 – 1 m from the ground. To help alleviate false triggering events, this height was occasionally allowed to be higher to accommodate snow accumulation and growth of low lying vegetation. Cameras were mounted so that the FOV's horizontal radius was parallel with the contour of the ground. Units were programmed with sensitivity set to "high", with each trigger corresponding to a burst of 5 pictures (1 picture/second) to aid in species identification. Each trigger was followed with a 30 second delay or "quiet period" where the camera was unable to be triggered. Camera units automatically recorded time and temperature in the digital metadata

for each photo. Each camera remained in its designated site from initial installation period (November 2011- February 2012) until removal (December 2012-January 2013).

FOV Detection Probability

The utilization measurement technique seeks the amount of time spent by an animal within the camera's field of view, where a detection event corresponds to the smallest unit of time set by the study. Events are recorded once an animal is detected by the camera's triggering system within the field of view. Multiple detections of the same animal may occur if the same animal resides within the plot for multiple 30 second triggering intervals. Detection events are suspected to decline as a function of increasing distance to the camera (Buckland et al. 2001), thus it is of interest to account for this decline in detection within the FOV (Rowcliffe et al. 2011). Assuming movements within the FOV are random with respect to the observer's position (the camera in this case), movement within is inconsequential, as it is the location of detection by the camera that is modeled. The initial location of detection is of concern for typical radial point-count distance sampling (i.e., animals moving in and out will only be detected near the outer limits of the plot); but is of less concern given the sector shaped plot typically used by camera traps as animals are allowed to enter the FOV in very close proximity to the observation platform (Rowcliffe et al. 2011).

The assumption of random plot placement is critical at two scales. In general cameras must be placed disregarding any prior knowledge of animal micro-habitat selection within a habitat or patch of interest. On a finer scale, placement of the camera's FOV must be done in a way so that animal movement paths within the FOV are random with respect to distance from the camera sensor. It is likely that micro-utilization of space within a single camera's FOV will show clustering (Figure 2.2), thus violating this assumption for any particular camera. However, a

sufficient sample of cameras allows detection probability to be modeled with observations from a pool of sites (Figure 2.2) in order to dilute aggregation effects (i.e., "pooling of robustness") (Buckland et al. 2001).

Preferably, cameras would have been allowed to trigger continuously or at 1 second intervals in order to minimize utilization measurement biases related to habitat specific movement rates (Chapter 1). However, the 30 second trigger delay was chosen to alleviate data processing and memory requirements. Only the initial picture from the sequence of five was retained for analysis of a detection to ensure that the picture record was dependent on the camera's infrared trigger. Distance and angular measures within the FOV were mapped for the initial picture using the methods described in Appendix 3. The number of individuals present for a particular event was determined by the minimum number of known animal individuals of a particular species visible in the photo.

Distance and angle measurements were collected on 31,456 photo records of small (rodent sized) to large (domestic equids) mammals and birds, spanning 33 mammalian (Appendix 3) and 33 avian species. Ideally, detection functions would be derived for each site and species separately, but some sites lacked a sufficient number of observations or exhibited a non-stationary spatial pattern within the FOV (Figure 2.2). Pooling the mammalian data for all sites, histograms of detection distances were inspected to assess whether data may adequately follow assumptions of distance sampling theory (i.e., a stationary process where detection probability is 1.0 at the surveyor's origin). Smaller sized species (<5 kg) appeared to occasionally pass close to the camera undetected as a result of camera mounting height, and thus were removed from further analysis. Species were classified into one of four groupings based on size and movement characteristics: Meso-slow (i.e., felids, procyonids), Meso-fast (i.e., canids),

Large (i.e., *Odoicoileus spp.* and large carnivores), and Xlarge (i.e., large ungulates) (Appendix 3). Depending on the grouping, histograms (1 m cut points) exhibited evidence of heaping at the furthest distance intervals (>10 m), which was expected given that distance measurement methods were less precise as distance increased. Therefore, distance sampling functions were created with custom distances bins (Appendix 3).

After pooling across sites, applying the species groupings, and setting appropriate binning distances, distance data behaved as expected; intensity of detection declined with increasing distance from the camera. A right truncation distance (w) was set so that the probability of detection for the furthest distance interval approximated no less than 0.1 once the key function was selected (Buckland et al. 2001). Right truncation standardized the plot sizes among camera locations but resulted in approximately10-26% of the observations being removed. If the plot area had been set based on the maximum distance observed for any animal, this truncation corresponds to retaining a plot area proportion of only 0.16, 0.20, 0.05, and 0.04 for the Meso-slow, Meso-fast, Large, and Xlarge groupings respectively (Appendix 3).Using program DISTANCE 6.0 (Thomas et al. 2010), hazard-rate and half-normal key functions, along with cosine and polynomial adjustment terms, were examined using chi-square goodness of fit tests and AIC model selection. A hazard-rate key function with no adjustment terms provided the best fit in all species groupings. Detection function $g(x)$ was modeled with a multi-covariate hazard-rate model (Marques and Buckland 2003).

Candidate model sets included site and observation level covariates thought to influence detection probability. Site level covariates only concerned visual obstruction measures. Vegetation strata of the cameras sampling strata were used as an indirect visual obstruction factor, after collapsing the “MIX” into the “DEC” strata (Table 2.2). Exploratory analysis

indicated these two strata yielded similar detection distance data. A direct visual obstruction measure (BANDMAX) was obtained as the maximum distance at which a technician could trigger the camera (Appendix 3).

The remaining were observation level covariates that may change from one detection event to another. The angular measure relative to the FOV center line (ANGLE) was used to index whether animals were detected closer to edges of the FOV. With this particular camera make, the triggering mechanism consists of an array of sensors arranged horizontally, and thus it is expected that animals near the left and right edges of the camera would have fewer opportunities to be triggered by multiple sensors, especially when a portion of the animal's body is outside the FOV. Ambient temperature (TEMP) was included because it could influence trigger probability given the use of a passive infrared sensor that detects differences in thermal energy between a target and the surroundings. Snow cover presence was indicated with a dummy factor (SNOWP) (Appendix 4). Other covariates included the calendar season (SEAS) and whether the infrared illuminator flash, which turns on automatically during night-time period, was used (NIGHT). Other covariates included the counts of individuals in each photo (INDIV) and species average weight (MASS) (Appendix 3). High co-linearity between some pairings of variables (BANDMAX with VEG and SEAS with TEMP or SNOWP) required inclusion into models separately. All additive combinations of variables were tested using Akaike information criterion (AIC) model selection techniques. From program DISTANCE, variance in overall detection probability never exceeded 2% (SE = 0.00965) for any species grouping.

The methods of Marques et al. (2007) were then employed for calculating a detection probability estimate conditional for covariates of each camera site *k* and each observation event *i*

($\hat{P}_{k,i}$). Assuming a selected truncation distance (w) and parameter values of the best fitting model of $g(x)$, $\hat{P}_{k,i}$ is derived by equation 3 described in Marques et al. (2007).

Habitat Utilization Model

Typically, distance sampling analyses produce a time-specific snapshot of the number of unique individual animals per unit area, correcting for the probability of detection (Buckland et al. 2001). For this study, I used a more asymptotic measure: the number of encounters over space and time rather than abundance of individuals. Space is the FOV area (a_k) represented by a sector with radius equal to the truncation distance (w) and central angle equal to the camera's fixed FOV angle (40.5°). Estimated encounter rate or usage by a single animal or group of animals per site k is:

$$\widehat{U}_k = \frac{1}{a_k}\sum_{i=1}^{n_k}\frac{1}{\hat{P}_{k,i}}$$

The temporal effort component of the rate enters as an offset term described in the statistical model below. If animals occur in groups, $\widehat{U}_k$ can be multiplied by the expected mean group size (S_k) for that site to give $\widehat{US}_k$ for the overall encounter rate in terms of animals per square meter per day. In the event that a site did not have any detections, $\widehat{U}_k$ existed simply as a zero value, as this method must have at least one triggering event to incorporate $\hat{P}_{k,i}$.

The site specific encounter rate ($\widehat{US}_k$) was input as a response variable in a GLM with the number of days functioning, η_k, as an offset term. For some species (i.e., domestic cat and raccoon), inspection of the response variable indicated a high proportion of sites with zero values (animal absence) (Table 2.3). The non-zero utilization response values ranged from 0.02 to 156 depending on species (Table 2.3). To allow response values to contain exact zero values and continuous non-integers, while accounting for potential over-dispersion, a compound-Poisson (Tweedie) error distribution was used within a GLM (R package 'statmod' or 'cplm'). This uses

an exponential dispersion model of the form $E(Y) = \mu = \eta e^{\mathbf{X}'\beta}$ with variance expressed as $Var(Y) = \phi\mu^p$. The ϕ is a dispersion parameter and p is an estimated power or "index" parameter (Dunn and Smyth 2005) fit by calling a profile likelihood function (R package 'cplm' or 'tweedie') (R Development Core Team 2013). An index value of 0, 1, 2, or 3 would indicate a normal, Poisson, gamma, and inverse Gaussian distribution respectively. In this case, the index is expected to take on a value between 1 and 2, which is a Poisson mixture of gamma distributions supporting all non-negative reals with a mass at zero (Bar-Lev and Stramer 1987, Smyth and Jørgensen 2002).

Covariate values of the design matrix $\mathbf{X}'$ were based on topography, vegetation structure, and measures of human housing development. For covariates derived at more than one spatial scale, all scales were tested when forming the best fitting global model. The number of covariate terms b allowed in each model was limited to $n/10$, where n is the number of camera sites with a non-zero count. Pairs of main effect terms with correlation coefficients > 0.6 were removed from consideration in the same model. A full list of the covariates, derivation methods, and scales examined, are described and mapped in Appendix 2 (housing development) and Appendix 4.

Models were ranked with AIC model selection using ΔAICc and AICc weight values (Burnham and Anderson 2002). To help protect against spurious inclusion of variables, coefficient estimates were examined of models with potential "pretender variables" (Anderson 2008, Arnold 2010). Models in the top set (ΔAICc < 7) were inspected by assessing changes in log likelihood with the addition of potential pretending variables, along with 95% bootstrap confidence intervals of coefficient estimates. Pretender variable coefficient estimates are near zero, have confidence intervals overlapping zero, and do not contribute to improving model fit; thus models with pretenders were removed. Any erroneous removal of these variables will have

little effect on prediction estimates as their standardized coefficient estimates were near zero. After recalculating AICc weight for the revised model set, if high model selection uncertainty was evident (top model held < 90% AICc weight), all models with ΔAICc < 7 were reported. A general sense of model fit was obtained by a Pearson correlation coefficient (ranging: -1 to 1) using the observed vs. predicted values. Model fit was graphically assessed using the quantile residuals, which can be approximated with a chi-square distribution (Dunn and Smyth 1996, Dunn 2009), to create residual versus predicted values, and q-q theoretical plots. Confidence intervals (0.95) were created for all models in the top set using a nonparametric bootstrap with 10,000 iterations. Plots of the predicted response are given with respect to the housing covariates (i.e., distance to structure and housing density) while holding all other variables at their observed mean or median values. Maps of the utilization predictions were created using the best model (if AICc weight > 0.9) or the model averaged predictions of the set of models with ΔAICc < 7. These maps were created based primarily on interpolation (rather than extrapolation), thus predictions were only made for covariate values falling within the domain sampled.

Spatial autocorrelation is a pervasive theme in species distribution and population distribution studies (Legendre 1993). To test for residual spatial autocorrelation, response data was scaled and transformed to integer values so that models can be fit under a simpler negative binomial GLM using the same covariate structure. Neighborhood contiguity calculations were made using a specified minimum distance to ensure that all sites had at least one neighbor. This informed the creation of a row-standardized spatial weights matrix. First permutation based (drawing from a negative binomial distribution) global and localized (using varying neighborhood lags) Moran's I statistics were calculated. A non-significant and low Moran's I statistic (< 0.1) was found in all models. Pearson's residuals from a null (intercept only) model

and the residuals from the model with covariates, were used as input for separate Moran's I tests. Directional and omni-directional robust (Cressie's) semi-variograms were inspected for a variety of distances again using the residuals as input. These Moran's I tests and semi-variograms revealed no additional spatial structure once the covariate structure was considered. Fortunately, much of the spatial autocorrelation was accounted for with the landscape covariates chosen in this study. However, it is noted that the covariate UTM_Y improved the fit of the mule deer usage model for reasons unexplained by any actual landscape measure. Lack of additional residual spatial autocorrelation may have resulted from: the stratified random sampling scheme conducted on highly heterogeneous sampling strata, the widely dispersed sampling sites (average nearest neighbor: 2277 m), and/or the nature of animal utilization at the small grain size measured.

RESULTS

The dataset included a total of 41,740 functioning camera trap nights of effort. Given the site specific installation and employment dates, the mean duration a camera could function was 334 nights. However, errors found during maintenance checks and removal (i.e., full memory card, camera malfunction, or dead batteries) resulted in a mean 318 nights of effort, η_k. After applying the species groupings, 25,237 observations remained with 1,534 Meso-slow, 2,547 Meso-fast, 17,380 Large, and 3,776 XLarge observations.

FOV Detection Probability

Model selection results of the detection probability models and respective coefficient estimates are shown in Table 2.4. AIC weights for the candidate set of models indicated that a single best parsimonious model could be chosen for the Meso-slow, Meso-fast, and Large groupings (weights $\geq$ 96%). For the Xlarge grouping, the top model carried 79% of the weight,

while the second best model (nested within the top model) carried 15% of the weight. The top models for each grouping always included ANGLE and one of the visual obstruction covariates, BANDMAX or VEG. The covariates NIGHT, SNOW, or TEMP did not appear in any of the top models. SEAS was included in the best models for all the groupings. INDIV was included in the Large and XLarge groupings, but was not tested in the Meso-slow and Meso-fast groupings, as most observations in these groupings were photos of only one individual. The MASS covariate was important in the Meso-fast and Meso-slow groupings. Exemplary detection curves for the Large grouping are shown in Figure 2.3.

Utilization Model

Model selection results of the habitat utilization models (eq. 5) are shown in Table 2.5 for each species. The most parsimonious model for any species held > 0.45 AICc weight. A single most parsimonious model (AICc weight > 0.9) was found for raccoon while two to five models were found for mule deer, coyote, red fox, domestic cat, and elk with a ΔAICc < 7. Much of the model uncertainty was caused by the inclusion of a single additional covariate (e.g., models nested within one another). Model diagnostics using the quantile-theoretical plots and residual vs. fitted plots indicated that quantile residuals were approximately normal, thus model fit was assumed to be sufficient (Appendix 5). Pearson correlation coefficients of the fitted and observed values were $\geq$ 0.5 for any particular animal grouping (Table 2.5).

The top models for each species always contained a human development covariate. However, the type of response differed from species to species (Figure 2.4). Mule deer appeared to have a quadratic concave relationship with housing density (HDM250); utilization peaked at high exurban or low suburban housing density levels (~2.5 houses/ha) while tapering off to the lowest predicted levels as housing density increased (Figure 2.4). Raccoon utilization was

positively associated with HDM250, with a dramatic increase observed once housing density reached mid-suburban (5 houses/ha) levels. Elk utilization showed some response to the kernel density housing intensity measure at a large spatial scale (bandwidth = 1500 m: KD1500). However, the interaction with ELEV indicated that a positive response was only observed at higher elevations (Figure 2.4). ELEV and KD1500 were also somewhat correlated (r = 0.51); a correlation expected to increase as elevation increased. Coyote utilization showed a clear decrease with housing density (HDM_pnt) (Figure 2.4). Domestic cat and red fox utilization decreased as distance to nearest structure (STRUC) increased, but showed a clear threshold once distances reached approximately 200 and 1000 m respectively (Figure 2.4). For red fox, an interaction with distance to nearest forest edge (FOREDGE) and STRUC indicated that a stronger response to STRUC was observed as FOREDGE increases (Figure 2.4).

Topographic covariates were important explanatory variables in the candidate sets of all species but raccoon (Table 2.5). Elevation (ELEV or ELEV_12k) appeared in top models of all other species except domestic cat. Topographic position index (TPI_150 or TPI_50) was in top models of mule deer and coyote utilization. Deer utilized positions relatively higher on hillsides rather than in drainages. Coyote's quadratic relationship with TPI indicated highest usage was at mid-slope or non-sloping positions. SLOPE was important in models for elk, coyote, and secondary top models of domestic cat, where utilization decreased as slope increased. However, in domestic cat, a modest amount of co-correlation (r = 0.44) was observed between SLOPE and human housing covariates such as STRUC. Solar aspect, ASP_NW and ASP_E, was important for mule deer and red fox respectively.

Vegetation structure covariates were important for predicting utilization of mule deer, elk, red fox (FOREDGE*STRUC interaction discussed above), and coyote (Table 2.5).

However, mule deer utilization models were only marginally better with the SHRUB covariate (Table 2.5). Elk utilization was lower where forest was the predominant vegetation type (FOREST3). The interaction between canopy cover and distance to forest edge observed in the coyote models demonstrated higher utilization further from forest edge in areas more devoid of trees (i.e., open grass or shrubs) (Table 2.5)

A full listing of coefficient estimates and bootstrap 95% confidence intervals for the top model set of each species are given in Appendix 6. Predicted utilization cast to the entire study area for each species is given in Appendix 7.

DISCUSSION

The detection probability function analysis demonstrated here supports the findings of the pioneering camera trap distance sampling study (Rowcliffe et al. 2011) and demonstrates some additional site and observation level variables influencing detection probability. This case study verified that encounter rates derived from camera trap surveys can be a useful measure of habitat utilization of a landscape unit by the population, which is a property of the number of animal individuals and the utilization patterns of those individuals (Chapter 1). When the metric is modelled with the appropriate landscape covariates, model predictions across a spatial domain can be viewed as the joint utilization distribution of all members in the population, in units of animal-time expended at any location. Model selection indicated that the utilization of animals was influenced by anthropogenic variables, but the response differed by species. Utilization by mule deer, raccoon, elk, and red fox was generally associated with increased measures of housing development, while coyote utilization was generally negative.

As found in Rowcliffe et al. (2011), seasonality and species differences influence probability of detection within the FOV as a function of camera to animal distance. Body mass

was especially important when considering the smaller groupings (Meso-fast and Meso-slow). Additionally, I demonstrated that measures of visual obstruction are associated with detection distance in all species groupings. Although cumbersome, the six vegetation factors appeared to contribute to a more parsimonious model for the Meso-fast and XLarge groupings. However, the actual interpretation of the coefficient estimates for these habitat levels was less intuitive. Ranking the six levels from smallest to largest influence on detection probability resulted in grasslands (assumed to have lowest visually obstructed FOV) to have lower detectability than some woodland types. The more intuitive and simple continuous BANDMAX covariate contributed to a more parsimonious model for the Meso-slow and Large grouping. As expected, the number of individual animals within the FOV corresponded to an increased detection probability.

In contrast to findings in a follow-up analysis of data from Rowcliffe et al. (2011) by Rowcliffe et al. (2014), my analysis indicated detectability was not affected by whether photos were collected at night or during the day. Using over 25,000 detections and a gradient of temperatures ranging from -17 to 37 °C, I found no direct influence of ambient temperature on detectability; despite being a concern for certain camera trap models (Swann et al. 2010). The presence of accumulated snow did not have any discernable effect on detection either. Interestingly, calendar season was an important factor in all models. Besides the fact that snow presence and temperature are variables correlated with season, the exact mechanism for season's influence on detection probability is unknown.

My analysis indicated that detection distance is reduced as detection angle increases (observations located more toward the left or right edges of the FOV). The basis for this relationship is unclear, but may stem from the particular sensor alignment of the camera. Using

angle as a covariate in the distance detection model was a slightly different approach than Rowcliffe et al. (2011), who modelled detection distances and detection angles separately in different models. However, their objectives were to obtain estimated dimensions of the camera's FOV, which differed from my goal to estimate detection probability given a truncation distance. Unlike the distance parameter, the angle parameter's maximum is already set by the alignment of the sensor. Besides giving a more robust fit in the tail of the detection function (Buckland et al. 2001), a maximum truncation distance allows plot sizes to be standardized, which simplifies interpretation of the response when making predictions on the landscape.

Population Level Habitat Utilization Patterns in Relation to Housing

For the six species examined, population landscape utilization appears to be influenced by human housing developments. Except for deer and elk, the species-specific responses generally fit that of previous studies (Table 2.1). For a species like coyote, housing developments appear to be utilized relatively less. For mule deer, a quadratic effect indicated utilization peaked at high exurban – low suburban levels (~2.5 houses/ha). For raccoon, utilization increased precipitously with housing densities > 2.5 houses/ha. Red fox and domestic cat utilization generally increased as distance to structure decreased. A threshold of ~ 250 m to nearest structure was observed with domestic cats; no animals were observed further than this. The association between structures and domestic cats was expected, as many of the individuals observed in the photos had signs of being non-feral (i.e., collars present). For elk, utilization with respect to housing development was less clear, but it appeared that housing development was utilized more when in relatively higher elevations (>2200 m). The high temporal and spatial heterogeneity of elk herding behavior and the historic utilization of certain areas (as indicated by the presence of the ELK_conc variable) makes elk utilization hard to predict. Adding a seasonal

effect would likely improve predictions for species like deer and elk, as a proportion of their populations are migratory (Kufeld et al. 1989, Huwer 2007). For any species, the exact shape of the response was difficult to predict in the parameter space concerning suburban housing densities. Including additional sites in the suburban housing density range (1.6 – 10 units/ha) would likely have resulted in improved predictions. However, including more samples in the suburban class was hard to justify during study design steps as suburban densities corresponded to only 3% of the study region's land area (Appendix 2).

Natural (topographic and vegetation) variables, such as elevation, were important given the strong east-west elevation gradient present in the study area. Seasonally, the higher elevations on the western edge contain steep terrain and deep snow pack (present for half of the year), a formidable movement barrier to almost all species examined. Topography underlies the utilization patterns for many of the species, even if it was not explicitly found as an important predictor variable. For instance, the strong affinity of raccoons to the presence and density of human dwellings is likely related to the food sources humans provide (Prange et al. 2003). However, the presence of human dwellings on the landscape has some relationship to topography as parcelization of the land has strong roots in historic land accessibility for resource extraction and ranching (Appendix 2). Additionally, the placement of modern housing sites in this region appears related to the proximity of natural amenities (Riebsame et al. 1996), land features also more or less favored by wild animals. Topography also influences the vegetation types present. As elevation increases, low-elevation conifer forests dominated by ponderosa pine (*Pinus ponderosa*) and douglas fir (*Psuedotsuga menziesii*) transition to lodgepole pine (*Pinus contorta*) and aspen (*Populus tremuloides*) (Peet 1981). Grasslands appear more prevalent where slopes are more gradual. Vegetation structure did appear important for all but raccoon and domestic cat.

Employing the three strata in the sampling design and the correlation coefficient tests helped alleviate co-dependence between predictor variables. However, it would be hard to make conclusive inferences on the utilization patterns of independent variables not used as a sampling stratum. The six vegetation strata (Table 2.7) merely served as a way to spread the sampled locations out so that a wide variety of localities could be surveyed. This sampling strategy was beneficial for making prediction maps (Appendix 7) over a heterogeneous landscape (Appendix 4), but less beneficial for drawing inferences on relationship types and effect sizes.

Suggestions for Future Studies

Using the hazard rate distance function, the assumption that animals are detected perfectly at close distances may have been violated with the smaller animals (Meso-fast and Meso-slow classes) that could possibly pass within a close range underneath the FOV. One possible solution for this would be to employ a mixture model to deal with imperfect detection at close distances (Rowcliffe et al. 2011). Another solution would be to utilize multiple camera sensors or even platforms with a greater vertical FOV range to adequately cover the region closest to the camera.

The heaping of detection distance measures occurred despite field measures being marked at 1.5 - 3 m intervals (Appendix 3). Distances between these could be estimated in the photo to some degree, but it became more difficult as distance increased. Fortunately, inaccuracies in the distance measures collected in the tails of the distance function have less of an effect on the outcome. However, distances near the shoulder and inflection points of the detection curves do have a greater proportional effect, and it is in these locations that additional efforts should be made to obtain the most accurate measurements. Future technologies will likely allow measurements to be more automated and precise, and perhaps even be integrated with the

camera platform to give three-dimensional maps of the cameras field of view (Azzari et al. 2013).

The model I employed to correct detection probability (eq. 3) was only valid for sites producing at least one detection event. It is logical that some utilization could have occurred in sites with zero observations, as a few animals may have passed through undetected at the furthest distance intervals. However, having no detections when heavy usage was indeed happening would be highly unlikely; the truncation distances were selected so that detection probability was at least 0.10 for the furthest distance interval.

Encounter rate data was addressed at a fine temporal scale (30-second delay). However, this interval may have been too long. As demonstrated in Chapter 1, it is important to realize that photographic rate is a measure of the amount of time spent by animals within the FOV. Using the 30-second delay period, utilization measures can be biased low in habitats where movements are slower (Chapter 1). Habitats where animal movements were slowest may have yielded utilization measures that were biased low. Future studies measuring utilization should take advantage of the ability of modern camera traps to record data continuously (i.e., 1 second delay or less); the temporal effort of human based observations is unmatched to that put forth by remote cameras.

Although not required, a larger spatial effort would likely improve results. Additional sites would have allowed a larger array of independent variables to be examined, thus potentially decreasing spatial prediction biases. The number of sites sampled ultimately depends on the degree of heterogeneity in utilization exhibited across the study area. The 41,740 trap-days of effort employed here is currently one of the highest reported among camera studies. Implementing additional sites, while not decreasing the study period length or total trap-days,

would require additional camera platforms. Camera cost, and the resources to maintain sites, can be limiting factors. The ability to maintain 131 camera sites continuously for nearly one year, with minimal human effort, was attributable to recent technological advances of the camera platforms themselves. The long battery life and large memory capacity only required a mean 2.5 (range: 1-7) visits per site in the approximate year long period between installation and removal.

It is assumed that cameras are able to survey the spatial domain used by animals; animals cannot hide from the camera. This is an assumption also shared with recent activity measurement techniques (Rowcliffe et al. 2014). For instance, arboreal or fossorial animals may only spend a portion of their time on the two-dimensional landscape where camera traps are commonly deployed. An example for this study would be the utilization patterns exhibited by domestic cats, as a portion of their time is spent in a location impenetrable by a camera's FOV (inside houses). Photographic detections of the large ungulates (mule deer and elk) revealed a large range of behaviors (i.e., resting, foraging, and travelling). Thus, large non-illusive animals are most likely to fulfill this assumption by being unable to hide from cameras.

I question the mismatch between the scale at which covariates were measured (i.e., 30 m grain size) and the fine scale at which utilization was derived (FOV area ranging from 18 – 75 m^2). However, the fine scale of the FOV is not the issue. Utilization heterogeneity occurs at scales much smaller than what most conventional resource selection/utilization studies on animals have measured. In the extreme case, fine scale utilization heterogeneity likely occurs at less than 1 m spatial scale. This is evident in the fact that animals utilize game trails (< 1 m wide). Technological advances in remote sensing are allowing covariates to be derived from finer spatial resolutions, as done in a GPS telemetry study that incorporated 1.12 m resolution

LiDAR to uncover resource selection behaviors of a large carnivore in relation to ground level woody vegetation (Loarie et al. 2013).

Conclusion

Using camera traps to derive an encounter rate response variable is not a new idea. However, using camera traps to derive an encounter rate response for modeling population-level utilization across the landscape is novel. Whether this metric is useful to researchers depends on the objectives. The utilization measure should not be relied on if both fine scale abundance and individual level resource utilization/selection measures are obtainable. Future practitioners are reminded that two processes comprising population level utilization (resource utilization at the individual level and relative abundance) cannot be inferred separately with this approach. Researchers conducting broad studies on a multitude of taxa to understand ecological relationships will likely find it of most use.

TABLES AND FIGURES

Table 2.1. Review of scientific literature on the response (positive, negative, quadratic) found in relation to human housing development for six mammalian species. Studies included those examining housing or structure density, parcel size, or proximity to housing developments, using a variety of survey techniques (camera traps, track plates, mark-recapture, and telemetry).

Study	Mule Deer	Raccoon	Elk	Red Fox	Domestic Cat	Coyote
Smith et al. 1989	Neg[E]					
Vogel 1989	Neg[E]					
Riley et al. 1998		Pos[λ]				
Gloor et al. 2001				Pos[ψ]		
Grinder and Krausman 2001						Neg[Ŧ]
Crooks 2002		Pos[E]			Pos[E]	
Odell and Knight 2002				Neg[E]	Pos[E]	Neg[E]
Gosselink et al. 2003				Pos[Ŧ]		Neg[Ŧ]
Prange et al. 2003		Pos[λ]				
Atwood et al. 2004						Neg[Ŧ]
Wait and McNally 2004			Neg[Ŧ]			
Hebblewhite et al. 2005			Pos[E]			
Kays and Dewan 2006					Pos[ψ]	
Randa and Yunger 2006		Pos[ψ]				Neg[ψ]
Gehrt et al. 2009						Neg[Ŧ]
Ordenana et al. 2010		Pos[ψ]				Neg/Pos[ψ]
Horn et al. 2011					Pos[Ŧ]	
Jantz 2011						Neg[Ŧ]
Cleveland et al. 2012			Neg/Quad[Ŧ]			
Cove et al. 2012				Pos[ψ]		
Goad et al. 2014	Pos[E]			Pos[ψ]		Neg[ψ]

[E]relative encounter rate study (camera trapping, pellet survey, track plate), [λ]animal density study, [ψ]occupancy study, [Ŧ]telemetry resource selection/movement/habitat utilization study

Table 2.2. Description of camera site sampling strata. Factorial combinations were created between the levels of each strata, which led to 3-4 sites being sampled per each unique combination. Not all combinations were realized in nature (i.e., level "House 3" never occured within "Suburban/Urban" levels).

Strata	Level	Description	# of Sites
Major vegetation*	DEC	Deciduous trees present	19
	GRS	Site dominated by grassland	20
	HEC	Dominated by coniferous forest >2400 m elevation	20
	LEC	Dominated by coniferous forest <2400 m elevation	27
	SHR	Dominated by scrub/shrub	20
	MIX	Located in a mixture of two of the above vegetation	8
	URB	Located within suburban densities but undefined by a vegetation level	18
Housing density†	Rural	Housing density >16.18 ha/unit (<0.0618 units/ha)	67
	Exurban	Housing density 0.68-16.18 ha/unit (0.618 - 1.4706 units/ha)	47
	Suburban/Urban	Housing density <0.68 ha/unit (>1.4706 units/ha)	18
Proximity to dwelling‡	House 1	Site located < 200 m of house	61
	House 2	Site located within 200-700 m of house	50
	House 3	Site located >700 m from house	21

* Levels collapsed from BASINWIDE Colorado Vegetation Classification land cover (CDOW 2003).

† Determined by SERGoM of year 2000 housing density (Theobald 2005) and HDM (Appendix 2)

‡ Determined by digitization of all structures in 2008 USGS 0.6 m ortho-photo (Appendix 2).

Table 2.3. Summary of the observed encounter rate measure, $\widehat{US}_k$, as derived by eq. 4, for the six focus species.

Species	Proportion of Sites with zeros	Encounter Rate Response*		
		Minimum Non-zero	Max	Mean
Mule Deer	0.03	0.086	137.41	20.28
Raccoon	0.82	0.285	156.12	1.68
Elk	0.41	0.020	36.21	1.32
Red Fox	0.39	0.039	13.90	1.02
Domestic Cat	0.87	0.301	36.04	0.80
Coyote	0.31	0.073	15.43	0.94

*Response values are in units of: 30 second time intervals per m^2

Table 2.4. Summary of the top candidate model selected via AIC model selection for Meso-slow, Meso-fast, Large groupings, and top models for XLarge grouping. Corresponding coefficient estimates are in parenthesis, along with an overall estimate of detection probability (*p*) and estimated detection radius (EDR) in meters. Vegetation factor coefficients (DEC, GRS, HEC, LEC, and SHR) are relative to the URB background level.

Grouping	$\beta_{0(scale)}$	Shape Par. (*b*)	Scale Function	p	EDR	Parameters	Delta AIC	AIC weight
Meso-fast	7.896	3.612	β_0* Exp(DEC (-0.496) + GRS (-0.464) + HEC (-0.557) + LEC (-0.416) + SHR (-0.768) + FALL (-0.076) + SPRING (0.039) + SUMMER (-0.114) + MASS (0.025)) + ANGLE (-0.070))	0.39	6.83	12	-	0.97
Large	2.267	2.325	β_0* Exp(BANDMAX (0.008) + FALL (0.145) + SPRING (0.263) + SUMMER (0.247) + INDIV (0.117) + ANGLE (-0.149))	0.19	5.97	8	-	1.00
Xlarge	8.953	2.619	β_0* Exp(DEC (-0.099) + GRS (-0.087) + HEC (-0.279) + LEC (0.220) + SHR (0.129) + FALL (-0.072) + SPRING (-0.277) + SUMMER (-0.143) +ANGLE (-0.144) + INDIV (0.031))	0.35	7.94	12	0.0	0.79
	9.964	2.542	β_0* Exp(DEC (-0.127) + GRS (-0.1384) + HEC (-0.341) + LEC (0.237) + SHR (0.091) + FALL (-0.085) + SPRING (-0.292) + SUMMER (-0.187) + ANGLE (-0.157))	0.34	7.83	11	3.3	0.15
Meso-slow	2.839	9.066	β_0 * Exp(BANDMAX (0.018) + FALL (-0.026) + SPRING (-0.092) + SUMMER (-0.021) + MASS (-0.023) + ANGLE (-0.028))	0.38	4.11	8	-	0.99

Table 2.5. AICc model selection tables for each species, where k = number of parameters, logLik = deviance, ΔAICc, *w* = relative AICc model weight, and *r* = Pearsons correlation coefficient (observed vs. fitted values).

Species	Ranking	Covariate Structure	k	logLik	AICc	ΔAICc	*w*	*r*
Mule Deer	1	ASP_NW + ELEV_12k + HDM250 + HDM250^2 + TPI_150 + UTM_Y + SHRUB	8	-480.9	978.9	0.00	0.48	0.56
	2	ASP_NW + ELEV_12k + HDM250 + HDM250^2 + TPI_150 + UTM_Y	7	-482.3	979.5	0.53	0.37	0.54
	3	ASP_NW + ELEV_12k + HDM250 + HDM250^2 + TPI_150 + SHRUB	7	-484.0	982.9	3.91	0.07	0.53
	4	ASP_NW + ELEV_12k + HDM250 + HDM250^2 + TPI_150	6	-485.8	984.4	5.41	0.03	0.50
	5	ASP_NW + ELEV_12k + HDM250 + HDM250^2 + UTM_Y	6	-486.5	985.7	6.76	0.02	0.49
Raccoon	1	HDM250 + STRUC	3	-83.3	172.7	0.00	0.98	0.99
Elk	1	ELEV + FOREST3 + SLOPE + KD1500 + ELEV*KD1500 + ELK_conc	7	-181.9	378.8	0.00	0.85	0.63
	2	ELEV + FOREST3 + SLOPE + KD1500 + ELEV*KD1500	6	-185.0	382.7	3.93	0.12	0.53
RedFox	1	ELVE_12k + ELVE_12k^2 + FOREDGE + HDM250 + HDM250^2 + STRUC + FOREDGE*STRUC + ASP_E	9	-160.7	340.9	0.00	0.81	0.55
	2	ELVE_12k + ELVE_12k^2 + FOREDGE + HDM250 + HDM250^2 + STRUC + FOREDGE*STRUC	8	-163.5	344.1	3.21	0.16	0.61
Domestic Cat	1	STRUC + HDM250	3	-69.6	145.3	0.00	0.45	0.61
	2	STRUC + SLOPE	3	-69.9	146.0	0.67	0.32	0.73
	3	STRUC_yard + SLOPE	3	-70.5	147.2	1.86	0.18	0.71
Coyote	1	SLOPE + TPI_50 + TPI_50^2 + FOREDGE + CC_avg90 + CC_avg90*FOREDGE + HDM_pnt + ELEV	9	-151.0	321.5	0.00	0.66	0.49
	2	SLOPE + TPI_50 + TPI_50^2 + FOREDGE + CC_avg90 + CC_avg90*FOREDGE + HDM_pnt	8	-152.8	322.9	1.39	0.33	0.50

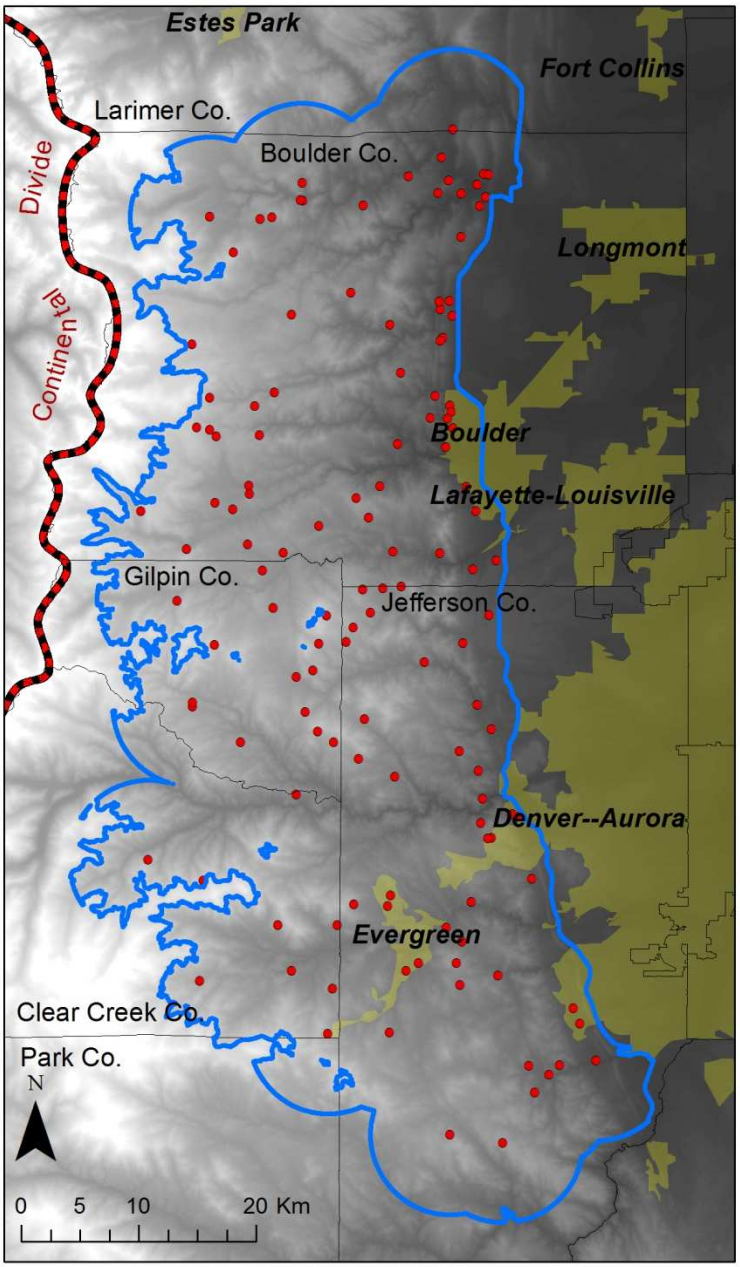

Figure 2.1. The 131 camera sites (red points) overlaid on the study area (blue polygon). County boundaries, 2010 Census Bureau Urban Areas (yellow shading) and digital elevation model (gray shading) (3,090 – 1,610 m west to east) are shown.

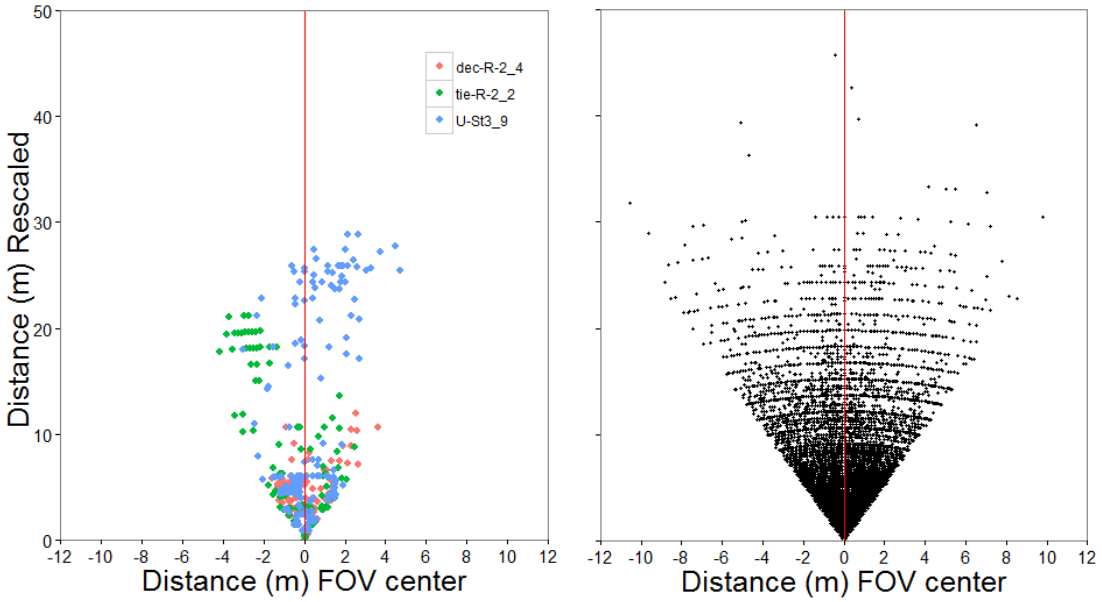

Figure 2.2. Observed locations of animals at detection mapped onto the camera FOV to demonstrate spatial clustering of observations when three sites (names coded by color: "dec-R-2_4", "tie-R-2_2", and "U-St3-9") are considered individually (left pane). Pooled observed locations at initial detection from all camera sites follows typical distance sampling stationarity assumptions (right pane). Y-axis and x-axis distance values only reflect quantities of the aerially mapped FOV, rather than the measures (radial distance and sector angle) collected in photos.

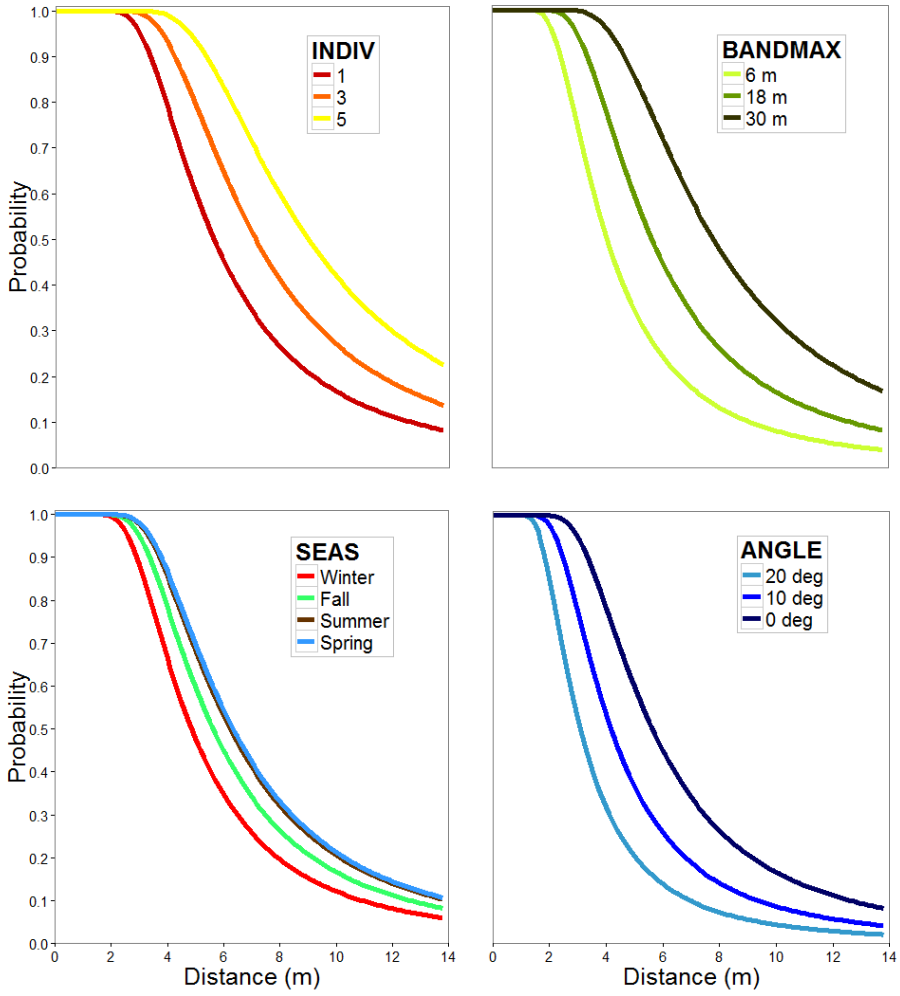

Figure 2.3. Detection probability curves for select values or levels of covariates (INDIV: number of individuals in a group within FOV, BANDMAX: maximum distance camera can be triggered, SEAS: four calendar seasons, ANGLE = angular difference from FOV center line) from the best fitting candidate model for the Large grouping.

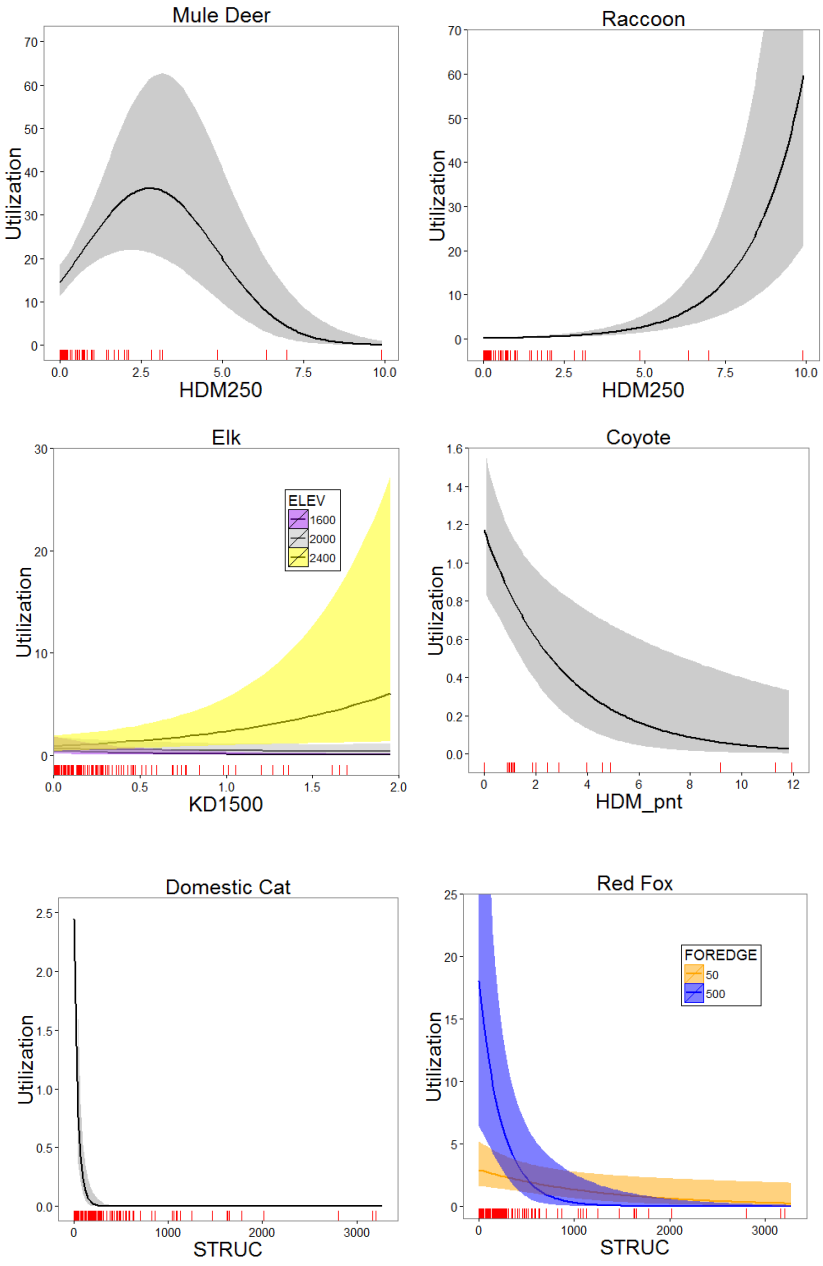

Figure 2.4. Modeled utilization for the six species to human housing covariates (HDM_pnt: Housing density at 1 ha scale, HDM_250: Housing density at 1 ha scale averaged over a 250 m radius, KD1500: kernel density index of housing density with 1500 m bandwidth, STRUC: Euclidean distance to nearest structure in meters). Rug plots (red ticks) indicate camera trap sampling intensity of the covariates domain.

LITERATURE CITED

Anderson, D. R. 2008. Model Based Inferences in the Life Sciences: A Primer on Evidence. Springer Science & Business Media, New York, NY, USA.

Arnold, T. W. 2010. Uninformative parameters and model selection using Akaike's Information Criterion. Journal of Wildlife Management 74:1175-1178.

Atwood, T. C., H. P. Weeks, Jr., and T. M. Gehring. 2004. Spatial ecology of coyotes along a suburban-to-rural gradient. Journal of Wildlife Management 68:1000-1009.

Azzari, G., M. L. Goulden, and R. B. Rusu. 2013. Rapid characterization of vegetation structure with a Microsoft Kinect sensor. Sensors 13:2384-2398.

Bar-Lev, S. K., and O. Stramer. 1987. Characterizations of natural exponential famlies with power variance functions by zero regression properties. Probability Theory and Related Fields 76:509-522.

Bowkett, A. E., F. Rovero, and A. R. Marshall. 2007. The use of camera-trap data to model habitat use by antelope species in the Udzungwa Mountain forests, Tanzania. African Journal of Ecology 46:479-487.

Buckland, S. T., D. R. Anderson, K. P. Burnham, J. L. Laake, D. L. Borchers, and L. Thomas. 2001. Introduction to Distance Sampling. Oxford University Press, New York, USA.

Burnham, K. P., and D. R. Anderson. 2002. Model selection and model inference: a practical information-theoretic approach. 2nd edition edition. Springer-Verlag, New York, NY, USA.

Burnham, K. P., D. R. Anderson, and J. L. Laake. 1980. Estimation of density from line transect sampling of biological populations. Wildlife Monographs 72:1-202.

Cagnacci, F., L. Boitani, R. A. Powell, and M. S. Boyce. 2010. Challenges and opportunities of using GPS-based location data in animal ecology. Philosophical Transactions of the Royal Society London B: Biological Sciences 365:2155.

Cleveland, S. M., M. Hebblewhite, M. Thompson, and R. Henderson. 2012. Linking elk movement and resource selection to hunting pressure in a heterogeneous landscape. Wildlife Society Bulletin 36:658-668.

Cove, M. V., B. M. Jones, A. J. Bossert, D. R. Clever, R. K. Dunwoody, B. C. White, and V. L. Jackson. 2012. Use of camera traps to examine the mesopredator release hypothesis in a fragmented midwestern landscape. The American Midland Naturalist 168:456-465.

Crooks, K. R. 2002. Relative sensitivities of mammalian carnivores to habitat fragmentation. Conservation Biology 16:488-502.

Cutler, T. L., and D. E. Swann. 1999. Using remote photography in wildlife ecology: a review. Wildlife Society Bulletin 27:571-581.

Dunn, P. K. 2009. Improving comparisons between models for CPUE. Fisheries Research 97:148-149.

Dunn, P. K., and G. K. Smyth. 1996. Randomized quantile residuals. Journal of Computational and Graphical Statistics 5:236-244.

_____. 2005. Series evaluation of Tweedie exponential dispersion model densities. Statistics and Computing 15:267-280.

Gurarie, E., and O. Ovaskainen. 2012. Towards a general formalization of encounter rates in ecology. Theoretical Ecology 6:189-202.

Gehrt, S. D., C. Anchor, and L. A. White. 2009. Home range and landscape use of coyotes in a metropolitan landscape: conflict or coexistence? Journal of Mammalogy 90:1045-1057.

Gessner, J., R. Buchwald, and G. Wittemyer. 2013. Assessing species occurrence and species-specific use patterns of bias in Central Africa with camera traps. African Journal of Ecology 52:59-68.

George, S. L., and K. R. Crooks. 2006. Recreation and large mammal activity in an urban nature reserve. Biological Conservation 133:107-117.

Gloor, S., F. Bontadina, D. Hegglin, P. dePlazes, and U. Breitenmoser. 2001. The rise of urban fox populations in Switzerland. Mammalian Biology 66:155-164.

Goad, E. H., L. Pejchar, S. E. Reed, and R. L. Knight. 2014. Habitat use by mammals varies along an exurban development gradient in northern Colorado. Biological Conservation 176:172-182.

Gosselink, T. E., T. R. Van Deelen, R. E. Warner, and M. G. Joselyn. 2003. Temporal habitat partitioning and spatial use of coyotes and red foxes in east-central Illinois. Journal of Wildlife Management 67:90-103.

Grinder, M. I., and P. R. Krausman. 2001. Home range, habitat use, and nocturnal activity of coyotes in an urban environment. Journal of Wildlife Management 65:887-898.

Gurarie, E., and O. Ovaskainen. 2012. Towards a general formalization of encounter rates in ecology. Theoretical Ecology 6:189-202.

Hamel, S., S. T. Killengreen, J.-A. Henden, N. E. Eide, L. Roed-Eriksen, R. A. Ims, N. G. Yoccoz, and R. B. O'Hara. 2013. Towards good practice guidance in using camera-traps in ecology: influence of sampling design on validity of ecological inferences. Methods in Ecology and Evolution 4:105-113.

Hebblewhite, M., C. A. White, C. G. Nietvelt, J. A. McKenzie, T. E. Hurd, J. M. Fryxell, S. E. Bayley, and P. C. Paquet. 2005. Human activity mediates a trophic cascade caused by wolves. Ecology 86:2135-2144.

Horn, J. A., N. Mateus-Pinilla, R. E. Warner, and E. J. Heske. 2011. Home range, habitat use, and activity patterns of free-ranging domestic cats. Journal of Wildlife Management 75:1177-1185.

Huwer, S. 2007. Elk Management Plan: Data Analysis Unit E-9 Game Management Unit 20: Ssaint Vrain Herd. State of Colorado, Denver, CO, USA.

Jantz, H. E. 2011. Home range, activity patterns, and habitat selection of the coyote (*Canis latrans*) along an urban-rural gradient. M.S., Auburn University, Auburn, AL, USA.

Karanth, K. U. 1995. Estimating tiger (*Panthera tigris*) populations from camera trap data using capture-recapture models. Biological Conservation 71:333-338.

Kays, R. W., and A. A. DeWan. 2006. Ecological impact of inside/outside house cats around a suburban nature preserve. Animal Conservation 7:273-283.

Kelly, M. J., and E. L. Holub. 2008. Camera trapping of carnivores: trap success among camera types and across species, and habitat selection by species, on Salt Pond Mountain, Giles County, Virginia. Northeastern Naturalist 15:249-262.

Krebs, C. J. 1994. Ecology: The Experimental Analysis of Distribution and Abundance (4th edition). HarperCollins College Publishers, Menlo Park, California, USA.

Kufeld, R. C., D. C. Bowden, and D. L. Schrupp. 1989. Distribution and movements of female mule deer in the Rocky Mountain Foothills. The Journal of Wildlife Management 53:871-877.

Legendre, P. 1993. Spatial autocorrelation: trouble or new paradigm? Ecology 74:1659-1673.

Loarie, S. R., C. J. Tambling, and G. P. Asner. 2013. Lion hunting behaviour and vegetation structure in an African savanna. Animal Behaviour 85:899-906.

Marques, F. F. C., and S. T. Buckland. 2003. Incorporating covariates into standard line transect analysis. Biometrics 59:924-935.

Marques, T. A., L. Thomas, S. G. Fancy, and S. T. Buckland. 2007. Improving estimates of bird density using multiple-covariate distance sampling. The Auk 124:1229-1243.

O'Brien, T. G., M. F. Kinnaird, and H. T. Wibisono. 2003. Crouching tigers, hidden prey: Sumatran tiger and prey populations in a tropical forest landscape. Animal Conservation 6:131-139.

Odell, E. A., and R. L. Knight. 2002. Songbird and medium-sized mammal communities associated with exurban development in Pitkin County, Colorado. Conservation Biology 15:1143-1150.

Ordeñana, M. A., K. R. Crooks, E. E. Boydston, R. N. Fisher, L. M. Lyren, S. Siudyla, C. D. Haas, S. Harris, S. A. Hathaway, G. M. Turschak, A. K. Miles, and D. H. Van Vuren. 2010. Effects of urbanization on carnivore species distribution and richness. Journal of Mammalogy 91:1322-1331.

Peet, R. K. 1981. Forest vegetation of the Colorado Front Range.Vegetatio 45:3-75

Prange, S., S. D. Gehrt, and E. P. Wiggers. 2003. Demographic factors contributing to high raccoon densities in urban landscapes. Journal of Wildlife Management 67:324-333.

R Development Core Team. 2013. Vienna, Austria.

Randa, L. A., and J. A. Yunger. 2006. Carnivore occurrence along an urban-rural gradient: a landscape-level analysis. Journal of Mammalogy 87:1154-1164.

Riebsame, W. E., H. Gosnell, and D. M. Theobald. 1996. Land use and landscape change in the Colorado Mountains I: Theory, scale, and pattern. Mountain Research and Development 16:395-405.

Riley, S. P. D., J. Hadidian, and D. A. Manski. 1998. Population density, survival, and rabies in raccoons in an urban national park. Canadian Journal of Zoology 76:1153-1164.

Rowcliffe, J. M., C. Carbone, P. A. Jansen, R. Kays, and B. Kranstauber. 2011. Quantifying the sensitivity of camera traps: an adapted distance sampling approach. Methods in Ecology and Evolution 2:464-476.

Rowcliffe, J. M., R. Kays, B. Kranstauber, C. Carbone, P. A. Jansen, and D. Fisher. 2014. Quantifying levels of animal activity using camera trap data. Methods in Ecology and Evolution 5:1170-1179.

Scheibe, K. M., K. Eichhorn, M. Wiesmayr, B. Schonert, and O. Krone. 2008. Long-term automatic video recording as a tool for analysing the time patterns of utilisation of predefined locations by wildlife. European Journal of Wildlife Research 54:53-59.

Smith, D. O., M. Conner, and E. R. Loft. 1989. The distribution of winter mule deer use around homesites. Transactions of The Western Section of the Wildlife Society 25:77-80.

Smyth, G. K., and B. Jørgensen. 2002. Fitting Tweedie's compound Poisson model to insurance claims data: dispersion modeling. Astin Bulletin 32:143-157.

Swann, D. E., C. C. Hass, D. C. Dalton, and S. A. Wolf. 2010. Infrared-triggered cameras for detecting wildlife: an evaluation and review. Wildlife Society Bulletin 32:357-365.

Thomas, L., J. L. Laake , E. Rexstand, S. Strindberg, F. F. C. Marques, S. T. Buckland, D. L. Borchers, D. R. Anderson , K. P. Burnham, M. L. Burt, S. L. Hedley, J. H. Pollard, J. R. B. Bishop, T. A. Marques. 2009. Distance 6.0 Release 2. Research Unit for Wildlife

Population Assessment, University of St. Andrews, UK. http://www.ruwpa.st-and.ac.uk/distance/

Vogel, W. O. 1989. Response of deer to density and distribution of housing in Montana. Wildlife Society Bulletin 17:406-413.

Wait, S., and H. McNally. 2004. Selection of habitats by wintering elk in a rapidly subdividing area of La Plata County, Colorado. Fourth International Urban Wildlife Symposium:200-209.

Williams, B. K., J. D. Nichols, and M. J. Conroy. 2002. Analysis and Management of Animal Populations. Academic Press, San Diego, CA.

CHAPTER 3 - RISK-REWARD TRADEOFFS OF A LARGE CARNIVORE FORAGING IN THE URBAN-WILDLAND INTERFACE

INTRODUCTION

Across anthropogenically modified landscapes, human-large carnivore conflicts (here after referred to as HLCCs) can directly or indirectly affect both species (Madden 2004). Understanding the indirect effects of HLCCs on carnivores is difficult (Shochat et al. 2006), but they appear to arise when habitat modifications and fragmentation result in reductions in genetic connectivity or foraging efficiency (Storfer et al. 2007, Shochat et al. 2010). For human losses, an indirect conflict occurs when carnivores compete for the same prey targeted for recreational and subsistence uses (Reynolds and Tapper 1996, Nilsen et al. 2005, Fa and Brown 2009). Direct losses to humans are often associated with carnivore feeding events, such as predation on livestock (Kaczensky 1999), pets (Torres et al. 1996), or humans (Beier 1991, Löe and Röskatt 2004). The offender can also suffer a loss when it is persecuted (Balme et al. 2009, Inskip and Zimmermann 2009, Maclennan et al. 2009). The most noticeable effect from HLCCs is the apparent association between increased anthropogenic development and the regional extirpations of some carnivores over the past century (Woodroffe 2000, Crooks et al. 2011).

Empirical explanations for the spatial patterns of HLCCs is that they occur where human and carnivore utilization overlaps the most, codependent on suitable carnivore habitat (Torres et al. 1996, Nyhus and Tilson 2004, Kertson et al. 2011) or the type of human activity (Baruch-Mordo et al. 2008, Balme et al. 2009). Foraging strategy, with respect to patch choice, has direct implications for understanding landscape utilization patterns (Brown 1988, Dupuch et al. 2009, Laundré 2010). Thus far, mechanistic explanations for patch choice are relatively simple and

one-dimensional for large carnivores. Explanations rooted in energy maximization principles indicate attraction toward prey availability or catchability for some species (i.e., cougar, *Puma concolor*) (Pierce et al. 1999). The same carnivore species may also engage in risk avoidance behaviors related to human development (Burdett et al. 2010). Studies focusing on either energy maximization (Pierce et al. 1999) or risk avoidance (Burdett et al. 2010, Wilmers et al. 2013) alone give contradictory predictions in the scenario where reward potential is positively correlated with increased risks near humans. Understanding whether a carnivore balances energy acquisition behaviors with risk avoidance behaviors may help reveal under which conditions an animal utilizes high risk locations when feeding, thus providing biological mechanisms for explaining HLCCs.

Classic optimal foraging theory (OFT) predicts that an organism makes choices when feeding to acquire a maximum level of energy gain per unit effort (MacArthur and Pianka 1966, Emlen 1968) where behavioral tradeoffs are made at the individual level between acquiring energy (McNamara and Houston 1987) and expending energy (Charnov 1976), ensuring offspring survival (Mangel and Clark 1986), avoiding mortality risks (Brown 1992), or avoiding injury risk (Berger-Tal et al. 2009, Embar et al. 2014). It is assumed that maximizing foraging efficiency results in a release of time constraints (Jeschke 2007) for the successful reproduction and rearing of offspring (Mangel and Clark 1986, Houston and McNamara 2014). However, all can be quickly lost if energy maximization choices are associated with increased mortality risk (McNamara and Houston 1987). For consumers (i.e., herbivores) at least, patches of lower food availability may be selected to avoid spatially mediated risks imposed by predators (Lima and Dill 1990).

Optimum foraging theory may also help explain space use patterns of a predator when faced with its own spatially mediated risks (i.e., housing development). In this scenario, the herbivore now serves as a mobile resource and the large carnivore is the mobile forager that in turn receives pressures from humans (Ordiz et al. 2011). Very little information is available on whether OFT can be useful for explaining the distribution of a mobile predator feeding on a mobile prey resource (Sih 1984, Lima 2002, Laundré 2010, DiRienzo et al. 2013), especially in three-way community-level interactions (i.e., herbivores, predators, humans). To judge whether or not a predator utilizes an optimal strategy with respect to balancing energy acquisition and human related risk, three assumptions must be fulfilled: 1) The forager places a reward value on certain patch types, 2) Certain patches are perceived as costly or risky by the forager, 3) Patch reward value must be correlated positively with risk of mortality in a portion of patches available to the forager.

Whether an animal can cope with and exploit the modifications associated with anthropogenic development is dependent on its species' characteristics (Noss et al. 1996, Johst and Brandl 1997, Crooks et al. 2011) and individual phenotype (Wilson et al. 1994, Reale et al. 2003, Nussey et al. 2007). Although the aim in many animal ecology studies is to provide an expected value for a population, patch-use choices are made at the individual level. Risk avoidance behaviors influencing patch selection are expected to vary inter-individually (Sih et al. 2004, Wolf and Weissing 2012). A tenet of OFT is that individuals can respond to energetically stressful temporal periods (i.e., age class, season, hunger) by increasing their foraging efficiency and subsequently choosing to make riskier patch selection choices (Berger-Tal et al. 2009, Embar et al. 2014). In other words, animals may be less selective when energy reserves are low (Emlen 1966). Testing for intra-individual differences related to temporal periods (periods of

stress experienced by all animal individuals) may reveal whether energetic stressors indeed influence foraging strategy.

The objective of this study was to test which foraging strategy best explains patch utilization in a model system with a top predator foraging in its own landscape of fear (Laundré et al. 2001). I used cougar foraging on mobile wild prey (i.e., mule deer [Odocoileus hemionus], meso-carnivores) in a patchwork of varying housing densities ranging from rural to suburban, which serve as a stationary human mediated risk. Similar to other large carnivores, various management and conservation concerns involving HLCCs with cougars exist (CMGWG 2005, Sweanor et al. 2008). Thus, understanding biological mechanistic explanations for cougar space use is of importance. While never tested directly for patch selection, large scale utilization patterns appear to be correlated with that of their prey (Pierce et al. 1999, Allen et al. 2014) or habitats known to be used by prey (Kertson et al. 2011), evidence for an energy maximization strategy. Other studies point out cougar aversion to human mediated risks (Burdett et al. 2010, Wilmers et al. 2013). I aim to provide a mechanistic understanding of space utilization of an apex predator foraging in human dominated landscapes on mobile prey by testing some optimal foraging theory predictions, especially concerning energetic stressors.

This study was carried out in a foothill-montane system of Colorado's Front Range situated between the continental divide and the Denver metropolitan area. The area is characterized by a patchwork of varying housing densities (Figure 3.1). Using a step-selection function (SSF) movement model, I tested whether cougar patch selection while foraging was influenced by: 1) an aversion to relatively higher housing density (risk avoidance), 2) an attraction to higher availabilities of prey (energy maximization), or 3) both risk aversion and prey attraction (optimal foraging). I also addressed whether cougars were motivated to utilize

risky habitat by testing whether housing density and/or prey availability influenced the probability of a hunting event manifesting into a feeding event (hunting success). Finally, I examined whether these foraging strategies were conditional on inter- and intra-individual factors concerning the individual animal, gender, age, season, and hunger level.

METHODS

Housing and Prey Distribution

A housing density distribution map was developed under a dasymetric approach (Wright 1936) combining information on the locations of man-made roofed structures with U.S. census bureau block-group housing density estimates (Appendix 2). Using the classifications given by Theobald (2005) it was found that rural (<0.068 housing units/ha) and exurban levels (0.068 – 1.47 housing units/ha) comprise a vast majority (69.7% and 27.3%, respectively) of the study area.

Unlike cursorial predators (Husseman et al. 2003), a stalking predator like the cougar (Banfield 2012) must get within a close distance (i.e., < 25 m) to prey before launching a successful attack (Beier et al. 1995, Holmes and Laundré 2006). An expected measure of prey availability should come from a similar scale in which hunting activities are carried out (Fraker and Luttbeg 2012, Birk and White 2014). Under a stratified random sampling design with varying levels of housing density, housing proximity, and natural landscape categories, 131 camera trap stations collected photographic encounter rate data of mule deer (the primary prey) and other alternative cougar prey species (i.e., raccoon (*Procyon lotor*), domestic cat (*Felis catus*), elk (*Cervus canadensis*)) over an annual period (2011 – 2012) (Chapter 2). The small confines of the field-of-view (FOV) of camera traps allowed the response to be interpretable for a fine spatial scale (< 30 m). Generalized linear models were used to associate encounter rate

data to various landscape covariates (Appendix 4), with special emphasis placed on various housing measurements (Appendix 2). It was found that the best utilization model for mule deer was one with natural variables (Appendix 6) and a quadratic housing density effect. Utilization increased as a function of increasing housing density when in the rural and exurban density range (the dominant housing types) but decreased once in the low suburban range (~2.5 houses/ha) (Figure 2.4). Raccoon and housecat utilization were positively associated with increasing suburban housing densities and decreased Euclidean distance to structure (Figure 2.4). For elk, utilization increased with higher housing when in higher elevations, but remained neutral in lower elevations (Figure 2.4).

Prey model predictions were interpolated to all 30 m pixels within the study area (Appendix 7). The resulting prediction at each location was used as an approximation for a population level utilization metric for a patch, which is the product of the number of individuals and the amount of time spent by any individual, given that certain study design components were adhered to (Chapter 1). Detailed field and model methods can be found in Chapter 2. Detailed spatial utilization results (model selection, coefficient estimates, and prediction maps) for these species can be found in Chapter 2, Appendix 6, and Appendix 7.

Defining Cougar Hunting and Feeding Locations

A sample of cougars (n = 54, 34 Female and 20 male) were captured (IACUC: 16-2008 – Colorado Parks and Wildlife USDA Registration # 84-R0045) and fit with GPS collars programmed to record locations every 3 hours at night and 3 or 4 hours during the day (Appendix 8). To identify feeding events, GPS locations were grouped into discrete clusters based on spatio-temporal characteristics using a customized algorithm (Appendix 8). The long duration of handling events (small prey: 3-24 hrs, large prey: 24 hrs to several weeks) made

identification of feeding events possible. For every cougar and month of the study period monitored (Jan 2008 – Dec 2012), a random sample of clusters was ground-truthed in the field (total visits = 1718) to confirm presence or absence of prey remains, which informed the creation of a GLM (binomial family) for predicting the locations of feeding sites (Anderson and Lindsey 2003). All prey types and sizes (lagomorphs – cervids) were included in the model. Cross validation indicated that the model predicted feeding events well (88.6% - Receiver Operator Characteristics: Area Under Curve measure). Detailed methods for the clustering algorithm, ground-truthing, and prediction model can be found in Blecha and Alldredge (*in prep*) and Appendix 8.

A total of 5,766 kill locations were identified with the prediction model, leaving non-feeding clusters and single GPS locations to remain. These remaining locations were identified as potential hunting locations by defined rules (details given in Appendix 9), but were mainly based on whether they occurred during the night (cougars are primarily nocturnal hunters) and whether they occurred at a time when no other prey handling activities were ongoing. This yielded a total of 39,268 potential hunting locations. Hunger level was assigned to each location as the amount of time that had passed since the commencement of the prior feeding activity, binned into one of 11 interval groupings (0-1 days,…, 9-10 days, 10+ days). Cougar age was assigned as a dynamic variable that incremented appropriately with time based on the estimated age at capture (Laundré et al. 2000).

Foraging Strategy Model

All single GPS locations and centroids of the identified clusters were used as input into a SSF analysis (Fortin et al. 2005, Thurfjell et al. 2014). The SSF used here incorporates the observed distribution of step distances and turning angles to inform the generation of matched

available locations (Appendix 9). To assess landscape choice, each "use" location is compared to the matched available locations (e.g., as in a case control design) (Figure 3.2) based on landscape covariates (Appendix 4 & Table A9.1) using a mixed effect conditional logistic regression model (Duchesne et al. 2010). Fixed effect coefficient estimates (β's) are given on their linearized scale along with confidence intervals (95% Walds). A positive β would indicate cougar selection for increasing values of a covariate, while a negative β would indicate selection against an increasing value of a covariate. Confidence intervals (C.I.) overlapping zero would indicate a lack of selection (neutral response) for the covariate. A detailed description of the model is found in Appendix 9.

To test which patch selection foraging strategy best described cougars, a candidate set of hypothesized models was examined using an information theoretic approach to find the most parsimonious model (Burnham and Anderson 2002). While focus was placed on the fit provided by the housing and prey covariates, other natural landscape covariates (Appendix 9) were included in the model as well. Because selection patterns can be scale specific (Wilmers et al. 2013, Zeller et al. 2014), a range of spatial scales was tested (Appendix 4). To indicate the presence risk-reward tradeoff, both a housing density (HDM) and the prey availability covariate (MDEER) must be in the most parsimonious model with coefficient signs aligned so that β_{HDM} is negative and β_{MDEER} is positive. A mixed effects parameterization with random slope terms, where the response to HDM and MDEER covariates were allowed to vary according to the individual animal ($\mathbf{b_{animal\_ID}}$) or calendar month (b_{Month}) should ensure that this interpretation supports a tradeoff, rather than it being the result of some animals responding solely to β_{HDM} and other animals solely to β_{MDEER} (Duchesne et al. 2010). Additional models specifying combinations of $\mathbf{b_{animal\_ID}}$ or $\mathbf{b_{Month}}$ and natural landscape covariates as random slopes were also

examined. All mixed effect candidate models were assessed by model fit and the overall variation contributed (σ^2) for the combination specified. A low σ^2 near zero would indicate that the random slope term did not vary with respect to the **b** term. Models were limited to three random effect terms to reduce computation load, but were also required to have random slope terms corresponding to both the HDM and MDEER covariates. Candidate model sets using various combinations of fixed effects terms and random slope terms were critiqued based on the model building and selection methods given in Appendix 9.

Hunting Success Model

Knowing whether a hunting location is more likely to be manifested into a successful kill , as a function of housing density or prey availability, is important for identifying drivers for why cougars may make the decisions revealed in the SSF model. In another case control analysis, I compared the attributes of kill locations to those of the hunting locations immediately preceding kills (Figure 3.2). In this case, "hunting success" is the joint probabilities of encountering a potential prey item, choosing to launch an attack, and successful submission of the prey. Any kill location not preceded by at least one hunting locations was removed (i.e., kills made back to back). Again using a mixed effect conditional logistic regression model (Appendix 9), it was determined if the probability of making a kill along a given hunting path was influenced by the landscape characteristics of the point locations (GPS locations) visited.

Inter- and Intra-individual Differences

In this system, several environmental and animal specific factors can introduce inter- and intra-individual differences. For cougars, inter-individual differences in foraging behaviors can arise based on sex and age classes (Knopff 2010) or possibly from individual traits such as the degree of boldness or shyness. It is hypothesized that older age classes (more experienced

cougars) will be more efficient at foraging and show a stronger degree of avoidance toward housing development and be able to capitalize on localities with a lower availability of prey. Intra-individual differences can be characterized as temporally changing. Availability of primary ungulate prey may vary seasonally, as a surge of ungulate prey availability occurs in relation to the summer ungulate birth pulse (June – July). Thus, in the months prior to the pulse, prey availability is likely at its nadir, especially considering over-winter ungulate deaths. On a shorter time scale, hunger level may influence foraging strategy. To examine whether the response to houses and prey availability depended on the above factors, the most parsimonious foraging strategy model was applied to subsets of the SSF data for each cougar, gender, age (yearly age classes), month, and hunger level. Random effects corresponding to the subset being analyzed were removed. For each subset, the β's and 95% confidence limits were assessed and compared among levels (e.g., across cougars, across age classes, etc). Standardized β's (covariate values centered and scaled by standard deviation) are given in all analyses.

Pertaining to the influence of hunger level on foraging strategy, it would be important to know at which hunger level kill events normally occurred. Thus, I characterized the distribution of the kill event timing with respect to hunger level by the mean and median.

RESULTS

Test of Foraging Strategy

For each cougar, 121 to 3087 locations (kill and hunting combined) were obtained for "use" locations (45,034 total use locations). The best fitting SSF model demonstrated an avoidance of locations with increased housing density ($\beta_{HDM150} = -0.769$) and a slight attraction to locations with increased mule deer utilization ($\beta_{MDEER} = 0.086$) (Table 3.1). A positive response (attraction) was also shown with respect to increased canopy cover, and increased

slope, and a negative response (avoidance) was shown to increased elevation (β_{ELEV}), forest edge ($\beta_{FOREDGE}$), and increasingly north facing aspects (β_{ASP180}) (Table 3.1). A general attraction toward edge was shown ($\beta_{FOREDGE}$), but the strength of the relationship was dependent on canopy cover (interaction with β_{CC_avg90}). Accounting for random effects with respect to individual and month as single random slope terms improved (Table 3.2), but the most inter-individual variation in site selection was related to housing density (HDM) ($\mathbf{b}_{animal\_id}$: $\sigma^2 = 0.818$).

Hunting Success Model

A total of 4,312 kill locations and 38,245 hunting locations were used for comparing the kill location to its respective preceding hunting locations. Hunting success was positively associated with increased housing density ($\beta_{HDM400} = 0.122$). Other natural covariates possibly associated with increased stalking cover, such as a decreasing topographic position index (locations closer to small drainages) ($\beta_{TPI\_100} = -0.384$) were also found in the top model. Little to no inter-individual or intra-individual variation in success was related to HDM (Table 3.1).

Inter- and Intra-individual Differences

With the SSF model, examining the response to increased housing density after applying the best model (after removing the random effect for individual) to each individual revealed that 26 of the 54 cougars displayed a clear (β 95% C.I. < 0) negative response with β_{HMD} ranging from -2.178 to -0.169 (Figure 3.3). Another 26 indicated a neutral response (95% C.I. overlapped zero) (Figure 3.3) with β_{HDM} ranging from -0.315 to 0.043. The remaining two individuals indicated a slight but clear attraction (β 95% C.I. > 0) with $\beta_{HDM} <= 0.120$ (Figure 3.3).

Applying the SSF model to sex class indicated that males showed a clear and stronger avoidance of housing ($\beta_{HDM} = -1.35$) than shown by females ($\beta_{HDM} = -0.41$) (Figure 3.4.A). For age classes, no discernable difference was shown in 12-60 month age classes (β_{HDM} ranged: -

0.282 to -0.605) (Figure 3.4.B). A stronger avoidance to housing was exhibited for the two 60+ month classes (β_{HDM}: -1.157 and -1.225) over the 12-60 month age classes, but the confidence limits nearly overlapped the mean β_{HDM} in all age classes (Figure 3.4.B).

The response to housing density varied greatly by month. From January - May, housing avoidance appeared to increase from moderate (β_{HDM} = -0.807) to very little avoidance (β_{HDM} = -0.070). In June, avoidance behavior increased intensely (β_{HDM} = -1.279), and then dropped off (β_{HDM} increased) throughout the remainder of the year (Figure 3.4.C).

As hunger increased, cougars became less selective when hunting. The strongest avoidance to houses was observed at 0-1 days post feeding (β_{HDM} = -0.779). The estimate showed a general increase in β_{HDM} the following 3 days, until leveling off and appearing the most neutral (β_{HDM} = -0.07 to 0.008) by 4-7 days post feeding (Figure 3.4.D). Hunting locations representing kill events occurred at a mean and median of 1.99 and 1.38 days (Figure 3.5).

DISCUSSION

I demonstrated that a large carnivore can balance the acquisition of energy with the risks imposed by its own predators. I provided much needed empirical knowledge of the influence of foraging strategy on landscape utilization patterns of a mobile predator seeking mobile prey (Sih 1984, Lima 2002). Support is provided for the foraging strategy being dependent on inter- and intra-individual differences. The heterogeneity observed in foraging strategy can occur at very fine temporal scales and can be directly linked to the predator's hunger level; cougars were more likely to take risks when hungry. Furthermore, cougars were more likely to utilize risky landscapes when numerical prey availability was assumed to be at its lowest.

Study Design

The SSF model used here explicitly accounts for animal choices conditional on what is available to an individual animal and the specific situation faced at the time. Standard tools for testing patch choice behaviors to understand predation costs and optimality behaviors rely on time allocation measures (i.e., "giving-up densities") (Krebs et al. 1974, Brown and Kotler 2004) or behavioral observations of vigilance (Roberts 1996, Bednekoff and Lima 1998), but are difficult to conduct for predators that intentionally avoid human detection. Recent attempts to understand cougar risk avoidance, from the perspective of foraging time on carcasses using GPS telemetry (Smith et al. 2015), reflect choices made during the handling process rather than the decisions for choosing that feeding location.

This study examines prey availability at any location based on an expected encounter rate for a prey animal at a small patch perspective. If faced with no risks, predators should choose patches with a higher baseline encounter probability with a potential prey item (Charnov 1976, Norberg 1977, Jaksić et al. 1981). The expected encounter rate for a potential prey item depends on the localized abundance for some area around the patch and the expected temporal utilization of the patch by any prey individual (Chapter 1). Previous studies assessing space utilization by the mule deer (Pierce et al. 2000, Laundré 2010) did so with sampled telemetry locations from individuals on the landscape that do not explicitly incorporate animal abundance. Passive camera trapping techniques have the potential to correctly quantify space utilization by prey (but not patch choice) at the level of the population more accurately than simple radio telemetry analysis (Chapter 1) alone, especially considering that telemetry sampling frequency can induce utilization inference biases (Reynolds and Laundre 1990, Johnson and Ganskopp 2008). Studies

using animal density alone to infer baseline encounter rates may have difficulties making inferences at fine spatial scales perceived by large predators (Holmes and Laundré 2006).

Tradeoff Assumptions

For the risk aversion – energy acquisition tradeoff to occur, the assumption defined earlier says that certain patch types are perceived as more rewarding to the predator. It was demonstrated here that cougars hunting success was improved in higher housing densities, which could imply that cougars are more likely to encounter prey in these habitats, or are simply more apt to make a kill based on improved ambush cover associated with housing. It appears that cougars were more successful in lower topographic positions (drainages or ditches with improved ambush cover) despite these localities having a lower availability of primary prey (Chapter 2). Since initial conceptions (Charnov 1976), much empirical support has been given for landscape utilization by large carnivores being positively associated with prey availability (Murray et al. 1994, Spong 2002, McPhee et al. 2012). However, hunting success did not improve with respect to the availability of primary prey species (mule deer), thus supporting the notion that accessibility can be more important than pure availability (Pierce et al. 2004, Hopcraft et al. 2005, Balme et al. 2007). Furthermore, demonstrating that prey availability is the single factor responsible for a predator making a successful kill would not validate a patch's reward value, as a predator engaged in simple Brownian motion would more likely encounter prey in areas where prey congregate. In this study, cougars may be placing reward value on certain landscape variables associated with some combination of the availability of prey and stalking cover.

The second assumption is that the predator must perceive humans as imposing a risk. While a few failed hunts may only result in a few missed meals, a single underestimation of the

predation risk present while foraging may result in instant injury or mortality, thus predation risk would be expected to have strong selective forces (Lima and Dill 1990, Bouskila and Blumstein 1992). Risk can be measured as the probability of being killed (Lima and Dill 1990) or possibly just injured (Brown and Kotler 2004, Berger-Tal et al. 2009) given exposure. Landscape of fear theories predict that animals will adjust their temporal or spatial utilization patterns based on fear of these risks (Brown et al. 1999, Altendorf et al. 2001), and has been applied to large carnivore response to foci of human mediated risks on the landscape (Burdett et al. 2010, Northrup et al. 2012, Valeix et al. 2012). Besides habitat selection studies indicating a general cougar avoidance to housing development (Burdett et al. 2010, Wilmers et al. 2013), a driver for avoidance is likely HLCCs, which can be a common mortality source of subjects in this study (approximately 33% of mortalities observed) (unpublished data) in other studied populations (Anderson et al. 1992, Torres et al. 1996, Cunningham et al. 2001, Orlando 2008, Burdett et al. 2010, Thompson et al. 2014).

Finally, patch reward value must be correlated positively with risk of mortality in some cases in order to demonstrate a tradeoff. Results of the camera study indicate that primary prey species availability is positively associated with increased housing density up to 2.5 houses/ha, and even more so for alternative prey species such as raccoon and domestic cat in suburban housing developments. A growing body of evidence supports these predictions (see review in Table 2.1). For the tradeoff to be tested, it is assumed that all combinations of relatively high and low housing development and relatively low and high prey availability are available, such as would be the case if using a factorial experimental design. However, defining what is considered low versus high levels of risk or prey availability is debatable. Positive risk-reward associations tend to occur when prey alter their distribution on the landscape to avoid the predator, especially

if that means seeking cover perceived as risky to the predator (Berger 2007). In this system, deer are faced with multiple predation pressures (Sih et al. 1998), such as those imposed by human hunting in rural localities and those by black bear and coyote on young deer (Pojar et al. 2004), additional forces that may drive deer to utilize exurban cover.

Conditions

The inter-individual heterogeneity found in cougar hunting behaviors is supported by others (Kertson et al. 2011, Wilmers et al. 2013, Zeller et al. 2014). However, additional testing needs to be carried out to understand if this was a reflection of personality (boldness/shyness) or resource availability at a larger scale. Understanding the latter could lead to a deeper understanding of the home range selection process (e.g., 2nd order selection; Johnson 1980). Some differences could be attributable to gender, considering males showed more risk-avoidance than females. Differences may also occur with respect to age, although the simple analysis done here was less clear. Age can also be viewed as an intra-individual influence, as age (to the nearest month) was allowed to increment throughout the study, with some cougars being monitored within all five years of the study.

On an intra-individual level, the waning risk-avoidance as a function of hunger level was most interesting, supporting the predictions of optimal foraging theory that decisions regarding trade-offs were actively being made. This phenomenon has rarely been tested in higher trophic levels (Berger-Tal et al. 2009, Embar et al. 2014) and with even fewer tests conducted on wild animals. Generally, kills are made at an expected hunger level of 1.99 days (median 1.34 days), while still exhibiting clear risk avoidance. After four days, little to no risk avoidance was exhibited. Over the longer timescale of the year, risk avoidance decreased with decreasing availability of prey (late winter through pre-ungulate birthing pulse). During periods with lower

primary prey availability, cougar may better able to capitalize on prey associated with human density by simply lowering their guard.

Besides being a novel demonstration of physiological state influencing large predator behavior, various ecological applications for this knowledge exist. Many studies have examined predator avoidance response to anthropogenic development (Burdett et al. 2010, Kertson et al. 2011, Wilmers et al. 2013). Yet these studies have done little to explain an animal's occasional (or generally rare) utilization of these inherently risky landscapes, which leads to a potential human-wildlife conflict. Decreases in risk avoidance would convey a higher overlap with humans, and thus a higher probability of conflict. Thus, any factor causing an increased level of hunger may also be a driver of increased conflicts. These factors include the sudden reduction in primary prey species (Inskip and Zimmerman 2009), and factors suggesting decreased hunting efficiency, such as younger age, sick, injured, or maternal status (Linnell et al. 1999).

Conclusion

An objective of this study was to place cougar space use of anthropogenically developed lands (and thus HLCCs) within the context of broader ecological theories to provide more generalizable applications. My findings demonstrate that a large carnivore can balance the acquisition of energy with the risks imposed by its own predators. I provide much needed empirical support for theoretical predictions concerning foraging strategies and their influence on landscape utilization patterns of a mobile predator seeking mobile prey. The intra-individual heterogeneity in foraging strategy can occur at very fine temporal scales and can be directly linked to the predator's physiological state. Reduced behavioral avoidance towards human development, as a function of physiological state, serves as a building block for understanding the influence of other energetic stressors when determining landscape utilization patterns.

TABLES AND FIGURES

Table 3.1. Fixed effect beta coefficient estimates, standard errors, and lower (LCL) and upper (UCL) 95% Walds confidence intervals for the most parsimonious mixed effect step-selection function (SSF) and hunting success models. Variance estimates σ^2 of random slope terms (Entity or Month), corresponding to the fixed covariate are given.

		Fixed Effects				Random Slope Effects σ^2	
Model	Covariate	β est.	SE	LCL	UCL	$\mathbf{b_{animal\_ID}}$	$\mathbf{b_{month}}$
SSF	ASP180*	-0.148	0.006	-0.159	-0.137	-	-
	ELEV	-0.278	0.012	-0.302	-0.254	-	-
	FOREDGE†	-0.202	0.007	-0.216	-0.188	-	-
	CC_avg90‡	0.204	0.007	0.190	0.218	-	-
	FOREDGE x CC_avg90	0.038	0.007	0.025	0.050	-	-
	HDM150§	-0.769	0.134	-1.032	-0.506	0.802	0.010
	MDEER¶	0.086	0.017	0.053	0.118	0.008	-
Kill Success	ASP45*	-0.071	0.018	-0.106	-0.035	-	-
	ELEV	-0.282	0.084	-0.448	-0.117	0.109	0.034
	TPI_100**	-0.384	0.039	-0.461	-0.307	0.014	0.010
	FOREDGE†	-0.001	0.021	-0.042	0.040	-	-
	FOREST***	0.007	0.021	-0.033	0.048	-	-
	FOREDGE x FOREST	-0.106	0.023	-0.152	-0.060	-	-
	HDM400§	0.122	0.016	0.090	0.154	-	-

* corresponds to decreasing southerly (180°) or northeasterly (45°) solar aspect

† Increasing Euclidean distance to forest edge

‡ average canopy cover percentage within 90 m radius

§ Housing density within 150 or 400 m radius respecitvely

¶ Mule deer utilization at 30 m grain size

** Topographic position index for for 100 m radius

***Binary indicator of forest presence at 30 m grain size

Table 3.2. SSF mixed effect model selection table with single random slope terms corresponding to each covariate random effect animal (animal_ID) or calendar month factors ("covariate | animal_ID" or "covariate | Month"). Accounting for individual animal variation (σ^2) in patch selection with respect to housing density (HDM150) by individual animal (Entity_ID) dramatically improved parsimony and greatly altered the HDM fixed effect coefficient estimate (-0.107 to -0.755). Other random slope terms improved model fit as well, but did not contribute greatly to explaining heterogeneity (σ^2 <= 0.025).

		Cofficient Estimates β of Fixed Covariate **x**								Model Selection			
Random Effect Term (covariate **z** | random factor **b**)	Random Slope σ^2	ASP	ELEV	SLOPE	FOREDGE	CC	FOREDGE * CC	HDM	MDEER	df	logLik	ΔAICc	AICc weight
(HDM150 | animal_ID)	0.818	-0.146	-0.275	0.004	-0.201	0.205	0.038	-0.755	0.089	53.5	-105041.5	0.0	1
(ASP180 | Month)	0.024	-0.086	-0.270	0.021	-0.193	0.220	0.037	-0.110	0.052	19.8	-105148.6	147.0	0.0
(SLOPE | animal_ID)	0.025	-0.150	-0.264	0.077	-0.192	0.203	0.035	-0.103	0.069	54.7	-105155.9	231.4	0.0
(ELEV | animal_ID)	0.081	-0.153	-0.252	0.023	-0.196	0.216	0.036	-0.132	0.069	52.2	-105204.4	323.2	0.0
(CC_avg90 | animal_ID)	0.017	-0.151	-0.266	0.013	-0.191	0.205	0.037	-0.112	0.069	51.0	-105264.6	441.2	0.0
(FOREDGE | animal_ID)	0.021	-0.149	-0.259	0.012	-0.218	0.202	0.025	-0.108	0.068	50.5	-105269.1	449.4	0.0
(SLOPE | Month)	0.006	-0.150	-0.264	0.014	-0.192	0.205	0.035	-0.107	0.069	18.4	-105363.4	573.7	0.0
(MDEER | animal_ID)	0.010	-0.152	-0.267	0.013	-0.193	0.203	0.034	-0.109	0.059	44.0	-105345.9	589.9	0.0
(MDEER | Month)	0.005	-0.150	-0.264	0.014	-0.192	0.204	0.035	-0.107	0.064	18.0	-105402.0	650.3	0.0
(CC_avg90 | Month)	0.004	-0.150	-0.262	0.014	-0.193	0.207	0.035	-0.108	0.068	18.0	-105405.1	656.2	0.0
(HDM150 | Month)	0.021	-0.149	-0.266	0.012	-0.194	0.205	0.036	-0.160	0.072	18.2	-105409.6	665.9	0.0
(ASP180 | animal_ID)	0.005	-0.151	-0.265	0.013	-0.189	0.206	0.036	-0.107	0.071	42.5	-105389.0	673.1	0.0
(FOREDGE | Month)	0.002	-0.150	-0.264	0.014	-0.194	0.204	0.034	-0.107	0.069	16.5	-105441.9	726.9	0.0
(ELEV | Month)	0.004	-0.150	-0.263	0.014	-0.192	0.205	0.035	-0.108	0.068	16.1	-105445.2	732.7	0.0
Null	-	-0.150	-0.264	0.014	-0.192	0.205	0.035	-0.107	0.069	8.0	-105462.1	750.4	0.0

Table 3.3. Hunting success mixed effect model selection table with single random slope terms corresponding to each random effect (identified as "covariate z| animal_ID" or "covariate z| Month"). Accounting for variation (σ^2) in hunting success with natural covariates as a function of individual cougar (Entity_ID) or calendar month (Month) appears to improve in parsimony (lower AICc) over the null model (in grey) in a few cases. Very little heterogeneity in housing avoidance (HDM400) ($\sigma^2 < 0.015$) was observed with respect to the factors.

		Cofficient Estimates β of Fixed Covariate **x**							Model Selection			
Random Effect Term (covariate **z** | random factor **b**)	Random Slope σ^2	ASP45	ELEV	TPI_100	FOREDGE	FOREST	FOREDGE * FOREST	HDM400	df	logLik	ΔAICc	AICc weight
(ELEV | animal_ID)	0.102	-0.071	-0.268	-0.374	-0.001	0.011	-0.102	0.124	32.5	-8014.2	16093.5	1.00
(TPI_100 | Month)	0.011	-0.070	-0.196	-0.391	-0.004	0.000	-0.108	0.143	15.2	-8040.5	16111.4	0.00
(ELEV | Month)	0.037	-0.070	-0.221	-0.378	-0.005	0.003	-0.108	0.140	15.0	-8045.5	16121.0	0.00
(ASP45 | Month)	0.007	-0.067	-0.198	-0.377	-0.005	0.003	-0.107	0.142	13.9	-8049.8	16127.5	0.00
(TPI_100 | animal_ID)	0.012	-0.070	-0.199	-0.376	-0.004	0.001	-0.108	0.140	25.7	-8040.1	16131.6	0.00
(FOREDGE | Month)	0.004	-0.070	-0.198	-0.378	-0.009	0.002	-0.108	0.141	12.2	-8055.1	16134.6	0.00
Null	-	-0.070	-0.198	-0.377	-0.004	0.003	-0.107	0.141	8.0	-8060.5	16135.0	0.00
(FOREST | Month)	0.000	-0.070	-0.198	-0.377	-0.004	0.003	-0.107	0.141	7.0	-8060.5	16135.0	0.00
(HDM400 | Month)	0.000	-0.070	-0.198	-0.377	-0.004	0.003	-0.107	0.141	7.0	-8060.5	16135.0	0.00
(HDM400 | animal_ID)	0.002	-0.071	-0.196	-0.378	-0.003	0.002	-0.107	0.151	11.5	-8056.4	16135.9	0.00
(ASP45 | animal_ID)	0.002	-0.067	-0.198	-0.377	-0.004	0.003	-0.106	0.141	11.8	-8057.7	16138.8	0.00
(FOREDGE | animal_ID)	0.003	-0.070	-0.197	-0.377	-0.007	0.006	-0.099	0.142	12.8	-8056.6	16138.8	0.00
(FOREST | animal_ID)	0.009	-0.070	-0.197	-0.377	-0.007	0.013	-0.103	0.141	21.5	-8048.0	16139.0	0.00

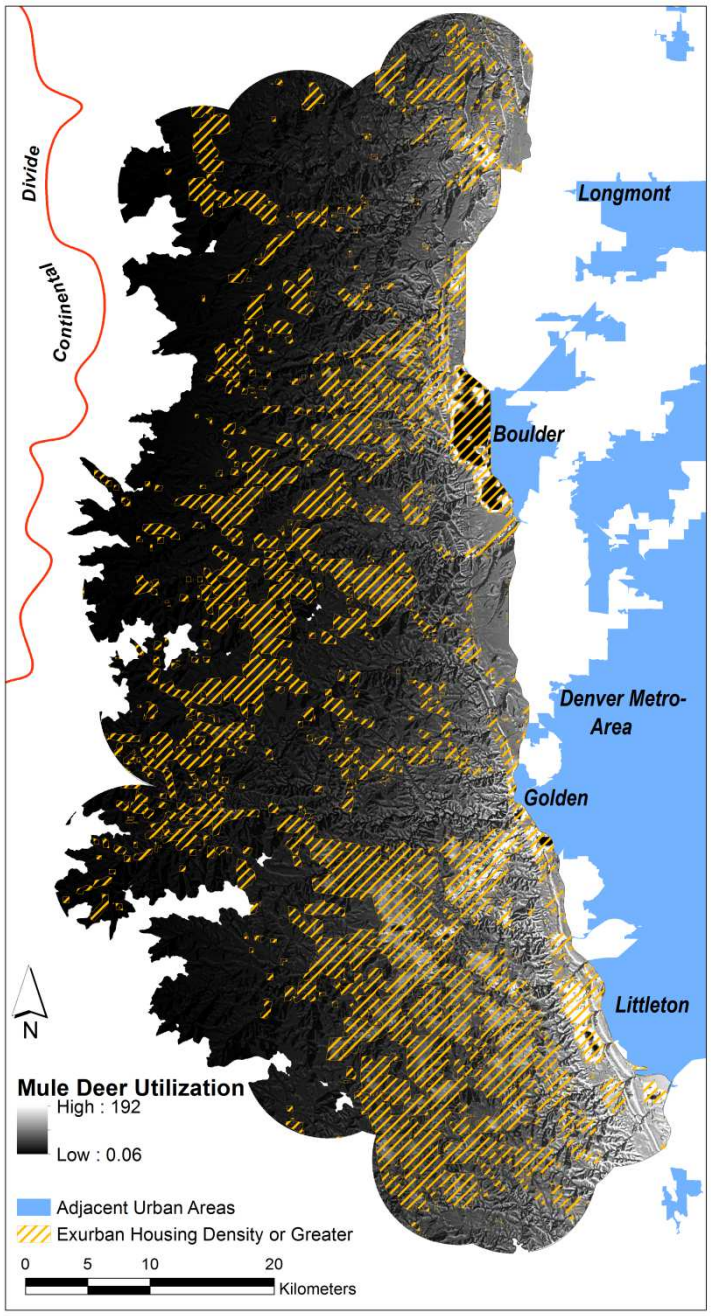

Figure 3.1. Colorado Front Range study area adjacent to the Denver metropolitan area with mule deer utilization gradient and patchwork of housing development marked by an exurban density (0.068 houses/ha) or greater.

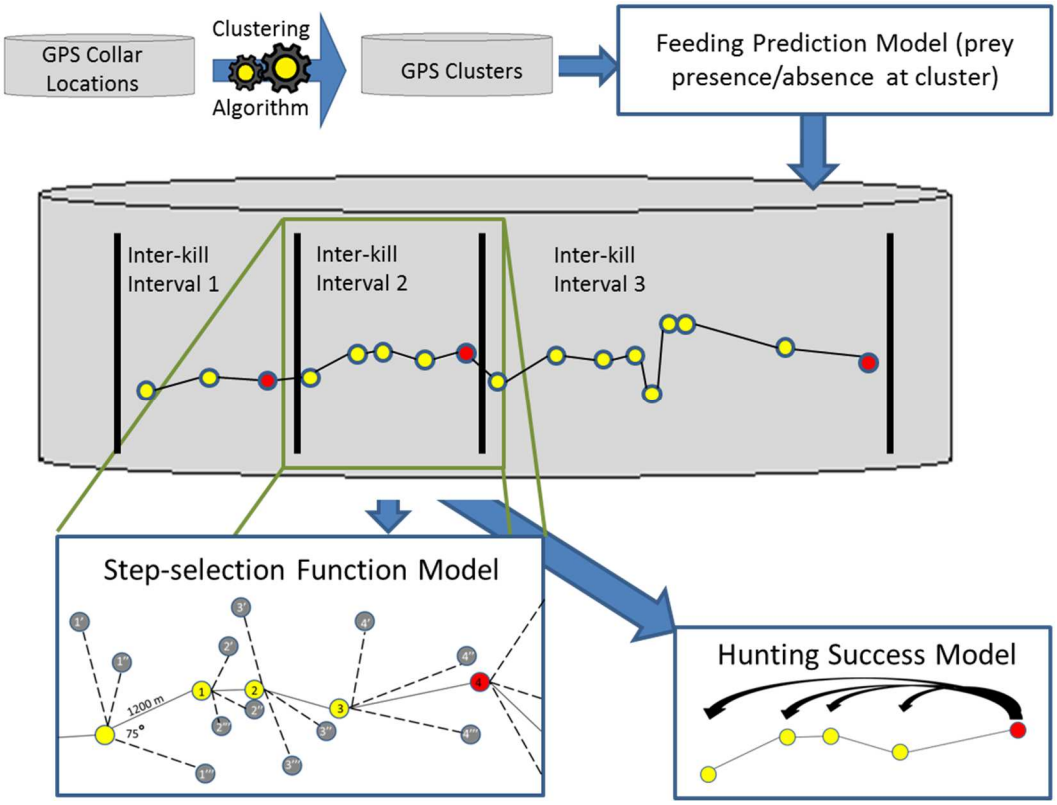

Figure 3.2. Processing steps for deriving kill-sites (red points) and hunting locations (yellow points) to be used as input into the SSF (step-selection function) and hunting success Models. The SSF compares the patch attributes at used locations (kill and hunting locations) to that of a set of generated matched locations (gray) based on the movement characteristics of the time steps. The hunting success model compares the kill site attributes to that of the preceding hunting locations within the respective hunting sequence.

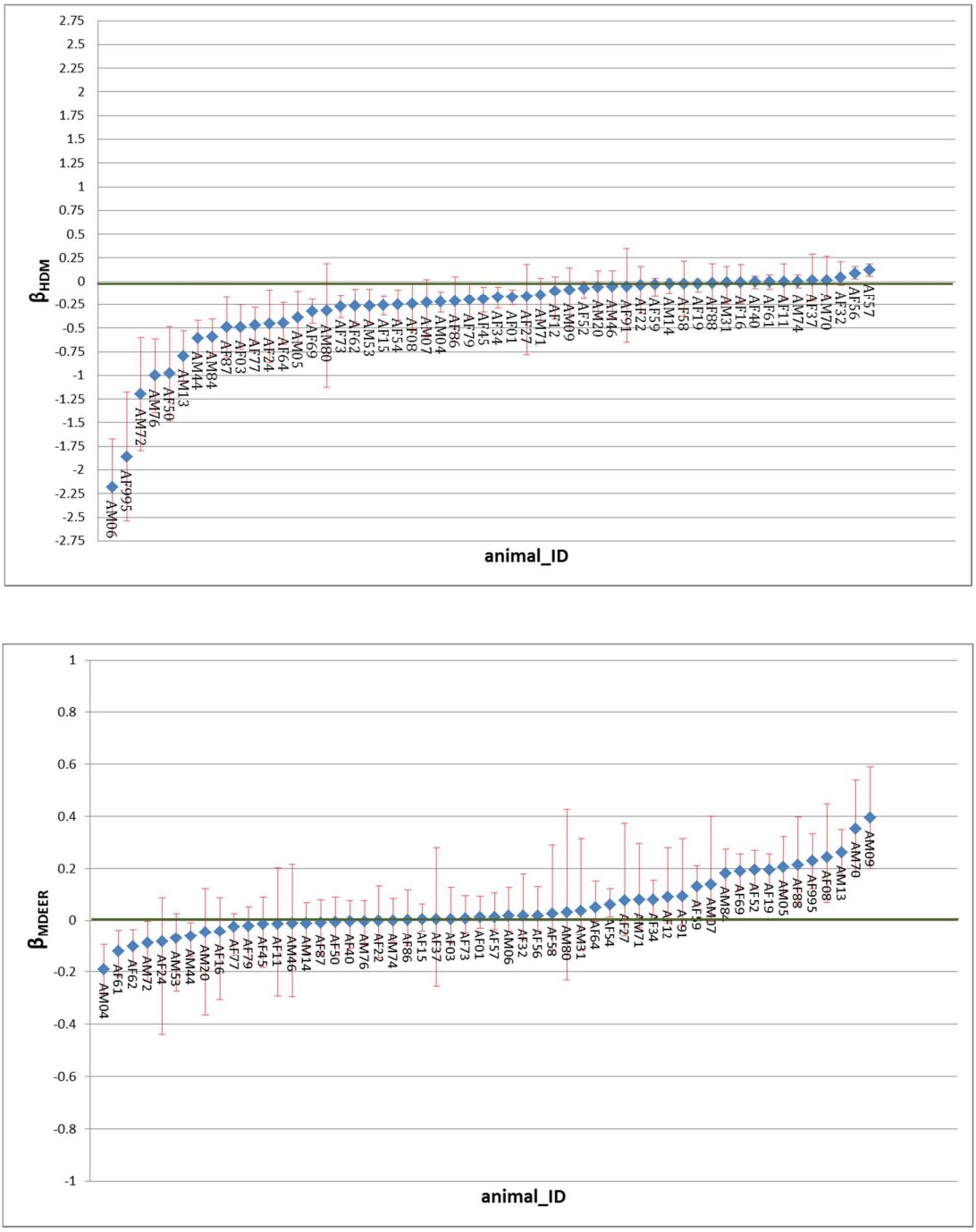

Figure 3.3. Responses of individual cougars to housing density (top pane) and prey (mule-deer) availability (bottom pane). Cougars are ordered by their effect sizes. Error bars represent 95% Walds lower and upper confidence limits. Error bars not overlapping zero indicate clear selection (if coefficient is positive) or avoidance (if coefficient is negative).

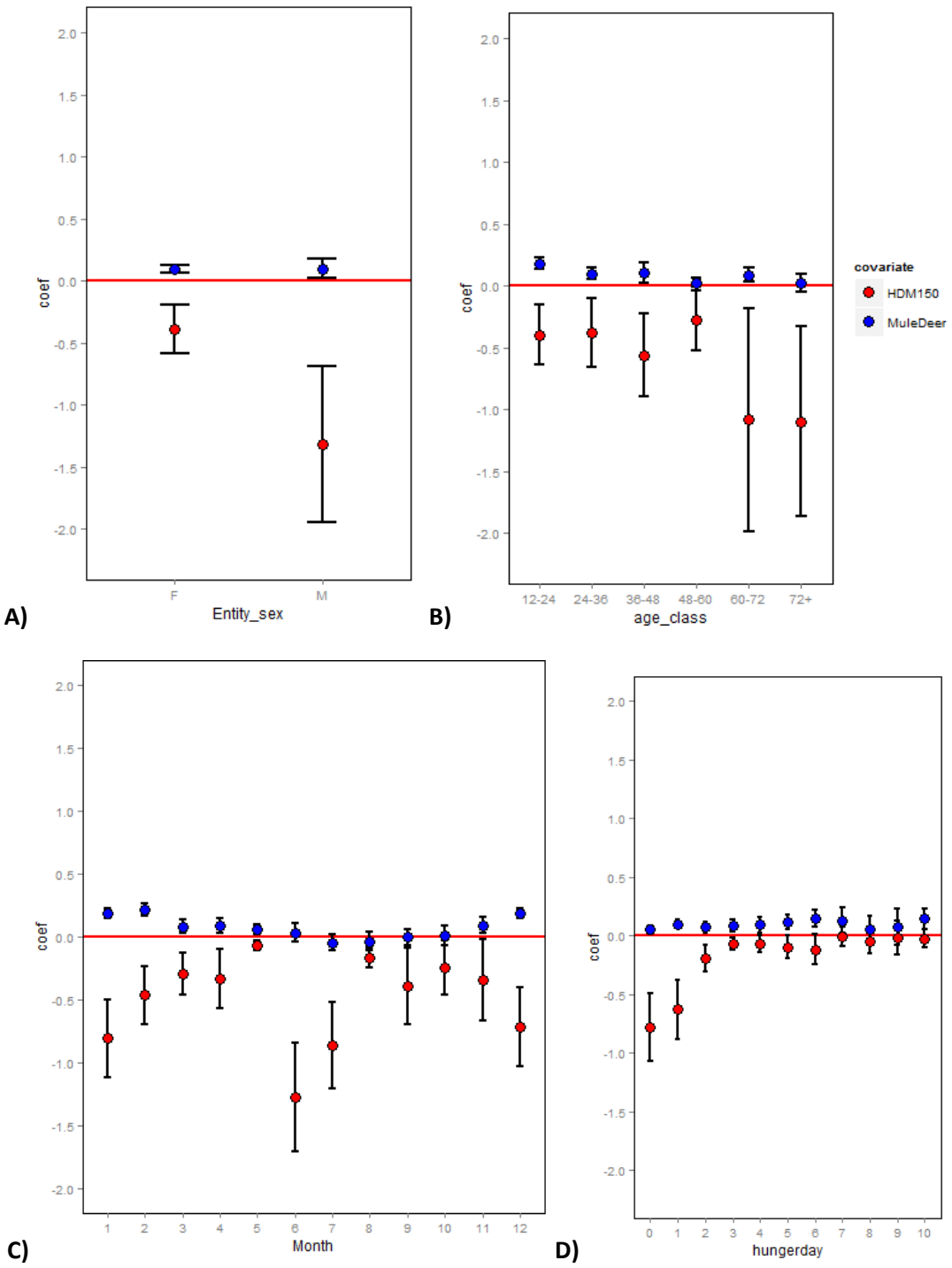

Figure 3.4. SSF (step-selection function) coefficient estimates (with lower and upper 95% Walds confidence intervals) with respect to housing density (red) and mule deer availability (blue) by levels of: A) gender, B) age class, C) calendar month, D) hunger level (days post feeding).

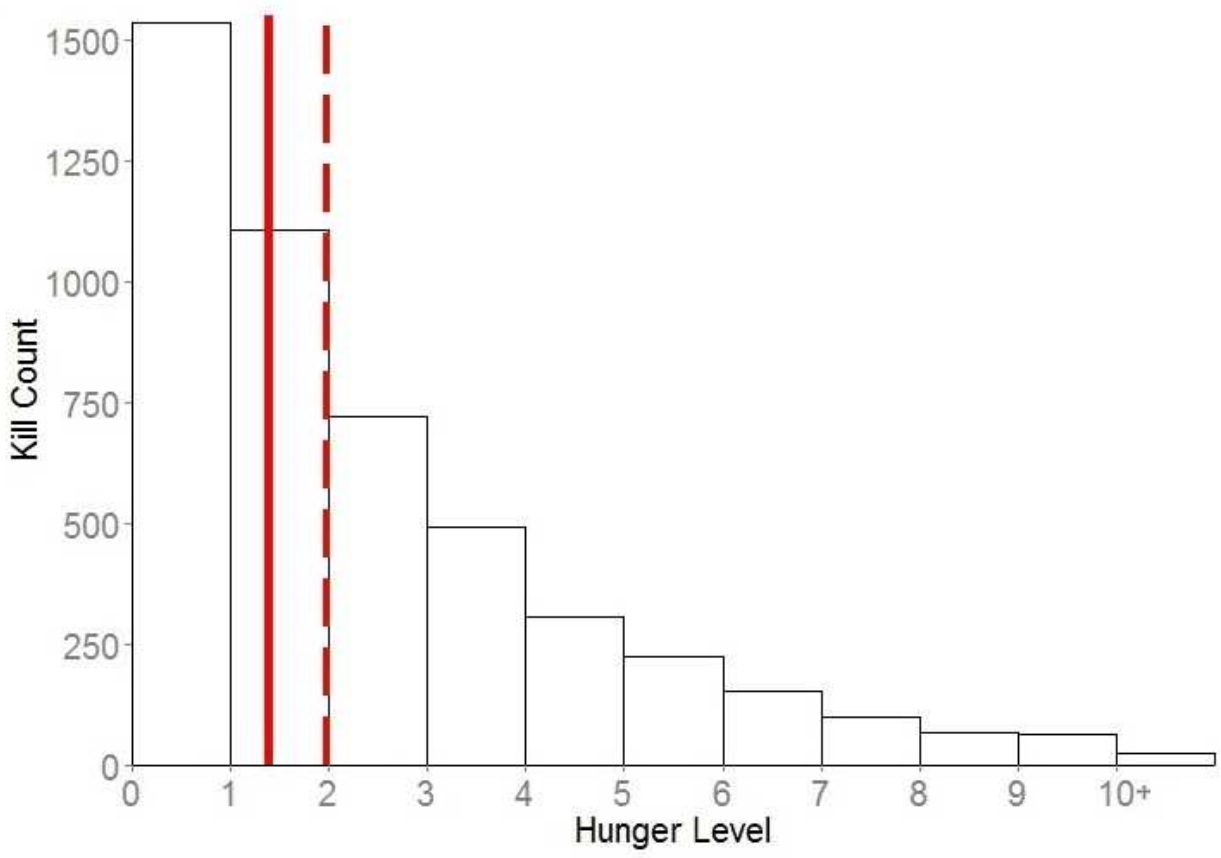

Figure 3.5. Histogram of kill events with respect to hunger level (days since last feeding event). Median and mean of the distribution are indicated with the solid and dashed lines respectively.

LITERATURE CITED

Allen, M. L., L. M. Elbroch, D. S. Casady, and H. U. Wittmer. 2014. Seasonal variation in the feeding ecology of pumas (*Puma concolor*) in northern California. Canadian Journal of Zoology 92:397-403.

Altendorf, K. B., J. W. Laundré, C. A. L. González, and J. S. Brown. 2001. Assessing effects of predation risk on foraging behavior of mule deer. Journal of Mammalogy 82:430-439.

Anderson, A. E., D. C. Bowden, and D. M. Kattner. 1992. The puma on the Uncompahgre Plateau, Colorado. Colorado Division of Wildlife Technical Publication 40. Colorado Division of Wildlife

Anderson, C., R., and F. G. Lindzey. 2003. Estimating cougar predation rates from GPS location clusters. Journal of Wildlife Management 67:307-316.

Balme, G., L. Hunter, and R. Slotow. 2007. Feeding habitat selection by hunting leopards Panthera pardus in a woodland savanna: prey catchability versus abundance. Animal Behaviour 74:589-598.

Balme, G. A., R. Slotow, and L. T. B. Hunter. 2009. Impact of conservation interventions on the dynamics and persistence of a persecuted leopard (*Panthera pardus*) population. Biological Conservation 142:2681-2690.

Banfield, J. E. 2012. Cougar response to roads and predatory behaviour in southwestern Alberta. University of Alberta.

Baruch-Mordo, S., S. W. Breck, K. R. Wilson, and D. M. Theobald. 2008. Spatiotemporal Distribution of Black Bear–Human Conflicts in Colorado, USA. Journal of Wildlife Management 72:1853-1862.

Bednekoff, P. A., and S. L. Lima. 1998. Re-examining safety in numbers: interactions between risk dilution and collective detection depend upon predator targeting behaviour. Proceedings of the Royal Society B: Biological Sciences 265:2021-2026.

Beier, P. 1991. Cougar attacks on humans in the United States and Canada. Wildlife Society Bulletin 19:403-412.

Beier, P., D. Choate, and R. H. Barrett. 1995. Movement patterns of mountain lions during different behaviors. Journal of Mammalogy 76:1056-1070.

Berger-Tal, O., S. Mukherjee, B. P. Kotler, and J. S. Brown. 2009. Look before you leap: is risk of injury a foraging cost? Behavioral Ecology and Sociobiology 63:1821-1827.

Berger, J. 2007. Fear, human shields and the redistribution of prey and predators in protected areas. Biology Letters 3:620-623.

Birk, M. A., and J. W. White. 2014. Experimental determination of the spatial scale of a prey patch from the predator's perspective. Oecologia 174:723-729.

Bouskila, A., and D. T. Blumstein. 1992. Rules of thumb for predation hazard assessment: predictions from a dynamic model. The American Naturalist 139:161-176.

Brown, J. S. 1988. Patch use as an indicator of habitat preference, predation risk, and competition. Behavioral Ecology and Sociobiology 22:37-47.

_____. 1992. Patch use under predation risk: I. Models and predictions. Annales Zoologici Fennici 29:301-309.

Brown, J. S., and B. P. Kotler. 2004. Hazardous duty pay and the foraging cost of predation. Ecology Letters 7:999-1014.

Brown, J. S., J. W. Laundre, and M. Garung. 1999. The ecology of fear: optimal foraging, game theory, and trophic interactions. Journal of Mammalogy 80:385-399.

Burdett, C. L., K. R. Crooks, D. M. Theobald, K. R. Wilson, E. E. Boydston, L. M. Lyren, R. N. Fisher, T. W. Vickers, S. A. Morrison, and W. M. Boyce. 2010. Interfacing models of wildlife habitat and human development to predict the future distribution of puma habitat. Ecosphere 1:art4.

Burnham, K. P., and D. R. Anderson. 2002. Model selection and model inference: a practical information-theoretic approach. 2nd edition edition. Springer-Verlag, New York, NY, USA.

Charnov, E. L. 1976. Optimal foraging, the marginal value theorem. Theoretical Population Biology 9:129-136.

CMGWG. 2005. Cougar Management Guidelines, First Edition. WildFutures, Brainbridge Island, Washington.

Crooks, K. R., C. L. Burdett, D. M. Theobald, C. Rondinini, and L. Boitani. 2011. Global patterns of fragmentation and connectivity of mammalian carnivore habitat. Philosophical Transactions of the Royal Society B: Biological Sciences 366:2642-2651.

Cunningham, S. C., W. B. Ballard, and H. A. Whitlaw. 2001. Age structure, survival, and mortality of mountain lions in southeastern Arizona. The Southwestern Naturalist 46:76-80.

DiRienzo, N., J. N. Pruitt, and A. V. Hedrick. 2013. The combined behavioural tendencies of predator and prey mediate the outcome of their interaction. Animal Behaviour 86:317-322.

Duchesne, T., D. Fortin, and N. Courbin. 2010. Mixed conditional logistic regression for habitat selection studies. Journal of Animal Ecology 79:548-555.

Dupuch, A., L. M. Dill, and P. Magnan. 2009. Testing the effects of resource distribution and inherent habitat riskiness on simultaneous habitat selection by predators and prey. Animal Behaviour 78:705-713.

Embar, K., A. Raveh, D. Burns, and B. P. Kotler. 2014. To dare or not to dare? Risk management by owls in a predator-prey foraging game. Oecologia 175:825-834.

Emlen, J. M. 1966. The role of time and energy in food preference. The American Naturalist 100:611-617.

_____. 1968. Optimal choice in animals. The American Naturalist 102:385-389.

Fa, J. E., and D. Brown. 2009. Impacts of hunting on mammals in African tropical moist forests: a review and synthesis. Mammal Review 39:231-264.

Fortin, D., H. L. Beyer, M. S. Boyce, D. W. Smith, T. Duchesne, and J. S. Mao. 2005. Wolves influence elk movements: behavior shapes a trophic cascade in yellowstone national park. Ecology 86:1320-1330.

Fraker, M. E., and B. Luttbeg. 2012. Effects of perceptual and movement ranges on joint predator-prey distributions. Oikos 121:1935-1944.

Holmes, B. R., and J. W. Laundré. 2006. Use of open, edge, and forest areas by pumas *Puma concolor* in winter: are pumas foraging optimally? Wildlife Biology 12:201-209.

Hopcraft, J. G. C., A. R. E. Sinclair, and C. Packer. 2005. Planning for success: Serengeti lions seek prey accessibility rather than abundance. Journal of Animal Ecology 74:559-566.

Houston, A. I., and J. M. McNamara. 2014. Foraging currencies, metabolism and behavioural routines. Journal of Animal Ecology 83:30-40.

Husseman, J. S., D. L. Murray, G. Power, C. Mack, C. R. Wenger, and H. Quigley. 2003. Assessing differential prey selection patterns between two sympatric large carnivores. Oikos 101:591-601.

Inskip, C., and A. Zimmermann. 2009. Human-felid conflict: a review of patterns and priorities worldwide. Oryx 43:18.

Jaksić, F. M., H. W. Greene, and J. Yáñez. 1981. The guild structure of a community of predatory vertebrates in central Chile. Oecologia 49:21-28.

Jeschke, J. M. 2007. When carnivores are "full and lazy". Oecologia 152:357-364.

Johnson, D. D., and D. C. Ganskopp. 2008. GPS Collar Sampling Frequency: Effects on Measures of Resource Use. Rangeland Ecology & Management 61:226-231.

Johnson, D. H. 1980. The comparison of usage and availability measurements for evaluating resource preference. Ecology 61:65-71.

Johst, K., and R. Brandl. 1997. Body size and extinction risk in a stochastic environment. Oikos 78:612-617.

Kaczensky, P. 1999. Large carnivore depredation on livestock in Europe. Ursus 11:59-72.

Kertson, B. N., R. D. Spencer, J. M. Marzluff, J. Hepinstall-Cymerman, and C. E. Grue. 2011. Cougar space use and movements in the wildland-urban landscape of western Washington. Ecological Applications 21:2866.

Knopff, K. H. 2010. Cougar predation in a multi-prey system in west-central Alberta. PhD, University of Alberta.

Krebs, J. R., J. C. Ryan, and E. L. Charnov. 1974. Hunting by expectation or optimal foraging? A study of patch use by chickadees. Animal Behaviour 22:953-964.

Laundré, J. W. 2010. Behavioral response races, predator-prey shell games, ecology of fear, and patch use of pumas and their ungulate prey. Ecology 91:2995-3007.

Laundré, J. W., L. Hernández, and K. B. Altendorf. 2001. Wolves, elk, and bison: reestablishing the "landscape of fear" in Yellowstone National Park, U.S.A. Canadian Journal of Zoology 79:1401-1409.

Laundré, J. W., L. HernÁNdez, D. Streubal, K. B. Altendorf, and C. A. L. González. 2000. Aging mountain lions using gum-line recession. Wildlife Society Bulletin 28:963-966.

Lima, S. L. 2002. Putting predators back into behavioral predator-prey interactions. Trends in Ecology and Evolution 17:70-75.

Lima, S. L., and L. M. Dill. 1990. Behavioral decisions made under the risk of predation: a review and prospectus. Canadian Journal of Zoology 68:619-640.

Linnell, John D., J. Odden, M. E. Smith, R. Aanes, and J. E. Swenson. 1999. Large carnivores that kill livestock: do "problem individuals" really exist. Wildlife Society Bulletin 27: 698-705.

Löe, J., and E. Röskatt. 2004. Large carnivores and human safety: a review. Ambio 33:283-288.

MacArthur, R. H., and E. R. Pianka. 1966. On optimal use of a patchy environment. The American Naturalist 100:603-609.

Maclennan, S. D., R. J. Groom, D. W. Macdonald, and L. G. Frank. 2009. Evaluation of a compensation scheme to bring about pastoralist tolerance of lions. Biological Conservation 142:2419-2427.

Madden, F. 2004. Creating Coexistence between Humans and Wildlife: Global Perspectives on Local Efforts to Address Human–Wildlife Conflict. Human Dimensions of Wildlife 9:247-257.

Mangel, M., and C. W. Clark. 1986. Towards a unified foraging theory. Ecology 67:1127-1138.

McNamara, J. M., and A. I. Houston. 1987. Starvation and predation as factors limiting population size. Ecology 68:1515-1519.

McPhee, H. M., N. F. Webb, and E. H. Merrill. 2012. Hierarchical predation: wolf (*Canis lupus*) selection along hunt paths and at kill sites. Canadian Journal of Zoology 90:555-563.

Murray, D. L., S. Boutin, and M. O'Donoghue. 1994. Winter habitat selection by lynx and coyotes in relation to snowshoe hare abundance. Canadian Journal of Zoology 72:1444-1451.

Nilsen, E. B., T. Pettersen, H. Gundersen, J. M. Milner, A. Mysterud, E. J. Solberg, H. P. Andreassen, and N. C. Stenseth. 2005. Moose harvesting strategies in the presence of wolves. Journal of Applied Ecology 42:389-399.

Norberg, R. A. 1977. An ecological theory on foraging time and energetics and choice of optimal food-searching method. Journal of Animal Ecology 46:511-529.

Northrup, J. M., J. Pitt, T. B. Muhly, G. B. Stenhouse, M. Musiani, M. S. Boyce, and N. Pettorelli. 2012. Vehicle traffic shapes grizzly bear behaviour on a multiple-use landscape. Journal of Applied Ecology 49:1159-1167.

Noss, R. F., H. B. Quigley, M. G. Hornocker, T. Merrill, and P. C. Paquet. 1996. Conservation biology and carnivore conservation in the Rocky Mountains. Conservation Biology 10:949-963.

Nussey, D. H., A. J. Wilson, and J. E. Brommer. 2007. The evolutionary ecology of individual phenotypic plasticity in wild populations. Journal of Evolutionary Biology 20:831-844.

Nyhus, P. J., and R. Tilson. 2004. Characterizing human-tiger conflict in Sumatra, Indonesia: implications for conservation. Oryx 38.

Ordiz, A., O. G. Stoen, M. Delibes, and J. E. Swenson. 2011. Predators or prey? Spatio-temporal discrimination of human-derived risk by brown bears. Oecologia 166:59-67.

Orlando, A. M. 2008. Impacts of rural development on puma ecology in California's Sierra Nevada. PhD, University of California Davis, Davis, CA, USA.

Pierce, B. M., V. C. Bleich, J. D. Wehausen, and R. T. Bowyer. 1999. Migratory patterns of mountain lions: implications for social regulation and conservation. Journal of Mammalogy 80:986-992.

Pierce, B. M., R. T. Bowyer, and V. C. Bleich. 2004. Habitat selection by mule deer: forage benefits or risk of predation? Journal of Wildlife Management 68:533-541.

Pierce, B. M., V. C. Vleich, and R. T. Bowyer. 2000. Social organization of mountain lions: does a land-tenure system regulate population size? Ecology 81:1533-1543.

Pojar, T. M., D. C. Bowden, and Morgart. 2004. Neonatal Mule Deer Fawn Survival in West-Central Colorado. Journal of Wildlife Management 68:550-560.

Reale, D., A. G. McAdam, S. Boutin, and D. Berteaux. 2003. Genetic and plastic responses of a northern mammal to climate change. Proceedings of the Royal Society B: Biological Sciences 270:591-596.

Reynolds, J. C., and S. C. Tapper. 1996. Control of mammalian predators in game management and conservation. Mammal Review 36:127-155.

Reynolds, T. D., and J. W. Laundre. 1990. Time intervals for estimating pronghorn and coyote home ranges and daily movements. Journal of Wildlife Management 54:316-322.

Roberts, G. 1996. Why individual vigilance declines as group size increases. Animal Behavior 51:1077-1086.

Shochat, E., S. B. Lerman, J. M. Anderies, P. S. Warren, S. H. Faeth, and C. H. Nilon. 2010. Invasion, Competition, and Biodiversity Loss in Urban Ecosystems. Bioscience 60:199-208.

Shochat, E., P. S. Warren, S. H. Faeth, N. E. McIntyre, and D. Hope. 2006. From patterns to emerging processes in mechanistic urban ecology. Trends in Ecology and Evolution 21:186-191.

Sih, A. 1984. The behavioral response race between predator and prey. The American Naturalist 123:143-150.

Sih, A., A. Bell, and J. C. Johnson. 2004. Behavioral syndromes: an ecological and evolutionary overview. Trends in Ecology and Evolution 19:372-378.

Sih, A., G. Englund, and D. Wooster. 1998. Emergent impacts of multiple predators on prey. Trends in Ecology and Evolution 13:350-355.

Smith, J. A., Y. Wang, and C. C. Wilmers. 2015. Top carnivores increase their kill rates on prey as a response to human-induced fear. Proceedings of the Royal Society B: Biological Sciences 282.

Spong, G. 2002. Space use in lions, Panthera leo , in the Selous Game Reserve: social and ecological factors. Behavioral Ecology and Sociobiology 52:303-307.

Storfer, A., M. A. Murphy, J. S. Evans, C. S. Goldberg, S. Robinson, S. F. Spear, R. Dezzani, E. Delmelle, L. Vierling, and L. P. Waits. 2007. Putting the "landscape" in landscape genetics. Heredity 98:128-142.

Sweanor, L. L., K. A. Logan, J. W. Bauer, B. Millsap, and W. M. Boyce. 2008. Puma and Human Spatial and Temporal Use of a Popular California State Park. Journal of Wildlife Management 72:1076-1084.

Theobald, D. M. 2005. Landscape patterns of exurban growth in the USA from 1980 to 2020. Ecology and Society 25:999-1011.

Thompson, D. J., J. A. Jenks, and D. M. Fecske. 2014. Prevalence of human-caused mortality in an unhunted cougar population and potential impacts to management. Wildlife Society Bulletin 38:341-347.

Thurfjell, H., S. Ciuti, and M. S. Boyce. 2014. Applications of step-selection functions in ecology and conservation. Movement Ecology 2:4.

Torres, S. G., T. M. Mansfield, J. E. Foley, T. Lupo, and A. Brinkhaus. 1996. Mountain lion and activity in california: testing speculations. Wildlife Society Bulletin 24:451-460.

Valeix, M., G. Hemson, A. J. Loveridge, G. Mills, and D. W. Macdonald. 2012. Behavioural adjustments of a large carnivore to access secondary prey in a human-dominated landscape. Journal of Applied Ecology 49:73-81.

Wilmers, C. C., Y. Wang, B. Nickel, P. Houghtaling, Y. Shakeri, M. L. Allen, J. Kermish-Wells, V. Yovovich, and T. Williams. 2013. Scale dependent behavioral responses to human development by a large predator, the puma. PLoS One 8:e60590.

Wilson, D. S., A. B. Clark, K. Coleman, and T. Dearstyne. 1994. Shyness and boldness in humans and other animals. Trends in Ecology and Evolution 9:442-445.

Wolf, M., and F. J. Weissing. 2012. Animal personalities: consequences for ecology and evolution. Trends in Ecology and Evolution 27:452-461.

Woodroffe, R. 2000. Predators and people: using human densities to interpret declines of large carnivores. Animal Conservation 3:165-173.

Wright, J. K. 1936. A method of mapping densities of population with Cape Cod as an example. Geographical Review 26:103-110.

Zeller, K. A., K. McGarigal, P. Beier, S. A. Cushman, T. W. Vickers, and W. M. Boyce. 2014. Sensitivity of landscape resistance estimates based on point selection functions to scale and behavioral state: pumas as a case study. Landscape Ecology 29:541-557.

APPENDIX 1: NETLOGO PROGRAMMING CODE

Code used in the NetLogo environment for "CamEncounter" (I) and "CamHabitat" (II) agent-based models for generating the theoretical datasets used in Chapter 1.

I. "CamEncounter"

```
;"CamEncounter"
;NetLogo 5.1.0
;Blecha K.A. and R.B. Boone
;October 2014
;Natural Resources Ecology Laboratory
;Department of Ecosystems Science and Sustainability
;Colorado State University

;************* INPUT PARAMTERS ********************************************
;Enter values for parameters of interest:
;Alternatively these could be included as sliders in the GUI
to input-parameters
  set MOVE 1
  set ABUND 5
  set DELAY 1
  set FOVDIST 13.0
  ;Study length of on normal day = 86,400 ticks (tick = 1 sec),
  ;while a week would equal 604,800 ticks.
  set study-length 86400
  set turning-stdv 5
  set HOMERAD 50
  ;Displaying the patches utilization counts will make the model run slower.
  ;Utilization will discontinue being tallied when this is toggled off.
  set display-utilization-distribution FALSE
end
;************************************************************
breed [ cameras camera ]
breed [ animal one-animal ]
breed [ rangecenters one-rangecenter ]
patches-own [ centroid
              x-edge-pixel
              y-edge-pixel
              usage]
globals [ ;other
          display-utilization-distribution
          xpos
          ypos
          seconds
          ;response variables:
          total-triggers
          mean-triggers
          cam0triggers
          cam1triggers
          cam2triggers
          cam3triggers
          ;parameters to test:
          MOVE ABUND DELAY FOVDIST HOMERAD study-length turning-stdv ]
cameras-own [ triggers waiting lag currentcount encounter-rate]
animal-own  [ center-xpos center-ypos current-distance ]
;************** SETUP *****************
to setup
  clear-all
  input-parameters
  setup-cameras
  setup-patches
  setup-agents
  reset-ticks
end

;************** SETUP-AGENTS ***************
to setup-agents
;: generate home range centers
 ask n-of ABUND patches with [pcolor = black] [set pcolor blue]
  ask patches with [pcolor = blue] [
    sprout-animal 1 [
```

```
      set size 7
      set color brown
      set center-xpos pxcor
      set center-ypos pycor ]
  ]
end
;************** SETUP-CAMERAS ***************
to setup-cameras
  let camcoordinates  [
    [50 50][150 50]
    [50 150][150 150] ]
;make the number of forest cameras created the length of the respective coordinate list above
create-cameras length camcoordinates
(foreach (sort cameras) camcoordinates [           ;not sure exactly how this line works...
  ask ?1 [ setxy item 0 ?2 item 1 ?2              ;not sure exactly how this line works...
           set shape "camera"
           set heading 0
           set size 7
           set color blue]
])
end
;************** SETUP-PATCHES ***************
to setup-patches
  ask cameras [
     ask patches in-cone ( FOVDIST ) 42  [
       set pcolor yellow
     ]
  ]
end
;************** GO **************
to go
  if ( study-length <= ticks )
    [
      ask patches [set pcolor scale-color (red - 5) usage 0 10]
      stop ]
  travel
  assess
  tick
end
;************** MOVE ****************
to travel
      ask animal [
         ifelse (current-distance > HOMERAD )
            [ facexy center-xpos center-ypos
              set heading heading + random-normal 0 20
              forward (MOVE)]
            [ let tangle  random-normal 0 turning-stdv
              set heading  heading + tangle
              forward ( MOVE )]
         set current-distance distancexy center-xpos center-ypos
         if display-utilization-distribution = TRUE [set usage usage + 1]
      ]
end
;*************** ASSESS ****************
to assess
  ask cameras
  [if lag <= 0 and waiting = FALSE
    [ set triggers triggers + (count animal in-cone FOVDIST 42)
      set currentcount (count animal in-cone FOVDIST 42)
      ifelse currentcount >= 1
        [set lag DELAY
         ask patches in-cone FOVDIST 42
           [ set pcolor red ] ]
        [ask patches in-cone FOVDIST 42
           [ set pcolor yellow ]
        ]
    ]
   ifelse lag > 1
      [ set waiting TRUE ]
      [ set waiting FALSE ]
   set lag lag - 1
   ]
  ; report the counts and encounter rate
  set total-triggers ( sum [ triggers ] of cameras )
  if display-utilization-distribution = TRUE [ask patches [set pcolor scale-color (red - 5) usage 0 15] ]
  set mean-triggers ( mean [ triggers ] of cameras ) ;averages the snaps across cameras for this camera type
  ask camera 0 [set cam0triggers triggers]
  ask camera 1 [set cam1triggers triggers]
  ask camera 2 [set cam2triggers triggers]
  ask camera 3 [set cam3triggers triggers]
end
```

II. “CamHabitat”

```
;”CamHabitat”
;NetLogo 5.1.0
;Blecha K.A. and R.B. Boone
;October 2014
;Natural Resources Ecology Laboratory
;Department of Ecosystems Science and Sustainability
;Colorado State University

extensions [ gis ]
globals [ thematic euc_forest euc_grass
          sec day
          movement-type? camera-id-list g-xlist g-ylist
          mean-gsnaps
          mean-fsnaps
          camera_forest_utilization
          actual_forest_utilization
          half-fov-width
          x-right-offset ]
patches-own [ code forest-dist grass-dist]
breed [ gcameras gcamera]
breed [ fcameras fcamera]
breed [ deer ]
gcameras-own [ gsnaps gdelay gwaiting gcurrentcount ]
fcameras-own [ fsnaps fdelay fwaiting fcurrentcount ]
deer-own [ ftime gtime f_utilization ]
;;************** SETUP ********************************************************************************
to Setup-Habitat
  clear-all
  __clear-all-and-reset-ticks
;;load appropriate asci layers
  set thematic gis:load-dataset "input/habitat.asc"
  set euc_forest gis:load-dataset "input/euc_forest.asc"
  set euc_grass gis:load-dataset "input/euc_grass.asc"
  gis:set-world-envelope gis:envelope-of thematic
  display-thematic-in-patches
  display-euc_forest-in-patches
  display-euc_grass-in-patches
  ask n-of ABUND patches with [ pcolor = green ]
       [
       sprout-deer 1
         [set size 8
          set color brown]
       ]
  set half-fov-width round((tan (0.5 * FOVANGLE)) * FOVDIST  )
  set x-right-offset round((100 - half-fov-width))
  setup-cameras
  set day 1
end
;;************** Habitat ************************************************************************************************
to display-thematic-in-patches
;;assigns raster values to the patches by "lining up" the raster with the world settings,
;;world settings in this case need to match the number of pixels in the raster
 let min-code gis:minimum-of thematic
  gis:apply-raster thematic code
  let max-code gis:maximum-of thematic
  ask patches
    [ if (code = 1) [ set pcolor yellow]   ;;grassland
      if (code = 2) [ set pcolor green] ]   ;;forested
end
to display-euc_forest-in-patches
  gis:apply-raster euc_forest forest-dist
  let min-forest-dist gis:minimum-of euc_forest
  let max-forest-dist gis:maximum-of euc_forest

end
to display-euc_grass-in-patches
  gis:apply-raster euc_grass grass-dist
  let min-grass-dist gis:minimum-of euc_grass
  let max-grass-dist gis:maximum-of euc_grass
end
to check-display
  ifelse show-euclidean-distance-rasters?
      [  gis:paint euc_forest green
         gis:paint euc_grass yellow ]
      [ clear-drawing   ]
end
```

```
;;************** SETUP-CAMERA ********************************************************************************
to setup-cameras
;;enter a list of the coordinates where the forest-cameras should be placed,
;;the number of xy sets will be the number of cameras created
let fcoordinates [
[0   0][400 0][200 200][600 200][0   400][400 400][200 600][600 600]
[100 100][500 100][300 300][700 300][100 500][500 500][300 700][700 700]  ]
let gcoordinates [
[200 0][600 0][0 200][400 200][200 400][600 400][400 600][0 600]
[300 100][700 100][500 300][100 300][300 500][700 500][500 700][100 700]  ]
;;make the number of forest cameras created the length of the respective coordinate list above
;;not sure exactly how this line works...
create-fcameras length fcoordinates
(foreach (sort fcameras) fcoordinates [
    ; limits the x and y camera positions so that FOV does not overlap adjacent habitats
     ask ?1 [
        setxy  ((item 0 ?2) + half-fov-width)
                + random ( ( (item 0 ?2) + x-right-offset ) - ((item 0 ?2) + half-fov-width) )
         (item 1 ?2) + random (100 - FOVDIST )
         set shape "camera"
         set shape "camera"
         set heading 0
          set size 15
          set color blue]
          set heading 0
          set size 15
          set color blue]  ]   )
create-gcameras length gcoordinates
(foreach (sort gcameras) gcoordinates [
;; limits the x and y camera positions so that FOV does not overlap adjacent habitats
  ask ?1 [
        setxy  ((item 0 ?2) + half-fov-width)
                + random ( ( (item 0 ?2) + x-right-offset ) - ((item 0 ?2) + half-fov-width) )
         (item 1 ?2) + random (100 - FOVDIST )
         set shape "camera"
         set shape "camera"
         set heading 0
         set size 15
         set color blue] ] )
ask gcameras
    [ask patches in-cone  FOVDIST FOVANGLE
       [set pcolor black ] ]
ask fcameras
     [ask patches in-cone  FOVDIST FOVANGLE
       [set pcolor red ] ]
end
;;************** GO*****************************************************************************************
to go
    if ( study-length-days * day-length <= ticks )
        [ stop ]
    set sec sec + 1

    if ( sec >= 0 and  sec < (forest-seeking-proportion * day-length ) )
       [set movement-type? "forest-seeking"]
    if (sec >= (forest-seeking-proportion * day-length ) and sec < (1 * day-length ) )
       [set movement-type? "grass-seeking"]
    if ( sec >= (1 * day-length ) )
       [set sec 0
        set day day + 1]
    assess-cameras
    assess-deer-patch-selection
    move
    check-display
    tick
end
;;************** MOVE ****************************************************************************************
to move
  ask deer
     [if (movement-type? = "forest-seeking")
        [  ifelse pcolor = yellow
          [downhill-forest-code
            forward f-move-rate]
          [random-walk]  ]
      if (movement-type? = "grass-seeking")
        [  ifelse pcolor = green
          [downhill-grass-code
            forward g-move-rate]
          [random-walk]  ]  ]
end
to random-walk
       let tangle  random-normal 0 turning-stdv
```

```
        set heading  heading + tangle
        ifelse (movement-type? = "forest-seeking" )
             [ forward  f-move-rate ]
             [ forward  g-move-rate ]
end
;;  deer will turn toward a lower patches with relatively lower crop-euclidean distance values
to downhill-grass-code
   ;;  sets the scent-ahead parameter to the patch the deer is currently facing:
 let scent-ahead grass-dist-at-angle 0
   ;;  sets the scent-right parameter angle to 45 degrees (right and ahead):
  let scent-right grass-dist-at-angle 45
  ;;  sets the scent-right parameter angle to -45 degrees (left and ahead):
  let scent-left grass-dist-at-angle -45
  ;;  determines if there is a difference between scent-right and scent-left:
   if ( scent-right < scent-ahead ) or ( scent-left < scent-ahead )
   ;;  if crop euclidean distance is lesser value to the right, then turn towards the right:
   ;;  if crop euclidean distance is lesser value to the left, then turn towards the left:
    [ ifelse scent-right < scent-left
        [ rt random-normal 45 turning-stdv]
        [ lt random-normal 45 turning-stdv]   ]
end
to downhill-forest-code
 let scent-ahead forest-dist-at-angle 0
 let scent-right forest-dist-at-angle 45
 let scent-left forest-dist-at-angle -45
   if ( scent-right < scent-ahead ) or ( scent-left < scent-ahead )
      [ ifelse scent-right < scent-left
        [ rt random-normal 45 turning-stdv]
        [ lt random-normal 45 turning-stdv]   ]
end
to-report grass-dist-at-angle [ angle ]
    let p patch-right-and-ahead angle 1
     if p = nobody [ report 0 ]
    report [ grass-dist ] of p
end
to-report forest-dist-at-angle [ angle ]
    let p patch-right-and-ahead angle 1
       if p = nobody [report 0 ]
      report [ forest-dist ] of p
end
;;*************** ASSESS ***************************************************************************************
to assess-cameras
  ask fcameras [
    if fdelay <= 0 and fwaiting = FALSE [
      ask deer in-cone FOVDIST  FOVANGLE
          [set color white]
      set fsnaps fsnaps + (count deer in-cone FOVDIST  FOVANGLE)
      set fcurrentcount (count deer in-cone FOVDIST   FOVANGLE)
      if fcurrentcount >= 1
        [set fdelay DELAY]    ]
    ifelse fdelay > 1
      [ set fwaiting TRUE ]
      [ set fwaiting FALSE ]
    set fdelay fdelay - 1     ]
 ask gcameras [
    if gdelay <= 0 and gwaiting = FALSE [
      ask deer in-cone FOVDIST  FOVANGLE
          [set color white]
      set gsnaps gsnaps + (count deer in-cone FOVDIST  FOVANGLE)
      set gcurrentcount (count deer in-cone FOVDIST  FOVANGLE)
      if gcurrentcount >= 1
         [set gdelay DELAY]   ]
    ifelse gdelay > 1
      [ set gwaiting TRUE ]
      [ set gwaiting FALSE ]
    set gdelay gdelay - 1     ]
  ask deer [
    if pcolor = green or pcolor = yellow
     [set color brown]
  ]
  ;;averages the snaps across cameras for this camera type
  set mean-fsnaps ( mean [ fsnaps ] of fcameras )
  set mean-gsnaps ( mean [ gsnaps ] of gcameras )
  if mean-fsnaps > 0 and mean-gsnaps > 0
      [ set camera_forest_utilization ( mean-fsnaps / (mean-fsnaps + mean-gsnaps ) ) ]
end
to assess-deer-patch-selection
  ask deer [
   if pcolor = green
        [ set ftime ftime + 1 ]
      if pcolor = yellow
```

```
        [ set gtime gtime + 1 ]
      if ftime > 0 and gtime > 0 [
      set f_utilization ( (ftime / (ftime + gtime) ) )    ]    ]
  set actual_forest_utilization ( mean [ f_utilization ] of deer )
end
;;***************** RESTORE-DEFAULTS ***************************************************************************
to restore-defaults
  set FOVANGLE 42
  set g-move-rate 0.8
  set f-move-rate 0.8
  set turning-stdv 5.0
  set ABUND 20
  set turning-stdv 5.0
  set FOVDIST  20.0
  set day-length 86400
  set study-length-days 1
end
```

APPENDIX 2: QUANTIFICATION OF HOUSING DEVELOPMENT ACROSS AN URBAN TO RURAL LANDSCAPE

SUMMARY

This appendix gives the methods for deriving the Housing Density Model used in Chapters 2 and Chapters 3. This appendix provides: 1) detailed methods for derivation of the HDM and discussion on how this model is an improvement over other published models, 2) detailed methods for derivation of a data layer depicting distance to man-made roofed structures (STRUC), 3) an additional description and discussion on the anthropogenic development nature of the section of the Front Range foothills for which the HDM and STRUC were initially created for.

INTRODUCTION

Identifying the presence and intensity of anthropogenic development is an important component in ecological studies whose goal is to understand whether anthropogenic development is perceived by the organism(s) of interest to be a behavioral disturbance or related to the population- or community- level perturbation of organisms. Consistently defining and quantifying what a human modified site actually is has been met with only little success in early models (Theobald 2004). Housing development is frequently measured as a potential anthropogenic disturbance as it is where most human activities take place. It is important that the human component be identified in a quantitative manner that provides measures meaningful to the system of interest. How housing developments are measured and the spatial scale of which measurements are gathered (Turner et al. 1989, Levin 1992) will likely influence analysis. For instance, if specific housing locations are known, distance based analysis can be conducted to

test influences of spatial proximity. In other cases, human or housing densities can be mapped on the landscape to give true areal density estimates on a per pixel basis.

When choosing a modeled dataset to represent the extent and intensity of human density on the landscape, one must consider several aspects; the spatial extent of the dataset, quantitative versus qualitative measures, accuracy, and grain size (Li and Wu 2004, Linke and Franklin 2006). Widely available datasets such as the National Land Cover Dataset (NLCD) (Homer et al. 2007) may be attractive to a researcher studying some forms of anthropogenic development at the national scale, but a poor choice for a study interested in housing intensities as it merely provides a qualitative depiction of human influence. For instance, NLCD defines four land cover types indexing the intensity of development, two landcover types indexing agricultural lands and one indexing natural or human modified barren land (no vegetative cover). Land cover maps such as NLCD and Southwest GAP (Prior-Magee et al. 2007) utilize measures of non-permeable surfaces or other remote sensing data to depict a qualitative classification of human development at fine scales (~30 m). While it is likely that housing development is correlated with more impervious surfaces, this relationship does not hold within the range of rural or even exurban (also known as "ranchette" or "exurbia") housing densities (Theobald 2001). Readily available landcover datasets perform poorly when quantifying the distinction between areas of little development (i.e., rural) and exurban developments (Theobald 2001, Theobald 2005). A vector based representation, such as the U.S. Census Bureau's Topographically Integrated Geographic Encoding and Referencing (TIGER) data gives distinct counts of housing units for a hierarchy of subsettable geographic scales (i.e., census tract, block-group, and block) to provide information for chloropeth mapping, but is subject to the modifiable areal unit problem (Jelinski and Wu 1996). Parcel polygons can also be converted into depictions of housing based on expected

parcel size (Thomas et al. 2009) and the premise that zoning regulations of rural areas are often limited to one housing unit per parcel.

A vast improvement from using land cover, census data, or parcel tract data alone, is the use of dasymetric mapping techniques (Wright 1936). With this approach, count data derived for a larger mapping unit, such as that provided by census data, is redistributed for a smaller mapping unit using ancillary data such as land cover (Yuan et al. 1997), roads (Reibel and Bufalino 2005, Theobald 2005, Shrestha and Conway 2013), or parcel data (Tapp 2010). The Spatially Explicit Regional Growth Model (SERGoM) (Theobald 2005) is one example using census bureau block level counts and road density, which provides a housing density map for a nationwide extent at a 1 ha grain size (100 x 100 m cell). Although SERGoM maintains pycnophylactic properties (Tobler 1979) down to the spatial scale of the census block, accuracy of cells within a block is questionable based on the assumption that housing densities are perfectly correlated with road densities. While this assumption is reasonable with respect to correlations between road density and housing density (Shrestha and Conway 2013), it is unreasonable to assume that housing densities are equivalent along the same linear stretch of road within the census block (Reibel and Bufalino 2005).

Spatial proximity to sources of disturbance is a common measure to represent the potential risk perceived by an organism. Measures and indices incorporating spatial proximity have become important in connectivity and meta-population analysis (Lima and Zollner 1996). The quantity may be measured in the field with survey equipment, but is increasingly measured with computerized spatial analysis techniques. Remote imagery can often provide housing locations with the aid of trained observers or automated imagery classification software. If all structure locations are obtained within a region of interest, Euclidean distance maps created on a

cell by cell basis provide areal quantities that may be further described by the inherent spatial patterns they exhibit across a landscape. A quantity that incorporates both the intensity of human development and the spatial proximity may also be of interest, such as that provided by kernel density estimation techniques.

The Rocky Mountains of Colorado have been a host to many studies on anthropogenic development. This area is particularly interesting as an influx of immigrants over the last few decades (Manfredo and Zinn 1996) appears to be driven by recreational opportunities or the charismatic landscape itself rather than economic opportunities associated with natural resource extraction (i.e., agricultural, mining) or large urban centers (Riebsame et al. 1996). Like much of the Rocky Mountain west, mining, logging, ranching, and provisions of the 1862 Homestead Act initially drew people to the Front Range region. However, the more rugged areas were inaccessible to the transportation methods of the time. These areas, mostly in higher elevations, remain under federal ownership to this day. Anthropogenic development of the rural Front Range region is driven not only by the charismatic landscape reasons mentioned above, but also by the proximity to larger urban centers (i.e., Denver), allowing people to take advantage of both natural and metropolitan amenities (Davis and Nelson 1994). Public lands occur as a result of the historic federal land holdings and more recent acquisitions by local government agencies to help curb urban sprawl. The matrix of public lands can influence the placement of housing sites, as housing sites located immediately adjacent to the public lands are preferred (Irwin 2002, Wade and Theobald 2010, Hannum et al. 2012). A characteristic of this patchwork of public and private land is the abrupt changes in housing density observed within a small area; thus presenting a challenge when quantifying spatial patterns of development.

The overarching goal for this project was to yield meaningful quantity-based data layers to represent the extent of anthropogenic development in a foothills ecosystem of the Colorado Front Range marked by a rural to urban gradient. The first objective was to create a vector based depiction of structure locations (point map) within the study area. The second objective was to create a flexible and accurate housing density model (HDM). The HDM was created with a dasymetric mapping technique (Wright 1936, Mennis 2003) similarly implemented for SERGoM, but instead utilized the density of man-made roofed structures rather than the density of roads to allocate housing units across a census block. The HDM was produced at a baseline grain size of 1 ha, but was intended to be utilized at more sensible aggregation of 1 ha cells (i.e., 200 x 200 m, 300 x 300 m, etc.). The third objective was to summarize model outputs of housing density and the housing proximity.

METHODS

Study Area

The study area (6,424 km^2) focuses on a selection of 266 U.S. Census Bureau block-groups situated in the eastern slopes of the Colorado Front Range, bordered by the continental divide on the west and the urban fringes of the urban census areas of Denver, Boulder, and Fort Collins - Loveland on the east (Figure A2.1). Topography is similar along the longitudinal gradient, but transitions from 1,500 m elevation in the eastern fringes with plateaus and historic prairies to rugged peaks greater than 3,800 m in the west. Vegetation cover, as determined by Southwest GAP landcover types (Prior-Magee et al. 2007), is a mix of Introduced Perennial Grasslands and Forbs, Short Grass Prairie, and Agriculture in the prairie transition zone just below the foothills on the eastern fringe. Inside the foothills, Lower Montane Foothill Shrublands and Ponderosa Pine (*Pinus ponderosa*) woodlands in lower elevations give way to

Subalpine Mesic Spruce-Fir Forest and Woodlands as elevations increase above 2,500 m. Elevations above 3,300 m are described by Alpine Bedrock and Scree with interspersed Sub-alpine Montane Riparian Shrublands. Population size was 345,200 persons with a total of 158,727 housing units in 2010 and a mean 1,323 persons and 608 housing units per block-group (U.S. Census Bureau 2010). When referring to housing densities in this area, I used the levels defined by Theobald (2005): urban (< 0.1 ha per unit), suburban (0.1 – 0.68 ha per unit), exurban (0.68 – 16.18 ha per unit), and rural (> 16.18 ha per unit) housing density levels (equivalent housing units per ha: >10 units/ha, 1.47 – 10 units/ha, 0.0618 – 1.4706 units/ha, and <0.0618 units/ha respectively).

Structure Locations

To create a point location map of man-made roof structures, heads-up digitization was done using USGS high resolution (0.6 m) aerial ortho-imagery (2008) obtained for the study area. Using vector point layers, technicians assigned the approximate center of all man-made roofed structures with at least two sides greater than 3.5 m across. This distance would usually be sufficient to ensure that large trucks and recreational vehicles were not mistaken for a more fixed structure. All digitization was done within ArcMap 10.0 (ESRI, Redlands, CA) with the map scale set to 1:1,500. Three trained technicians were assigned a random subset of 4 km^2 quadrats (~2,400 total quadrats) superimposed over the study area along with a 2.5 km buffer of the perimeter. Quadrats were digitized in a randomized order to ensure that effort and potential errors were distributed evenly. If the identification of any particular structure was questionable, USDA Farm Service Agencies: National Aerial Imagery Program, which has 1 m resolution aerial photos (2006, 2009 and 2011 collection years) were consulted.

Ideally, each man-made roofed structure would equally represent one housing unit. However, a large number of uninhabited man-made roofed structures (out-buildings, barns, detached garages) were apparent in rural and exurban areas. To address this issue, parcel data was used to restrict the number of man-made roofed structures to just one randomly chosen digitized structure location per parcel. This was possible as local zoning regulations of the counties composing the study area only allow one housing unit per parcel, aside from parcels deemed multiple family units. This restriction was only applied to parcels lying within census block-groups where the housing unit density for the overall block-group was characterized by either rural (< 0.068 housing units / ha) or exurban quantities (0.068 – 1.47 housing units / ha) (Figure A2.1). In block-groups characterized by an overall suburban or urban density (> 1.47 units / ha) (Figure A2.1), a structure may actually hold multiple housing units (i.e., duplexes, apartment complexes, etc). However, the size of the suburban and urban block-groups (mean: 1.51 and 0.45 km^2) are much smaller than that of the rural and exurban block-groups (mean: 263.04 and 25.47 km^2), thus rendering less potential intra-block-group spatial error.

Housing Density Model Creation

Dasymetric processing steps using the parcel restricted point locations of man-made roofed structures and the TIGER polygon census block group boundaries containing the housing unit counts are shown in Figure A2.1. Dividing the study area into 1 ha cells, the count of man-made roofed structures (from the restricted layer created above) for cell (i) was identified as m_i. For each cell (i), the respective census block-group polygon (j) containing the cell's center was identified. Dividing the number of man-made roofed structures identified in a particular cell and block-group (m_{ij}) by the summation of all (k) man-made roofed structures in the block-group allowed a weighting factor for each cell of the block-group (ψ_{ij}) to be calculated. This

weighting factor was then multiplied by the total housing unit count of the block-group (n_j) for an estimated housing unit density (d_i) for each cell in units of "housing units per ha":

$$\psi_{ij} = \frac{m_{ij}}{\sum_{m=1}^{k} m_{ij}}$$

$$d_i = \psi_{ij} * n_j$$

Output of the 1 ha cell size was then aggregated to form other raster layers with multiples of the 1 ha (i.e., 200 m, 400 m, 600 m). Housing densities were classified into four discrete quantities, as defined by Theobald (2005). I assessed the effect of cell size choice on the measured areal extent of the four housing development levels with a simple scatter plot. A schematic of the processing steps is given in Figure A2.2

Spatial Proximity Layer Creation

Using the unrestricted man-made roofed structure layer, the Euclidean distance was measured for every cell within the study area boundary and its associated 2.5 km buffer. Because the algorithm searches all cells within the spatial extent defined, this buffer region was important to include for the more remote areas of the study area, whose quantities are easily influenced by the inclusion of just a single housing location. The 2.5 km buffer for the final product was then removed to ensure accuracy near the edges. To preserve the distance based measure from being too coarse while balancing processing time and accuracy associated with structure digitization, a 10 m grain size was retained in the final output. A summary of the final mapped product (layer: STRUC) using descriptive statistics is given.

RESULTS

A total 156,565 man-made roofed structures were manually digitized. Retaining one random man-made roofed structure for each parcel in the rural and exurban block-groups, 132,348 man-made roofed structures remained for the restricted structure layer. After creating the HDM at a range of grain sizes, the proportion of land area classified as rural, exurban, and a combined suburban-urban level varied depending on the scale chosen (Figure A2.3). The proportion of rural land was very high (>0.9) while the proportion of exurban land appeared low (<0.1) at the native grain size of 100 m. The proportion of suburban (~0.03) and urban (0.003) areas were relatively low and were thus combined for further analysis. In general, the rural areas were more apt to be classified into exurban as grain size increased, with a threshold appearing to be reached past 400 m, where proportions of rural and exurban areas leveled out, in terms of the rate of change, near 0.75 and 0.22 respectively. Output of the HDM classified into rural, exurban, suburban, and urban levels at an aggregated grain size of 500 m is shown in Figure A2.4.

The output Euclidean distance to man-made roofed structure raster (STRUC) is summarized using a histogram of the areal proportion and 400 m break points in Figure A2.5. The distribution follows a negative exponential pattern, where the most commonly encountered distance class was less than 400 m. Classifying the observed Euclidean distance into three natural quantiles (given the distribution of values produced for the study area) results in bins of 0-250 m, 250-1085 m, and 1085-10,640 m (Figure A2.4).

DISCUSSION

Having a full understanding of anthropogenic development is crucial for ecological studies attempting to assess the influence of humans on a species or system of interest.

Ecological studies generally incorporate anthropogenic spatial data as explanatory covariates in statistical models. Too often, landcover data is grabbed haphazardly from GIS libraries without an understanding of what is actually being represented. This project demonstrates a model of housing unit density produced from dyasmetric techniques combining remotely sensed aerial imagery depicting man-made roofed structures to spatially allocate counts of housing units throughout polygons provided by census data. The HDM is an improvement over previously published land cover models by providing a quantitative measure of human disturbances associated with housing developments. Specifically, the goals were to produce a model that maintained the ability to characterize abrupt changes in housing density across small spatial domains, to be spatially accurate at sensible grain sizes, and scalable to other resolutions of interest.

Abrupt Spatial Heterogeneity

Using man-made roofed structures as the fine-scale data source seems to be an improvement over past dasymetric models in the ability to depict abrupt spatial changes in housing densities. The fine-scale data source used to scale census counts in the SERGoM was derived using a moving neighborhood (a form of aggregation) with a search radius of 800 m when calculating road densities. This moving average approach produces a smoothed spatially autocorrelated quantity that obscures any spatially abrupt heterogeneity. Like many other cartographic works, the SERGoM used a binary mask informed by the presence of water bodies and public lands to define areas of zero housing densities. While these land features are a common source of abrupt housing density heterogeneity in much of our study area, they are unlikely to capture the source of heterogeneity in all localities (i.e., between high density exurban and adjacent rangelands).

Sensible Grain Size and Rescaling

The HDM model was created for a relatively small spatial extent, typical for ecological studies interested in large mammalian movement studies of individuals. If one were to develop this for a larger extent, it would be preferred that consistent aerial imagery is utilized. When examining the possible imagery sources available for this Front Range study area, obvious differences were apparent among the sources with respect to resolution, snow and cloud cover, and overall visual contrast between structures and the surrounding cover. For instance, if the HDM were to be created at the national scale, the USDA Farm Service Agencies: National Aerial Imagery Program provides this for the conterminous United States at a grain size of 1 m.

Most importantly, caution should be given when interpreting models of housing density giving output at small grain sizes (i.e. 1 ha). Users of the HDM presented here should take post-processing measures to aggregate the data to a larger grain size greater than 400 m to ensure that a more accurate representation of housing density is given at a per cell basis. Alternatively, one could take a moving window approach to calculate mean housing density from a specified search radius. If finer scales are needed (< 100 m grain), then a kernel density approach may be taken that accounts for the structure count within a specified search radius from focal points of interest (sampling points, animal locations, nesting or feeding sites) while also accounting for the number of structures within the radius. Other dasymetric modeling efforts, such as the SERGoM, give a misleading quantity for rural and exurban areas at the cell level given its native grain size of 100 m (1 ha). This small scale was implemented to ensure that the mapped areas conformed to the boundaries of blocks whose edges follow landscape features that often control the distribution of housing units. However, this scale is unable to characterize a gradient of densities within the rural setting, as a 1 ha cell of this size will usually only contain 0 or 1 house. If a single house is realized, then the density is automatically classified to be 1 house per ha, a

quantity that would automatically classify the cell to be of the exurban level rather than the rural level (assuming classification to levels is carried out). Given the processing steps related to binary masking of uninhabitable areas and the 800 m moving neighborhood approach, it is uncertain whether SERGoM output could be aggregated safely to larger more sensible grain sizes.

Suggested Future Improvements

While a human observer based digitization approach was used to identify the man-made roofed structures, future efforts could implement a more automated approach using supervised image classification. A total of 240 man hours of volunteer and student labor time was used to digitize the structures, which was more cost efficient than purchasing image classification software and professional time required for training an image classification algorithm, even if the volunteer time had been compensated with paid labor. However, if the spatial extent was any larger or covered more suburban and urban areas, then automated approaches would likely become more cost efficient. While inter- and intra-observer error was controlled for to ensure that these errors were not aggregated at any region of the study area, it is likely that some structures were missed in areas of high topographic relief where shadows were prone to occur. After structure digitization was complete, a cursory scan of other imagery sources (i.e., USDA NAIP imagery, ESRI, and Google Earth [accessed Dec 2010 – Dec 2012]) was made of privately owned, north-facing, steep hillsides where shadows were more likely to occur. No gross digitization errors, such as the complete exclusion of a small neighborhood or subdivision, appeared to have been made.

The HDM could have been produced using census counts from the block level, the smallest unit used by the Census Bureau, rather than the larger block-group, to further ensure a

high level of accuracy. However, polygons can be very small at the block level, and thus problematic to fit any 1 ha cells within the polygon when it has an odd or linear shape. Even with the block-group data, odd linear shapes sometimes occurred near the boundaries, thus some error may have been introduced when assigning the 1 ha cells to the appropriate polygons.

Future studies may also benefit from utilizing detailed data derived from parcel data attributes that may provide clues to the number of occupants, the zoning type (i.e., residential or rural), and the number of structures. One could generate parcel centroids in all residential parcels to derive a proxy for housing locations, and forego aerial photo digitization. However, error would be expected to increase as parcel size increases, as there is no reason to believe that housing locations are more likely to occur in the center of every parcel, especially in the case of long linear parcels. Given that our study area covered several counties, parcel attributes, such as those concerning the presence or absence of structures were not consistently available.

Anthropogenic Development Characteristics in the Front Range

For this foothill system, rural densities characterized a vast majority (0.765) of the study area at the 500 x 500 m resolution. This was expected as 59% of the study area is public land (COMaP; Theobald et al. 2010), which is generally free of housing unless associated with the management and maintenance of those public lands. Despite the areal majority being composed of rural housing densities, after visually inspecting the HDM output of the mapped exurban areas, it appears that development in the foothills is sprawling, but relatively concentrated to bands and certain vicinities bounded by the public lands. Suburban and urban developments (e.g., towns or cities) were relatively scattered and present for only a small proportion of land area (0.033). The housing density model revealed that exurban levels represent a large areal proportion (0.202) of the east slope of the foothills of this Front Range system. Exurban housing

developments were clustered in localities far from incorporated towns, with densities occasionally reaching suburban levels. The relative areal ratio of suburban/urban to exurban housing of 0.16 approximated that reported for a nationwide trend (Theobald 2005). However, it is important to recognize that the composition measure is sensitive to where study area boundaries are drawn.

While various efforts have studied the influence of cities (suburban/urban) on animals (McKinney 2002, Ditchkoff et al. 2006), the influence from exurban development is understudied with the exception of a few published case studies (Hansen et al. 2005). It is possible that exurban development will be viewed negatively by some species, but positive by others (Goad et al. 2014). For this foothill region, I revealed that relatively few areas exist distant from a man-made structure. The sprawling nature of the exurban developments and the scattered single houses composing the rural extent create a situation where one third of this area is within 250 m of a housing unit, a distance within line of sight of many fauna.

The major roadways of the Front Range foothills appear to be highly correlated with canyon bottoms and drainages. On these roadways, housing developments have sprung up immediately adjacent to or completely within the canyon bottoms (Riebsame et al. 1996). In some canyons, recreation opportunities such as fishing, kayaking, rafting, and trail development are increasing. The rugged terrain and streams characterizing some of these canyons alone can exist as geographic barriers for some species. Combining the natural barriers, roadways, recreational areas, and housing developments, it is likely that fragmentation will eventually increase given future human population and development projections (Theobald 2005). Further exploration of the HDM and STRUC data may include formal statistical tests to gain a deeper

understanding into which natural, social, and historic factors may contribute to the placement of housing developments at the landscape and site scales.

FIGURES

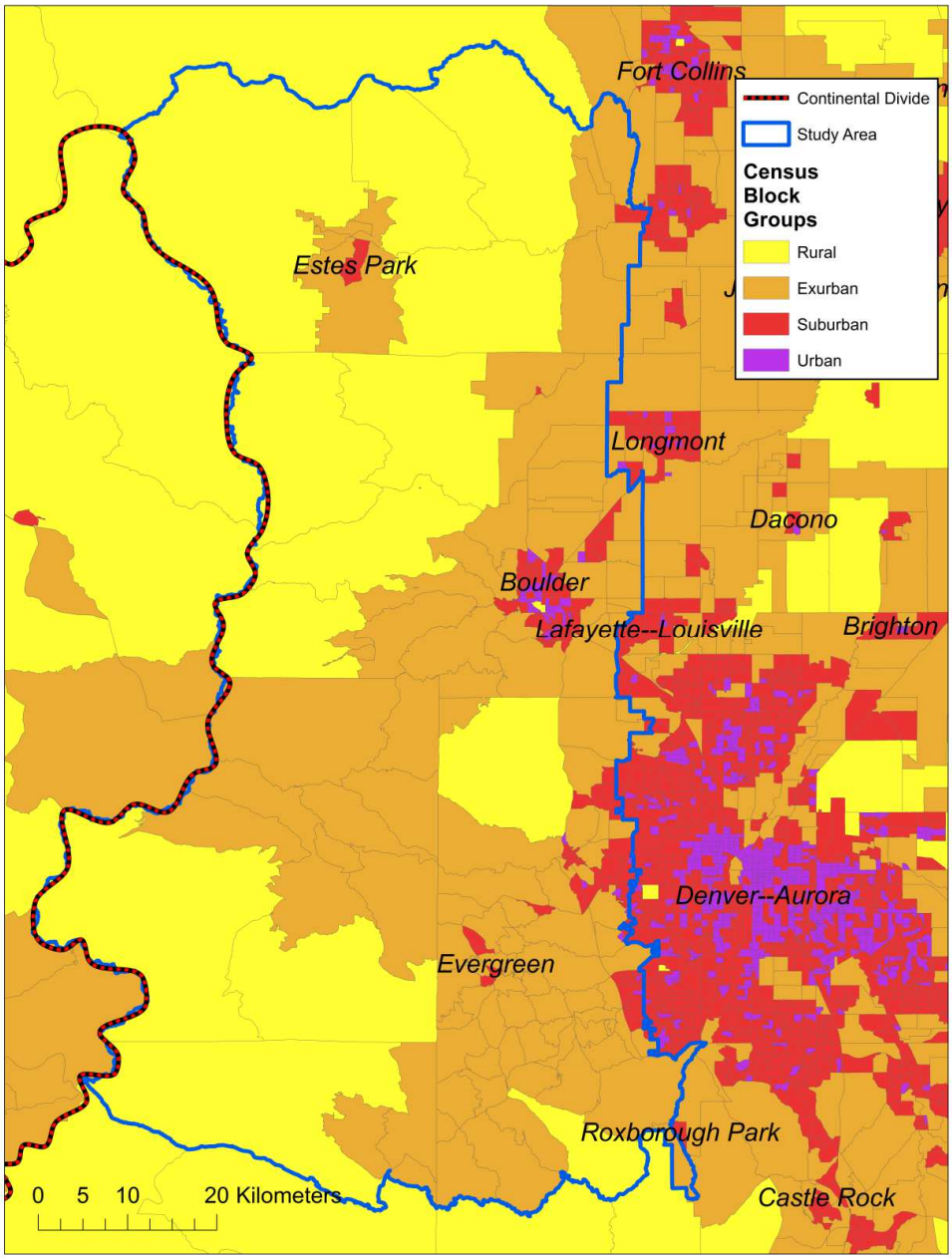

Figure A2.1. Study area depicted by U.S. Census Bureau's TIGER block-group delineations and chloropeth representation of overall housing density levels. Blue polygon delineates the block-groups where inferences (HDM model and STRUC) were made. Labels indicate "urban areas" as defined by 2010 TIGER shapefiles.

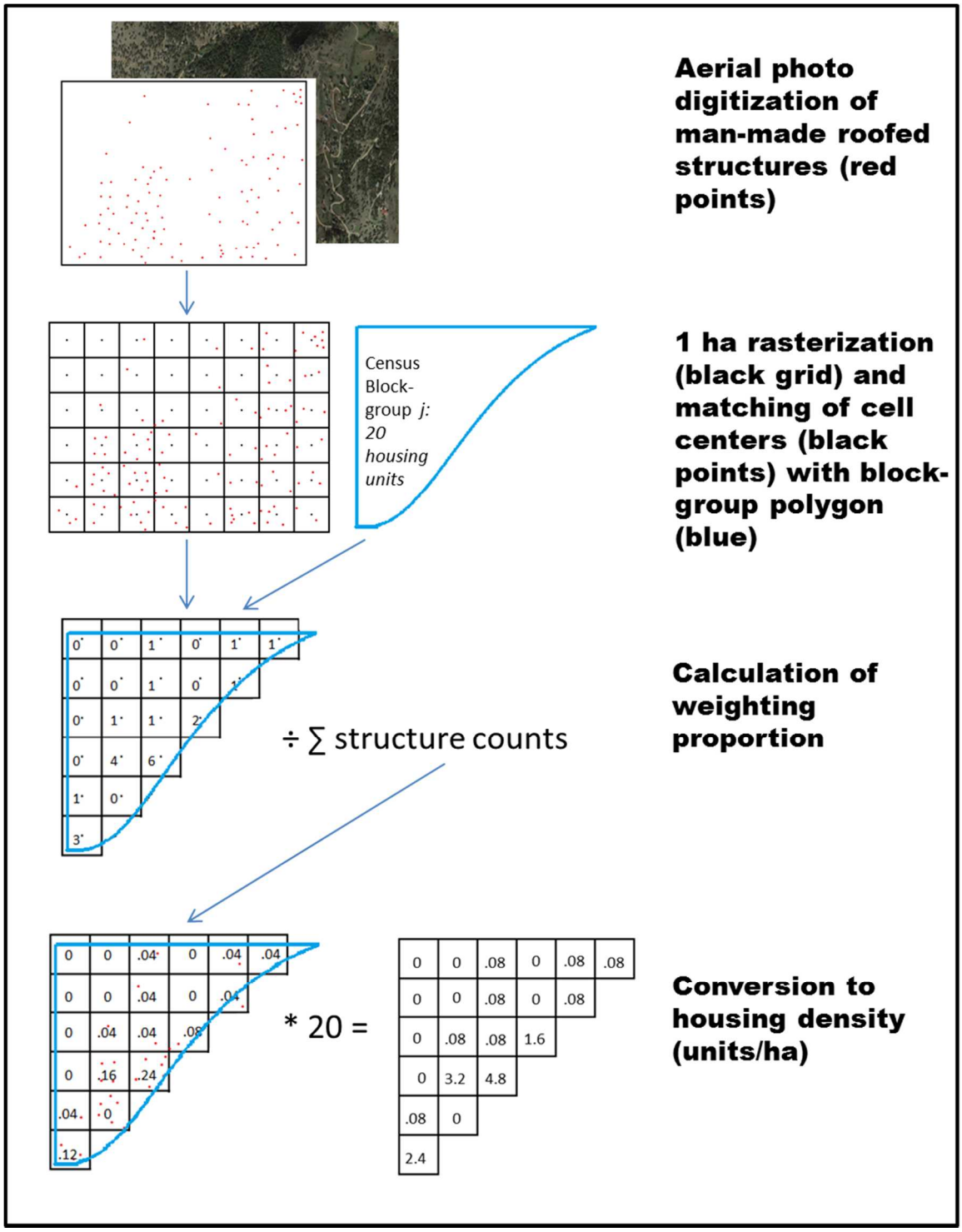

Figure A2.2. Diagram depicting daysmetric approach of the housing density model from aerial photo interpretation of man-made roofed structures and U.S. Census Bureau block-group housing counts.

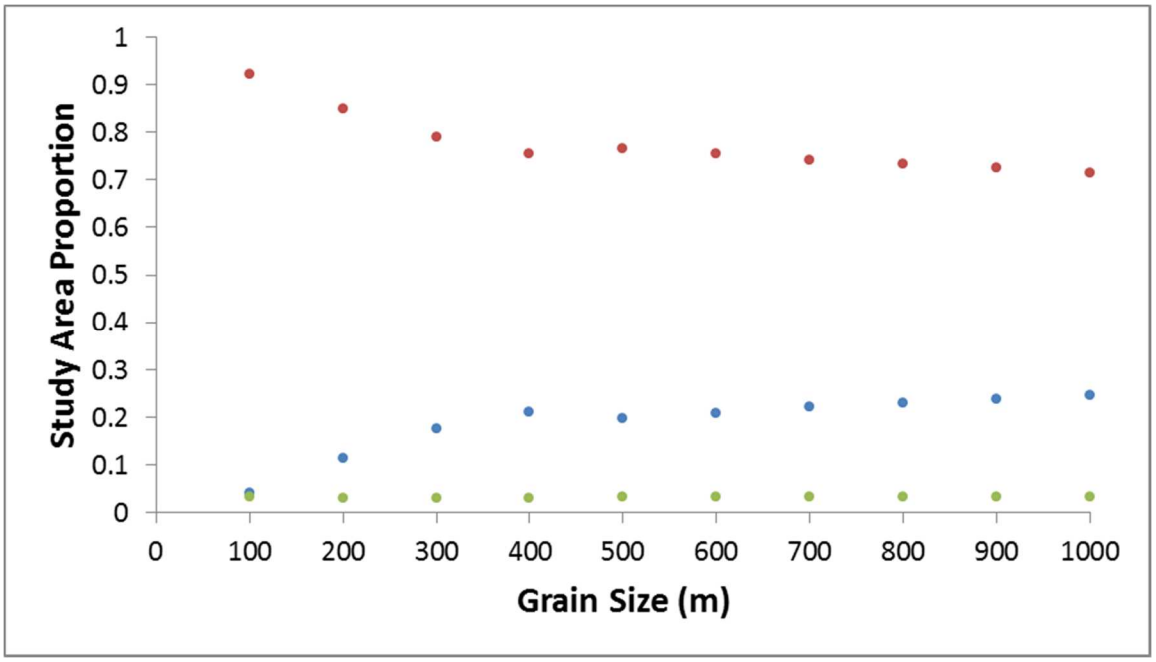

Figure A2.3. Proportion of study area composed of rural (red), exurban (blue), and combined suburban/urban levels (green), derived from the HDM with grain sizes ranging from 100 m to 1000 m.

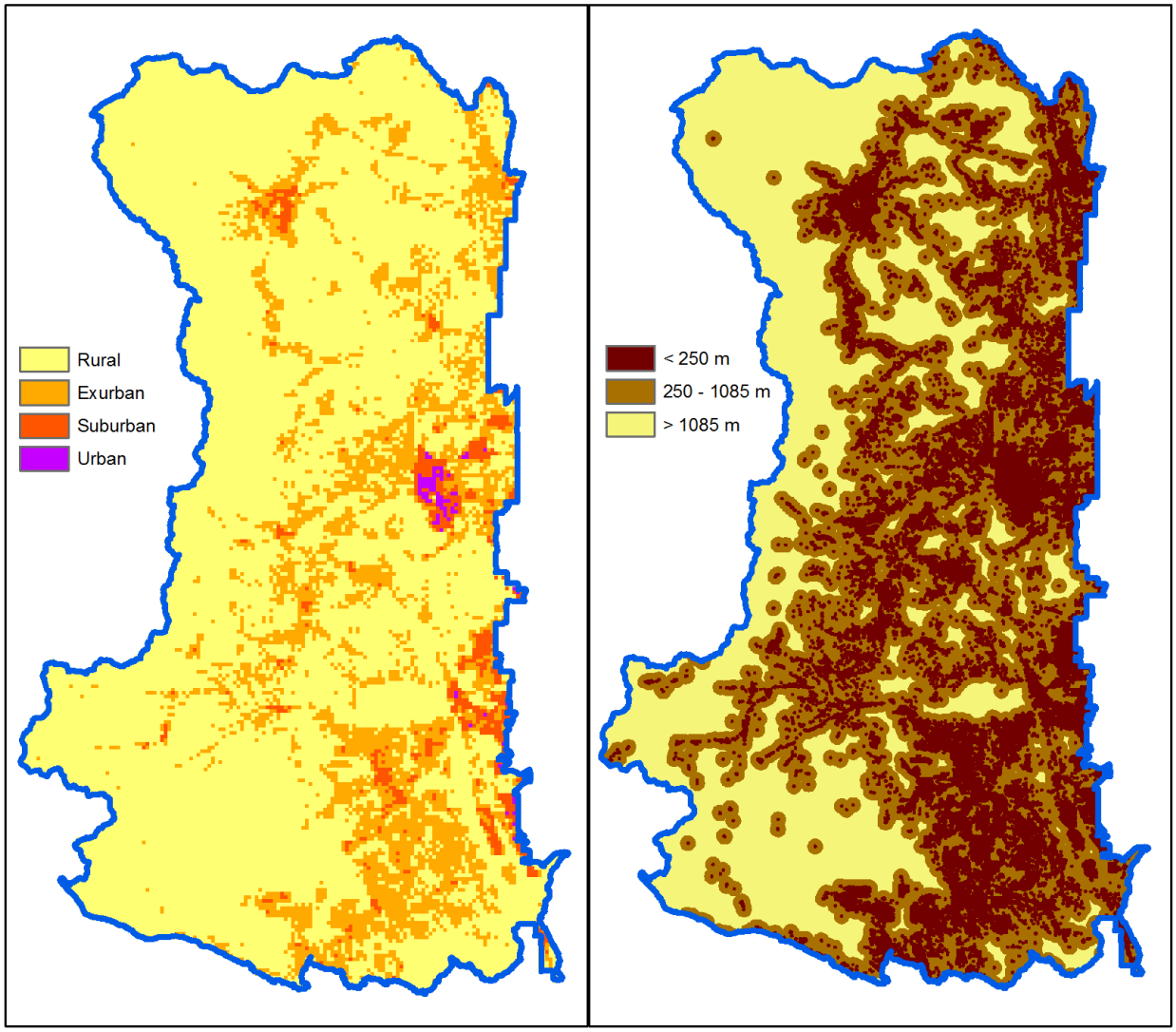

Figure A2.4. Left pane: Resulting output of the HDM at the aggregated 500 m grain size, displayed with four levels of housing unit density. Right pane: Resulting output of the nearest distance to man-made roofed structure (STRUC) displayed by classifying into three quantiles of equal area.

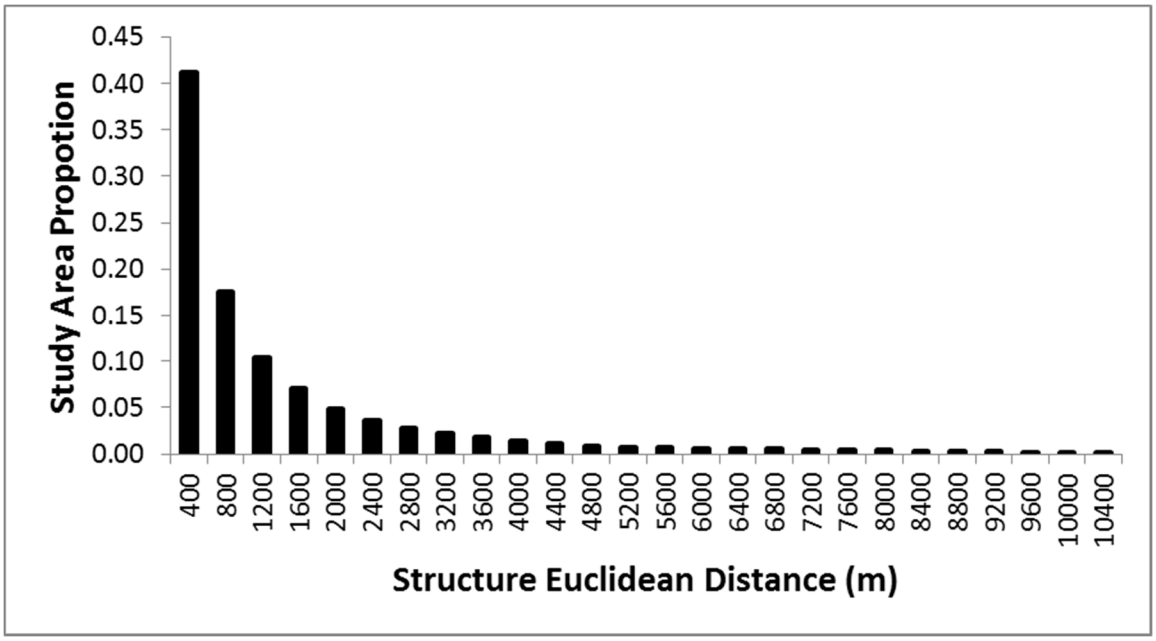

Figure A2.5. Histogram describing the composition of the study area, classified by the distance to nearest (Euclidean) digitized man-made roofed structure, at 400 m intervals.

LITERATURE CITED

Davis, J. S., and A. C. Nelson. 1994. The new 'burbs': The exurbs and their implications for planning policy. Journal of the American Planning Association 60:45-49.

Ditchkoff, S. S., S. T. Saalfeld, and C. J. Gibson. 2006. Animal behavior in urban ecosystems: Modifications due to human-induced stress. Urban Ecosystems 9:5-12.

Goad, E. H., L. Pejchar, S. E. Reed, and R. L. Knight. 2014. Habitat use by mammals varies along an exurban development gradient in northern Colorado. Biological Conservation 176:172-182.

Hannum, C., S. Laposa, S. E. Reed, L. Pejchar, and L. Ex. 2012. Comparative analysis of housing in conservation developments: Colorado case studies. The Journal of Sustainable Real Estate 4:149-176.

Hansen, A. J., R. L. Knight, J. M. Marzluff, S. Powell, K. Brown, P. H. Gude, and K. Jones. 2005. Effects of exurban development on biodiversity: patterns, mechanisms, and research needs. Ecological Applications 15:1893-1905.

Homer, C., J. Fry, J. Dewitz, M. Coan, N. Hossain, C. Larson, N. Herold, A. McKerrow, J. N. VanDriel, and J. Wickham. 2007. Completion of the 2001 National Land Cover Database for the Conterminous United States. Photogrammetric Engineering and Remote Sensing 73:337-341.

Irwin, E. G. 2002. The effects of open space on residential property values. Land Economics 78:465-480.

Jelinski, D. E., and J. Wu. 1996. The modifiable aeral unit problem and implications for landscape ecology. Landscape Ecology 11:129-140.

Levin, S. A. 1992. The problem of pattern and scale in ecology: the Robert H. MacArthur award lecture. Ecology 73:1943-1967.

Li, H., and J. Wu. 2004. Use and misuse of landscape indices. Landscape Ecology 19:389-399.

Lima, S. L., and P. A. Zollner. 1996. Towards a behavioral ecology of ecological landscapes. Trends in Ecology and Evolution 11:131-135.

Linke, J., and S. E. Franklin. 2006. Interpretation of landscape structure gradients based on satellite image classification of land cover. Canadian Journal of Remote Sensing 32:367-379.

Manfredo, M. J., and H. C. Zinn. 1996. Population change and its implications for wildlife management in the New West: A case study of Colorado. Human Dimensions of Wildlife 1:62-74.

McKinney, M. L. 2002. Urbanization, biodiversity, and conservation. Bioscience 52:883-890.

Mennis, J. 2003. Generating surface models of population using dasymetric mapping. The Professional Geographer 55:31-42.

Prior-Magee, J. S., K. G. Boykin, D. F. Bradford, W. G. Kepner, J. H. Lowry, D. L. Schrupp, K. A. Thomas, and B. C. Thompson. 2007. Ecoregional Gap Analysis of the Southwestern united States: The Southwest Regional Gap Analysis Project Final Report. U.S. Geological Survey, Gap Analysis Program.

Reibel, M., and M. E. Bufalino. 2005. Street-weighted interpolation techniques for demographic count estimation in incompatible zone systems. Environment and Planning A 37:127-139.

Riebsame, W. E., H. Gosnell, and D. M. Theobald. 1996. Land use and landscape change in the Colorado Mountains I: Theory, scale, and pattern. Mountain Research and Development 16:395-405.

Shrestha, N., and T. M. Conway. 2013. Mapping exurban development: can raod and census data act as surrogates? Cartographica 48:237-249.

Tapp, A. F. 2010. Areal interpolation and dasymetric mapping methods using local ancillary data sources. Cartography and Geographic Infromation Science 37:215-228.

Theobald, D. M. 2001. Land-use dynamics beyond the american urban fringe. Geographical Review 91:544-564.

Theobald, D. M. 2004. Placing exurban land-use change in a human modification framework. Frontiers in Ecology and Evolution 2:139-144.

Theobald, D. M. 2005. Landscape patterns of exurban growth in the USA from 1980 to 2020. Ecology and Society 25:999-1011.

Theobald, D. M., G. Wilcox, S. E. Linn, N. Peterson, and M. Lineal. 2010. Colorado ownership, management, and protection v8 database. Human Dimensions of Natural Resources and Natural Resources Ecology Lab, Colorado State University.

Thomas, N., G. Dobson, P. Dezendorf, M. Cantrell, and D. Abernathy. 2009. Development of a parcel-based density analysis tool to evaluate growth patterns in Western North Carolina. Journal of Conservation Planning 5:38-53.

Tobler, W. R. 1979. Smooth pycnophylactic interpolation for geographical regions. Journal of American Statistics 74:519-536.

Turner, M. G., R. V. O'Neill, R. H. Gardner, and B. T. Milne. 1989. Effects of changing spatial scale on the analysis of landscape pattern. Landscape Ecology 3:153-162.

Wade, A. A., and D. M. Theobald. 2010. Residential development encroachment on U.S. protected areas. Conservation Biology 24:151-161.

Wright, J. K. 1936. A method of mapping densities of population with Cape Cod as an example. Geographical Review 26:103-110.

Yuan, Y., R. M. Smith, and W. F. Limp. 1997. Remodeling census population with spatial information from Landsat TM imagery. Computers, Environment, and Urban Systems 21:245-258.

APPENDIX 3: MEASUREMENT AND PROCESSING STEPS FOR DISTANCE SAMPLING WITHIN CAMERA TRAP FIELD-OF-VIEW

This appendix provides supplementary methods for Chapter 2 for the detection probability component. To acquire approximate distance measurements between animals appearing in images and the camera's mounting point, reference measurements were collected upon installment of the camera and/or at the time of camera removal. First, a tape measure was aligned down the center of the camera's field of view. Pictures were allowed to be recorded by the camera while a technician walked in perpendicular passes to the tape measure at every 10 ft (3 m) to a maximum distance of at least 100 ft (30 m) (Figure A3.1). In some cases, 5 ft (1.5 m) intervals were marked. Several attempts (5-10 passes) were made for each distance interval to trigger the camera and record an image of the technician. Additional passes (>5) were sometimes required at the furthest distance intervals to trigger the camera. Using the resulting photos of the technician, reference locations of the horizontal distance intervals were determined from the point of contact of the technician to the ground while making the passes. These locations were compiled with image processing software (Adobe Photoshop CS6: Adobe Systems Inc, San Jose, CA, USA) into a single digital layer for each respective site (Figure A3.1). If cameras position moved at some point during the deployment (camera "bumped" by animal), separate reference overlays were made for the corresponding time period. An additional layer was created to designate eight equally spaced vertical line intervals spanning the cameras 42 degree FOV (every 5.25 degrees), with lines indexed relative to being either left (negative value) or right of the center line (positive value) (Figure A3.1). Assuming that the manufacturer had aligned the infrared trigger mechanism accurately with the cameras FOV and distortion from the camera lens was minimal, it was not necessary to measure these angular interval lines in the field. The

respective horizontal distance and vertical angular line overlay were then transferred to actual images with animals (Figure A3.2) using batch image processing techniques.

Aided by the overlay, an observer iterated through the images to visually assess the point of contact between the animal and the ground to measure distance (Figure A3.2). Distances between horizontal bands were visually approximated to the nearest foot. The angular measurement was approximated as the center of the animal's body visible in the picture, which was usually mid-thoracic region (Figure A3.2). Only the distance to the closest animal was recorded in photos with multiple individuals.

Photos where species identification was known (~99.9% of the photo records) were grouped based on body mass accounts (Armstrong et al. 2011) into one of three size groups: Meso, Large, and XLarge (Table A3.1). A fourth group was made by splitting Meso into fast moving ("MesoFast": canids) and slow moving ("MesoSlow": felids, procyonids). Distances were binned into intervals appropriate for each grouping (Table A3.2) to alleviate issues related to heaping of measurements (Buckland et al. 2001). A large proportion of the sector's area was cut off after applying the truncation distance; only 0.04 – 0.2 of the FOV area (given a maximum observation distance) was retained (Table A3.2). Fortunately, this still corresponded to 0.76 – 0.9 of the observed detection events being retained (Table A3.2).

Table A3.1. Mammalian species photographed, and their respective size groupings and body mass.

Size Class	Common Name	Latin Name	Mass (kg)		
			Minimum	Maximum	Average*
Xlarge	Domestic cow	*Bos taurus*	22.0	1361.0	692.0
	Horse	*Equus caballus*	54.0	998.0	526.0
	Moose	*Alces alces*	380.0	550.0	465.0
	Elk	*Cervus elaphus*	220.0	450.0	335.0
Large	Unknown ungulate	*Cervid* spp.	70.0	450.0	260.0
	Mule Deer	*Odoicoileus hemionus*	70.0	200.0	135.0
	Black Bear	*American black bear*	90.0	113.0	102.0
	Human	*Homo sapien*	50.0	100.0	75.0
	Cougar	*Puma concolor*	36.0	103.0	70.0
	Domestic Goat	*Capra* spp.	18.0	91.0	55.0
Meso	Domestic Dog	*Canis lupus familiaris*	1.00	79.0	40.0
	Unknown canid	*Canidae* spp.	3.00	70.0	37.0
	Coyote	*Canis latrans*	8.00	20.0	14.0
	Bobcat	*Lynx rufus*	5.00	14.0	9.50
	River Otter	*Lontra canadensis*	5.00	14.0	9.50
	Raccoon	*Procyon lotor*	3.00	9.00	6.00
	Domestic Cat	*Felis catus*	2.30	9.00	5.65
	Gray Fox	*Urocyon cinereoargenteus*	3.00	7.00	5.00
	Red Fox	*Vulpes vulpes*	3.00	7.00	5.00
	Unknown fox	*Vulpes or Urocyon* spp.	3.00	7.00	5.00
Small	Yellow-bellied Marmot	*Marmota flaviventris*	1.60	5.20	3.40
	Striped Skunk	*Mephitis mephitis*	1.80	4.50	3.15
	Unknown Lagomorph	*Lepus or Sylvilagus* spp.	0.50	5.00	2.75
	Snowshoe Hare	*Lepus americanus*	1.00	1.50	1.25
	Unknown Sylvilagus	*Sylvilagus* spp.	0.50	1.50	1.00
	Mountain Cottontail	*Sylvilagus nuttallii*	0.90	1.10	1.00
Micro	Rock Squirrel	*Otospermophilus variegatus*	0.65	1.00	0.83
	Fox Squirrel	*Sciurus niger*	0.40	1.10	0.75
	Mink	*Neovison vison*	0.53	0.78	0.65
	Aberts Squirrel	*Sciurus aberti*	0.55	0.75	0.65
	Unknown squirrel	*Sciurus* or *Tamiascirus* spp.	0.19	1.10	0.65
	Western Spotted Skunk	*Spilogale gracilis*	0.40	0.70	0.55
	Bushy-tailed woodrat	*Neotoma cinerea*	0.27	0.29	0.28
	Golden-mantled Ground Squirrel	*Spermophilus lateralis*	0.17	0.29	0.23
	Red Squirrel	*Tamiasciurus hudsonicus*	0.19	0.26	0.23
	Unknown Weasel	*Mustela* spp.	0.03	0.30	0.17
	Unknown Chipmunk	*Tamias* spp.	0.03	0.09	0.06
	Unknown Bat	*Chiroptera* spp.	0.00	0.03	0.02

*Average Mass calculated as mid-point of minimum and maximum values given by Armstrong et al. (2011).

Table A3.2. Summary of maximum observed distances, post processed distance interval assignments, and the areal proportion of sector retained after right-truncation for each species grouping.

Grouping	Maximum observed distance (m)	Interval 1	Interval 2	Interval 3	Interval 4	Interval 5	Interval 6	Proportion of sector retained	Proportion of events retained
Meso-slow	16.8	3.05	3.96	4.88	5.79	6.71*	-	0.16	0.76
Meso-fast	24.4	2.44	4.57	6.71	8.84	10.97*	-	0.20	0.90
Large	45.7	1.98	3.96	5.94	7.92	9.91	13.87*	0.05	0.89
Xlarge	67.1	4.48	6.71	8.95	11.18	13.42*	-	0.04	0.74

* Corresponds to the right truncation distance

Figure A3.1. Compiled layer of horizontal and vertical measurement liens (red) overlaid on a photo of a technician making passes at the distance intervals. Horizontal lines indicate approximate distance intervals at 10 – 100 ft (3 – 30 m) in 10 ft (3 m) intervals. This particular example image has distance intervals marked at 10 ft intervals with a maximum distance of 80 ft. Vertical lines indicate the center or 0° (index 0), 5.04° (index 1), 10.08° (index 2), 15.11° (index 3), and 20.15° (photo edge) to the left (negative index) or right (positive index) of the center line.

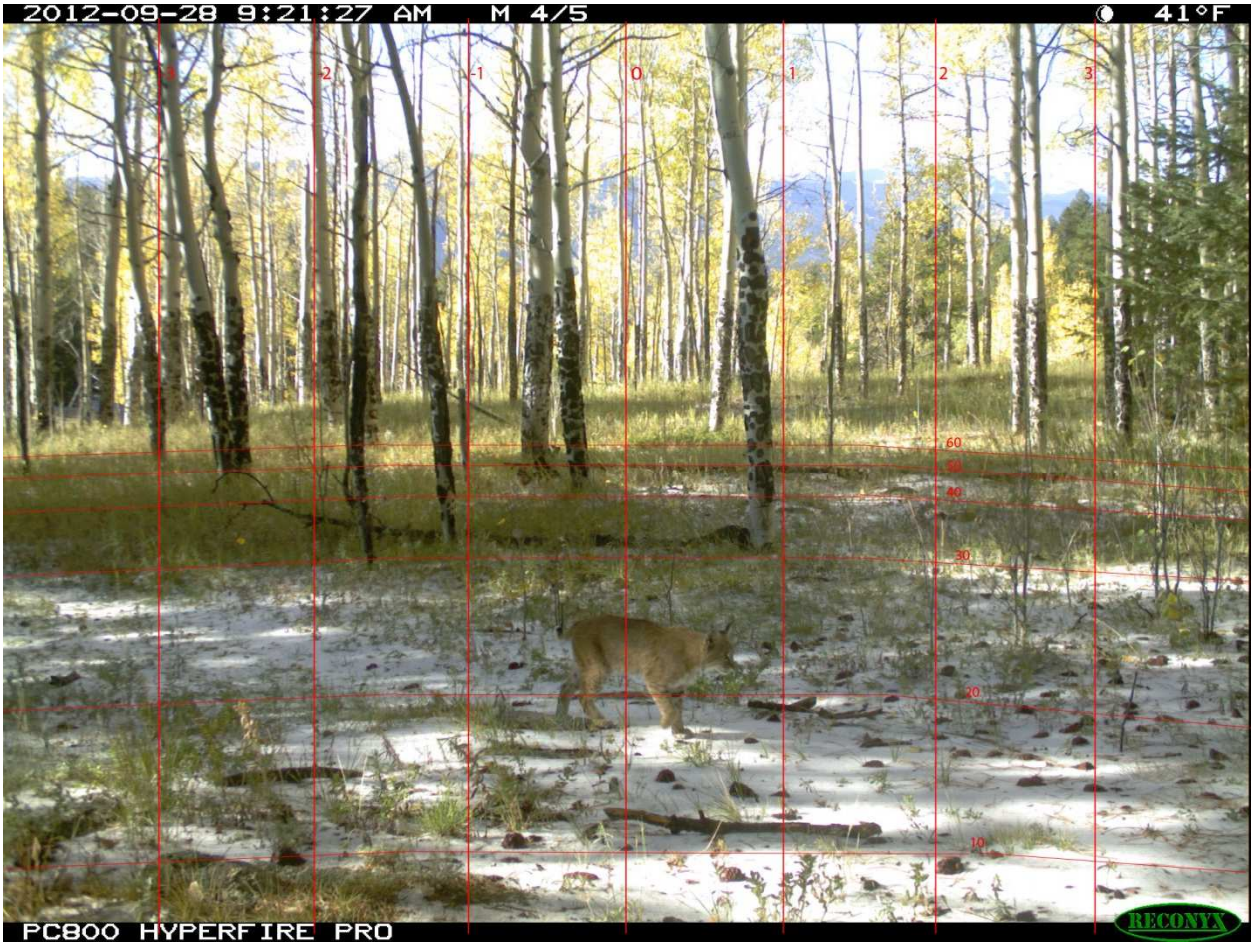

Figure A3.2. Example of photograph with the overlaid horizontal distance intervals (ft) and vertical angle intervals. The distance and angle index approximated for the bobcat (*Lynx rufous*) in this photo would be 18 ft and 0.1 respectively.

APPENDIX 4: LANDSCAPE COVARIATE MEASUREMENT METHODS

This appendix gives detailed information for the various landscape covariates utilized in Chapter 2 and Chapter 3 of this thesis. A complete listing of the covariate naming conventions and short covariate descriptions can be found in Table A4.1.

Topographic Measures

Topographic measures were derived from a 1/3-arc-second (~10 m) digital elevation model (USGS: National Elevation Dataset). Aggregating the elevation model to a 30 m grain size gave the primary elevation measure (ELEV) (Figure A4.1). For a coarse scale metric, a moving window average was calculated on ELEV with a radius of 6, 9, and 12 km. Using the 30 m ELEV data, solar aspect (ASP) was calculated for the four cardinal directions (N: 315 – 45°, E: 45 – 135°, S: 135-225°, W: 225 – 315°) and the four ordinal directions (NE: 0-90°, SE: 90-180°, SW: 180-270°, NW: 270-360°). Using the scale of the original elevation model, slope (SLOPE) was measured in degrees (Figure A4.2). A topographic position index (TPI) (Jenness 2006) was calculated from the original elevation model at scales ranging from 50 – 500 m radius windows in 50 m intervals at a 10 m grain size. A TPI with a 50 m window (TPI_50) would be able to capture any narrow deviation such as a ditch or knoll. A 500 m window (TPI_500) (Figure A4.3) would be able to capture any larger valley or ridge while averaging smaller deviations. A more negative TPI index would indicate that the location was a narrower or more "enclosed" drainage, while a more positive TPI index would indicate a narrower or more pronounced ridge line. A TPI near zero would indicate a flat location or mid-slope.

Hydrological Measures:

Hydrological features were derived from the U.S. Geological Survey's National Hydrological Dataset using flow-line and water-body datasets. Flow-lines were classified as either perennial or intermittent water sources, while all water bodies were classified as perennial sources. Euclidean distance layers were created using a 10 m grain size considering the perennial (NHD_per) (Figure A4.4) and intermittent (NHD_int) sources separately and then jointly (NHD_int_per).

Vegetation Measures

Vegetation data was derived using the readily available land-cover models: National Land Cover Dataset (U.S. Geological Survey), LANDFIRE (U.S. Forest Service), Southwest Regional GAP (U.S. Geological Survey) and BASINWIDE (Colorado Parks and Wildlife). All four of these datasets were derived from models combining imagery from various remote sensing platforms. Validation steps were conducted by the dataset's respective source entities with ground-truthing measures. However, it would be expected that certain land-cover types are more easily distinguishable by certain models; thus performance of these models to give a true characterization would vary spatially across the domain (i.e., NLCD: national level, BASINWIDE: state level). Therefore, I conducted a validation analysis specific to the vicinity of the Front Range Cougar Project study area in order to choose the best data source.

First, each of the four data sources were collapsed into three basic vegetation structure types (forest, shrub, and open) based on attribute data included with each data set. For Landfire, this corresponded to the "NVCSOrder". For BASINWIDE, it was the "Class_Names" and "Description" fields. For SWRGAP, the "NVC_CLASS" and "NVC_SUBCL" fields provided a

breakdown. For NLCD, reclassification was done simply by using the descriptions of the 17 classes found in the study area (http://www.mrlc.gov/nlcd11_leg.php). Land cover types depicted as grasses, open (barren), forbs, cropland, and snow were considered as the "open" vegetation type. For each of the data sources, three separate binary raster layers were created indicating the presence/absence of the vegetation structure (forest, shrub, open). Pixels related to human development (i.e., NLCD's "Developed", SWRGAP's "Developed & Other Human Use") were set to null values. Because not all layers shared the same grid resolution or spacing, I resampled with a regular grid of points spaced in 30 m intervals. For each of the three vegetation structure types, the union of the binary datasets was calculated across various combinations of the four data sources to create new binary datasets. Combining binary datasets allowed a more liberal estimate of the presence of a vegetation structure type, while also allowing a particular location to be classified by more than one vegetation structure type.

Next, ground-truthing data were collected for 2371 point locations visited in the field by human observers while conducting surveys for other ecological studies ongoing in the Front Range. These locations spanned all vegetation types, but forested vegetation types were likely overrepresented (versus a completely randomized sampling scheme). During these visits, the major vegetation form was recorded by an observer within a 50 m radius of the sampled point.

To rank the performance, ground-truthed point locations were spatially matched to the datasets' (individual and union of multiple) binary classification. Receiver Operator Characteristics (ROC) analysis was conducted with Area Under the Curve (AUC) as the primary ranking argument. AUC measures range from 0 – 1, with 1 yielding a perfect binary prediction (all 0's and 1's matching), and 0 yielding a completely opposite prediction. An AUC near the mid-point (0.5) indicated that the data source did not yield predictions of presence/absence any

better than a random binary assignment. Sensitivity (true-positive rate) and specificity (true-negative rate) are also given.

Performance measures for each data set (or union of multiple data sets) are given in Table A4.2. For the forest structure, NLCD alone gave the highest AUC score (0.803). For the open type, the union of NLCD, SWRGAP, and BASINWIDE data sets gave the best AUC score (0.753). Shrub type was best described by the combination of NLCD and SWRGAP data sets (AUC = 0.794). Using the top ranked individual or combined data source, final binary presence/absence raster layers were created to represent the basic FOREST, SHRUB (Figure A4.5), and OPEN presence/absence covariate. These layers were then used to calculate a moving window "majority" focal statistic layer. These "majority" layers represented whether the vegetation type was the predominant vegetation type in a 3x3 pixel or 5x5 pixel (pixels = 30 m) rectangular window.

The FOREST binary layer was used to create a layer for depicting the distance to nearest forest edge (FOREDGE). After resampling FOREST's native 30 m grain size to a 10 m grain size, a moving window "smoothed" the hard edges, resulting in an interpolated representation of FOREST. This new 10 m resolution layer was then used to create forest edge lines, which then was put into a simple Euclidean distance calculation for all locations on the landscape.

Canopy cover estimates are available separately from the LANDFIRE data source (year 2010 version) given canopy cover percentages in increments of 10 for a 30 m grain size. Using a moving window approach, the mean canopy cover percentage was calculated across a 90 m radius (CC_avg90) (Figure A4.6).

Human Development Measures

Appendix 2 gives a detailed description of methods employed to obtain housing density and Euclidean distance to man-made roofed structure layers (HDM_pnt [Figure A4.7] and STRUC respectively). Additionally, the man-made roofed structure point layer was summarized by density of structures as well as spatial proximity in a single covariate (KD). KD was calculated with a Gaussian kernel density analysis (grain size of 10 m) for a moving window defined by a radius of *h*, which took on a range of values from 100 – 2500 m. See Figure A4.8 for a kernel density conducted on structures at a 1500m radius (KD1500).

Roadways were depicted with the 2013 U.S. Census Bureau TIGER roads data set. After removing all off-road trails and private roads a Euclidean distance layer was created using a 10 m grain size (RDS_euc).

Snow Accumulation

Data pertaining to the accumulation of snow on the ground was obtained using the Snow Data Assimilation System (SNODAS) (Barrett 2003). At a 1 km^2 grain size, SNODAS predicts snow depth with a RMSE of 15 cm in forested landscapes of the Colorado mountains (Clow et al. 2012) on a daily basis. I considered snow depth as a continuous measure (SNOWD), and as a categorical presence/absence covariate with any snow depth measure > 0 given as binary presence "1" (SNOWP).

Other Landscape Measures

While elk are a species potentially found anywhere within the study area, concentrations of populations are evident. Agency biologists have compiled expert opinions to develop generalized polygons depicting known areas with higher probability of having elk. This population range information is available for elk across the state of Colorado ("Species Activity

Mapping": Colorado Parks and Wildlife) for the summer and winter season. Additionally, seasonal concentration maps are provided for areas with a higher probability of usage. The summer concentration and winter elk concentration map were converted to binary raster layers (30 m grain size) individually (ELK_sumconc and ELK_winconc) and as the union of the two layers (ELK_conc) (Figure A4.9).

TABLES AND FIGURES

Table A4.1. List of covariate naming conventions, grain size, and description.

Type	Covariate	Grain Size	Description
Topographic	ELEV	10	Digital elevation model at native 10 m scale
	ELEV_1k		Moving window average for a 1000 m radius
	ELEV_6k		Moving window average for 6000 m radius
	ELEV_9k		Moving window average for 9000 m radius
	ELEV_12k		Moving window average for 12000 m radius
	SLOPE	10	
	TPI_50	10	Topographic position index with 50 m radius window
	TPI_100		Topographic position index with 100m radius window
	TPI_150		Topographic position index with 150 m radius window
	TPI_200		Topographic position index with 200 m radius window
	TPI_250		Topographic position index with 250 m radius window
	TPI_500		Topographic position index with 500 m radius window
	ASP_N	30	Solar aspect (90 degree window, i.e.: SE = 90 - 180 degrees)
	ASP_E		
	ASP_S		
	ASP_W		
	ASP_NE		
	ASP_SE		
	ASP_SW		
	ASP_NW		
	ASP135	30	Continuous measure indicating solar aspect absolute difference from a azimuth of 135 degrees
	ASP45		Continuous measure indicating solar aspect absolute difference from a azimuth of 45 degrees
Hydrological	NHD_per	10	Distance to any perrenial water source
	NHD_int		Distance to intermittent stream
	NHD_int_per		Distance to intermittent and perrenial water sources (streams or water bodies)
Vegetation	OPEN	30	Binary presence of union of NLCD, GAP, and BASINWIDE open landcover types
	SHRUB		Binary presence of the union of NLCD and GAP shrub landcover types
	FOREST		Binary presence of NLCD forest landcover types
	OPEN3	30	Binary indicator of whether OPEN veg structure is dominate class within a 90x90 m window
	OPEN5		Binary indicator of whether OPEN veg structure is dominate class within a 150x150 m window
	SHRUB3		Binary indicator of whether SHRUB veg structure is dominate class within a 90x90 m window
	SHRUB5		Binary indicator of whether SHRUB veg structure is dominate class within a 150x150 m window
	FOREST3		Binary indicator of whether FOREST veg structure is dominate class within a 90x90 m window
	FOREST5		Binary indicator of whether FOREST veg structure is dominate class within a 150x150 m window
	FOREDGE	10	Distance to forest edge (smoothed edge of NLCD forest layer)
	CC_pnt	30	Point estimate of percent canopy cover from LANDFIRE (v. US110) dataset
	CC_avg90		Average of percent canopy cover within a 90m radius

…Continued

Continued from previous page

Type	Covariate	Grain Size	Description
Housing / anthropogenic development	HDM_pnt	100	Housing density 100 m cell size (Appendix 2)
	HDM100		focals statistics on HDM_pnt layer with a 2x2 window
	HDM150		focals statistics on HDM_pnt layer with a 3x3 window
	HDM200		focals statistics on HDM_pnt layer with a 4x4 window
	HDM250		focals statistics on HDM_pnt layer with a 5x5 window
	HDM300		focals statistics on HDM_pnt layer with a 6x6 window
	HDM350		focals statistics on HDM_pnt layer with a 7x7 window
	HDM400		focals statistics on HDM_pnt layer with a 8x8 window
	HDM450		focals statistics on HDM_pnt layer with a 9x9 window
	HDM500		focals statistics on HDM_pnt layer with a 10x10 window
	STRUC	10	Euclidean distance (m) of the closest man-made roofed structure (Appendix 2)
	STRUC_yard		From STRUC, indicating whether it is within 50 m (1 = < 50, 2 > 50) of a structure or not
	KD20	10	Kernel density (measured in ha) of the structures layer, within a search radius equal to the distance (m) given in the suffix.
	KD50		
	KD100		
	KD200		
	KD300		
	KD400		
	KD500		
	KD600		
	KD700		
	KD800		
	KD900		
	KD1000		
	KD1500		
	KD2000		
	KD2500		
	RDS_prlo_euc	10	Euclidean distance within a primary or local road
	RDS_euc		Euclidean distance to nearest road
Snow accumulation	SNOWD	1000	Snow depth as determined by SNODAS daily data
	SNOWP		Presence of snow (SNOWD > 0) as determined by SNODAS daily data.
Other	ELK_sumconc	30	As determiened by Colorado Parks and Wildlife "SAMs" database
	ELK_winconc		
	ELK_conc		Union of ELK_sumconc and ELK_winconc
	UTM_X	30	Universal Transverse Mercator coordinate (Zone 13)
	UTM_Y		

Table A4.2. Classification performance of various land cover data sources to depict three major vegetation structure types in the Front Range Cougar Project study area. Data sources were ground-truthed with 2,371 field visits. Table rows indicate a single source or combined data sources (dataset presence indicated with "1"). Area under the curve (AUC) is derived from receiver operator characteristics analysis as an overall accuracy measure.

Major Vegetation Structure	Land Cover Data Sources Considered				Performance Measure		
	NLCD	LANDFIRE	SWRGAP	BASINWIDE	Sensitivity	Specificity	AUC
Forest	1	1	1	1	0.982	0.275	0.275
	-	1	-	-	0.932	0.429	0.681
	-	-	-	1	0.661	0.773	0.717
	1	-	-	1	0.860	0.674	0.767
	-	-	1	-	0.830	0.749	0.789
	1	-	-	1	0.830	0.749	0.789
	1	-	-	-	0.776	0.830	0.803
Open	-	1	-	-	0.196	0.966	0.581
	1	-	-	-	0.282	0.948	0.615
	-	-	1	-	0.400	0.925	0.662
	-	-	-	1	0.573	0.872	0.722
	-	-	1	1	0.671	0.834	0.752
	1	-	1	1	0.698	0.808	0.753
Shrub	-	-	-	1	0.367	0.768	0.567
	-	1	-	-	0.291	0.942	0.617
	-	-	-	-	0.558	0.876	0.717
	1	1	1	1	0.912	0.578	0.745
	-	1	1	-	0.657	0.837	0.747
	1	-	-	-	0.749	0.796	0.772
	1	-	1	-	0.853	0.735	0.794

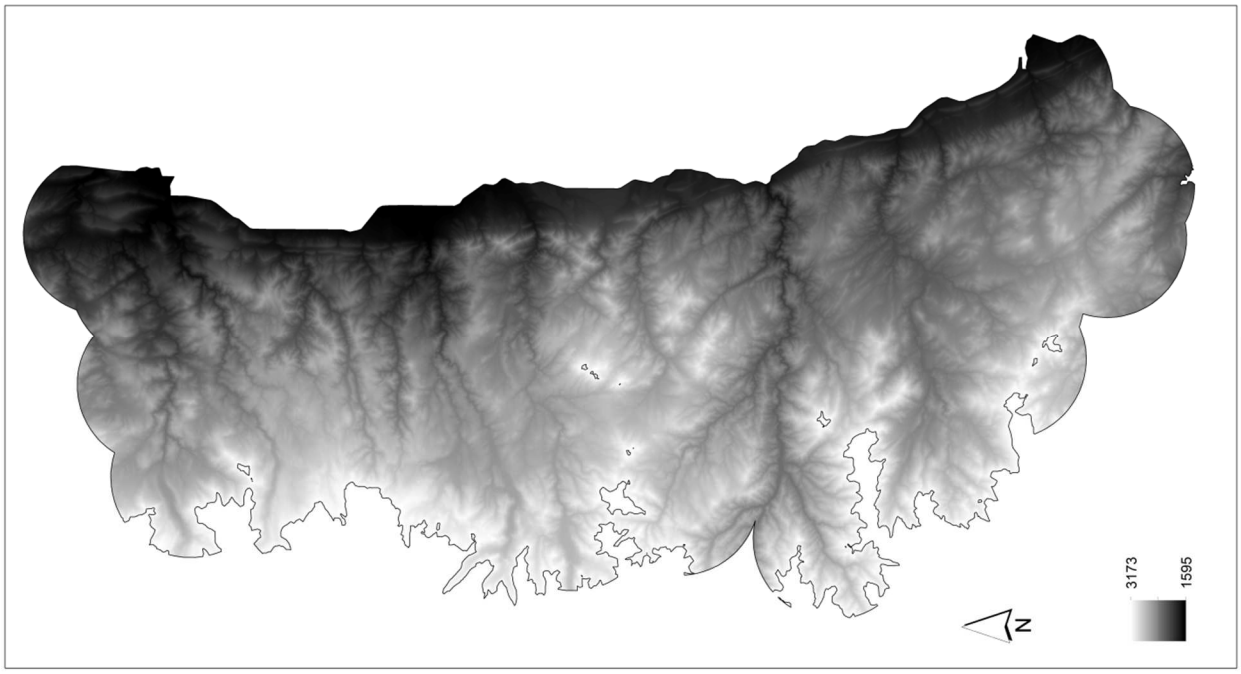

Figure A4.1. Elevation at 30 m grain size in units of meters above sea level (ELEV)

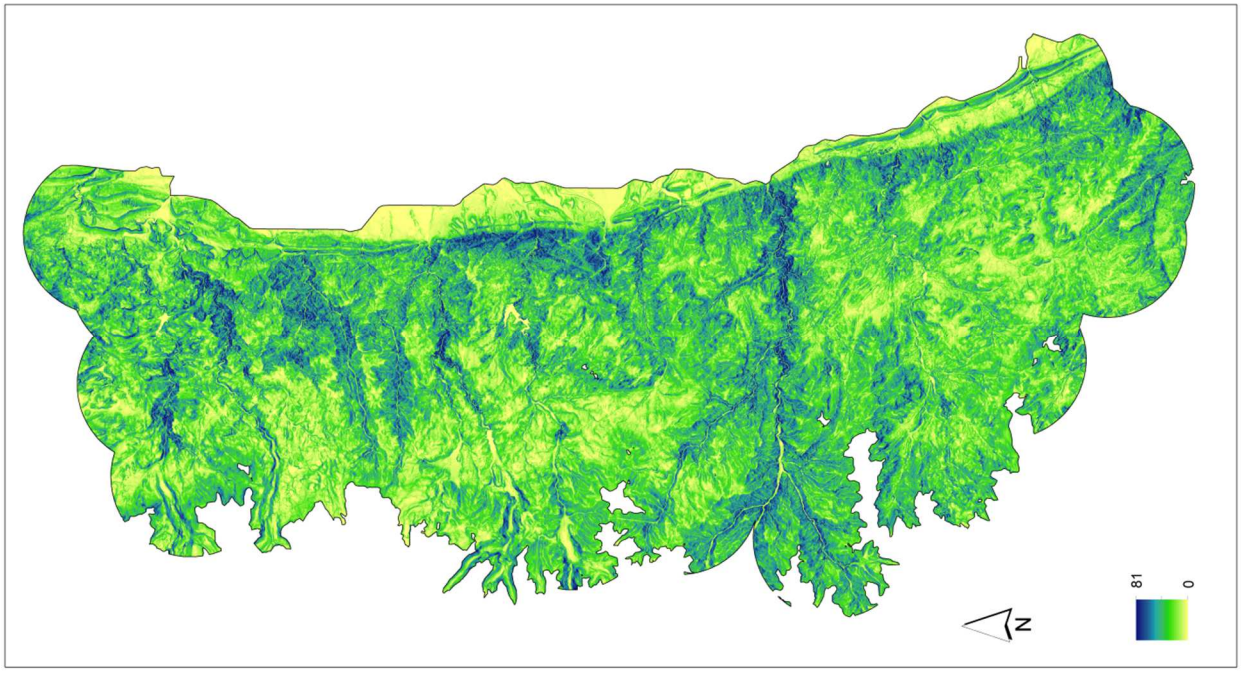

Figure A4.2. Slope in units of degrees (SLOPE)

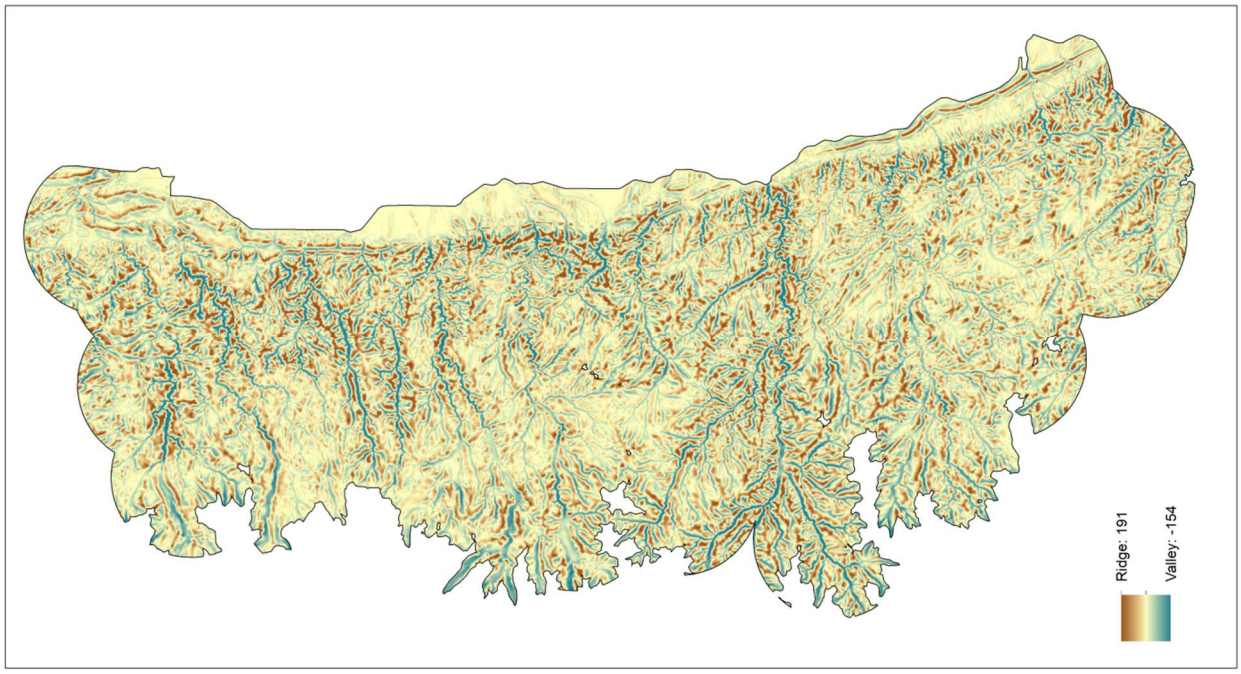

Figure A4.3. Topographic Position Index (TPI_500)

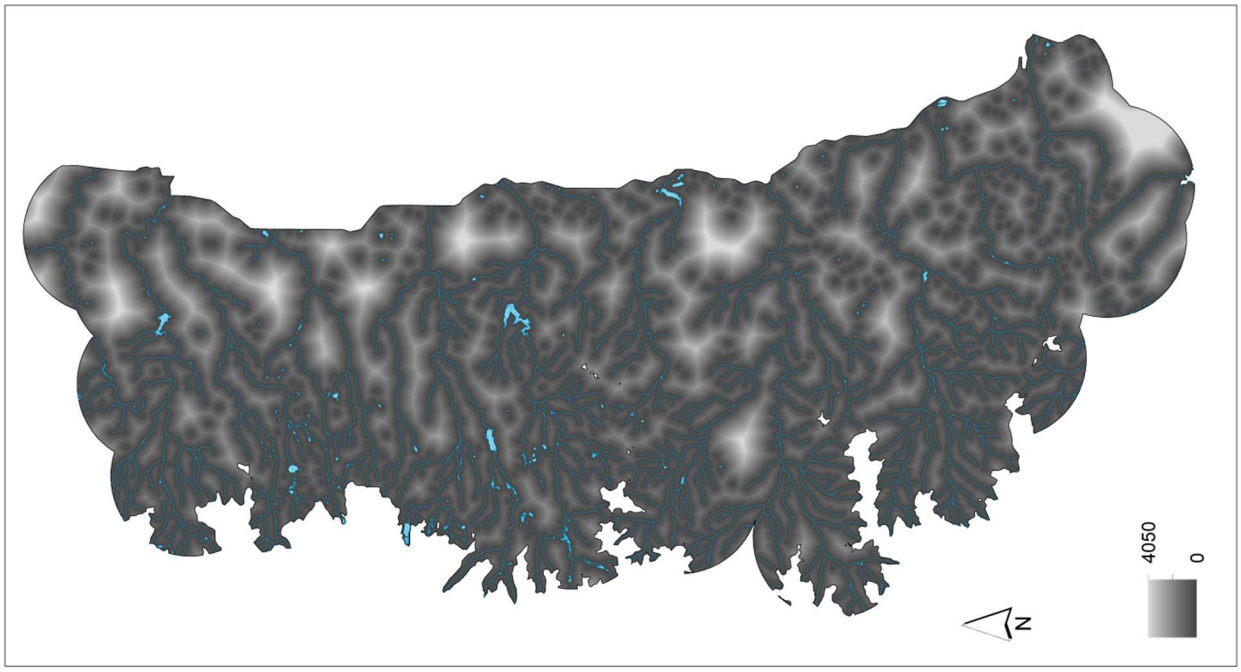

Figure A4.4. Perennial water sources Euclidean distance (NHD_per). Blue lines indicate perennial waterbodies or flow lines.

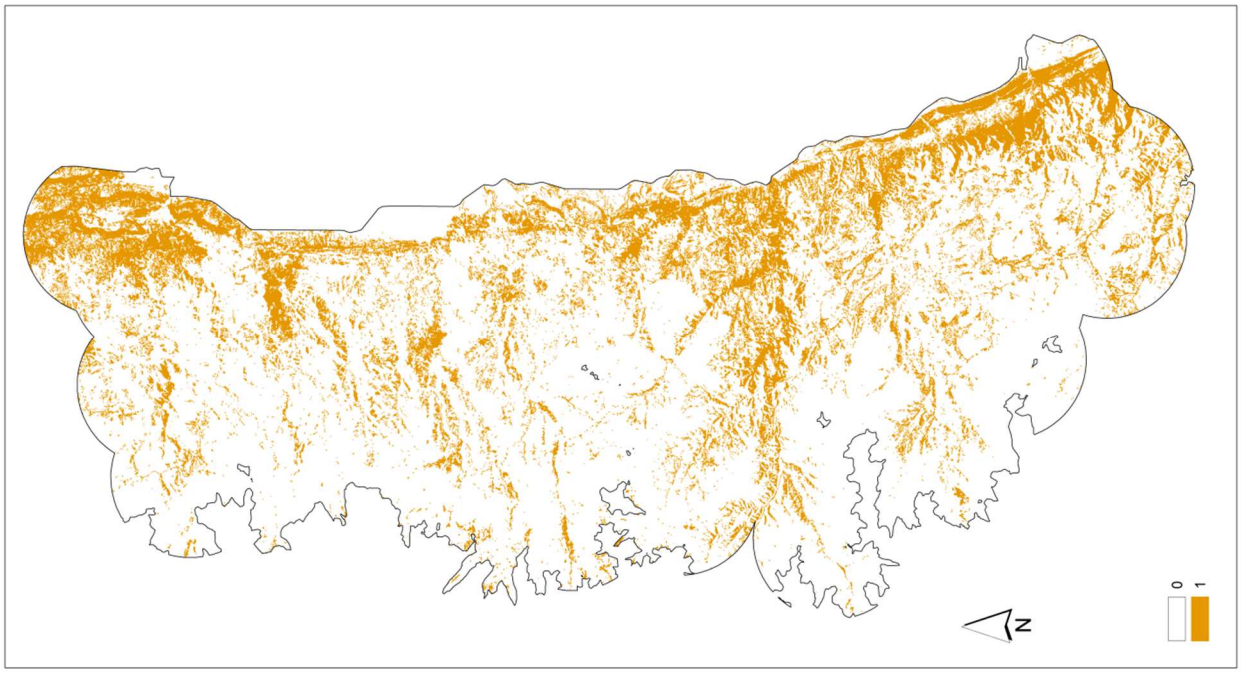

Figure A4.5. Binary depiction of SHRUB as derived from the union of NLCD and SWRGAP data sources shrub classes.

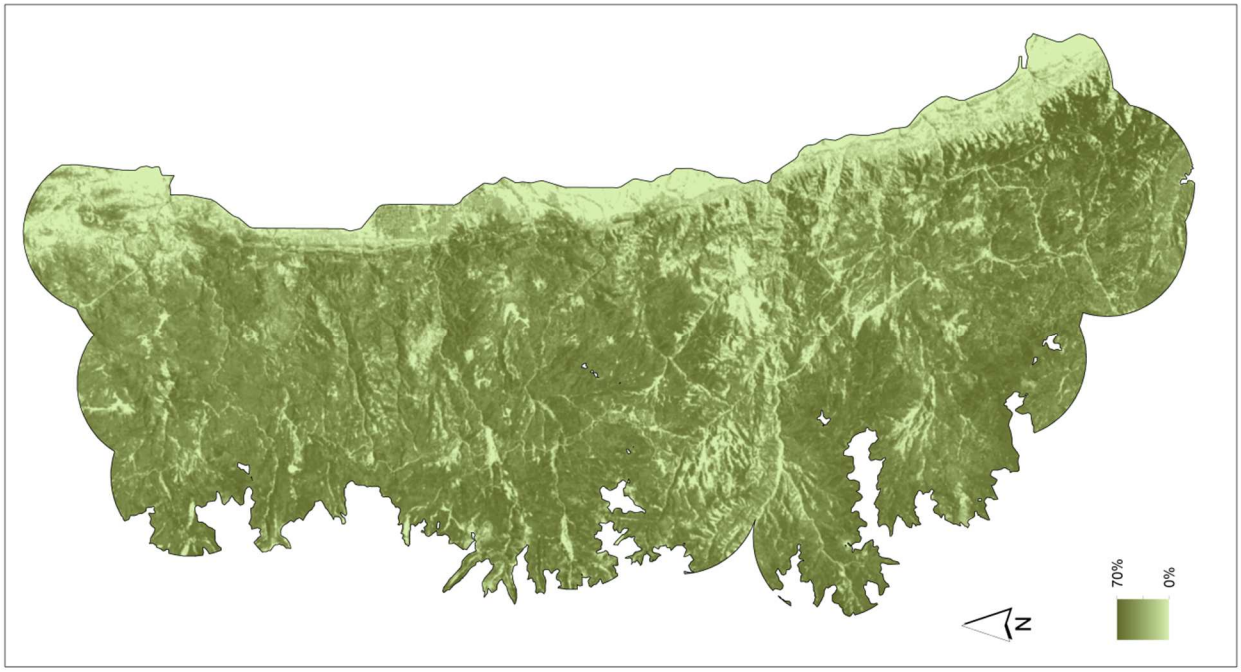

Figure A4.6. Canopy cover percentage averaged over 90 m radius window (CC_avg90).

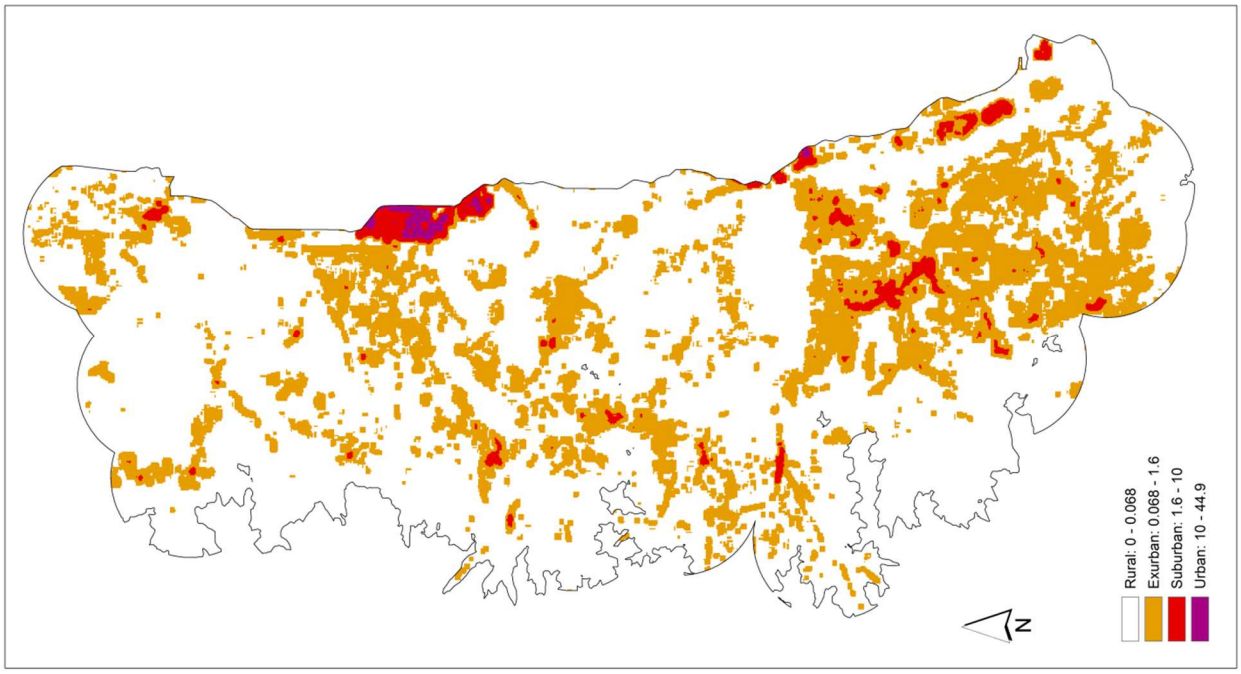

Figure A4.7. Housing density model in housing units/ha (see Appendix 2) discretized into rural, exurban, suburban and urban housing density levels (levels defined by Theobald (2005)).

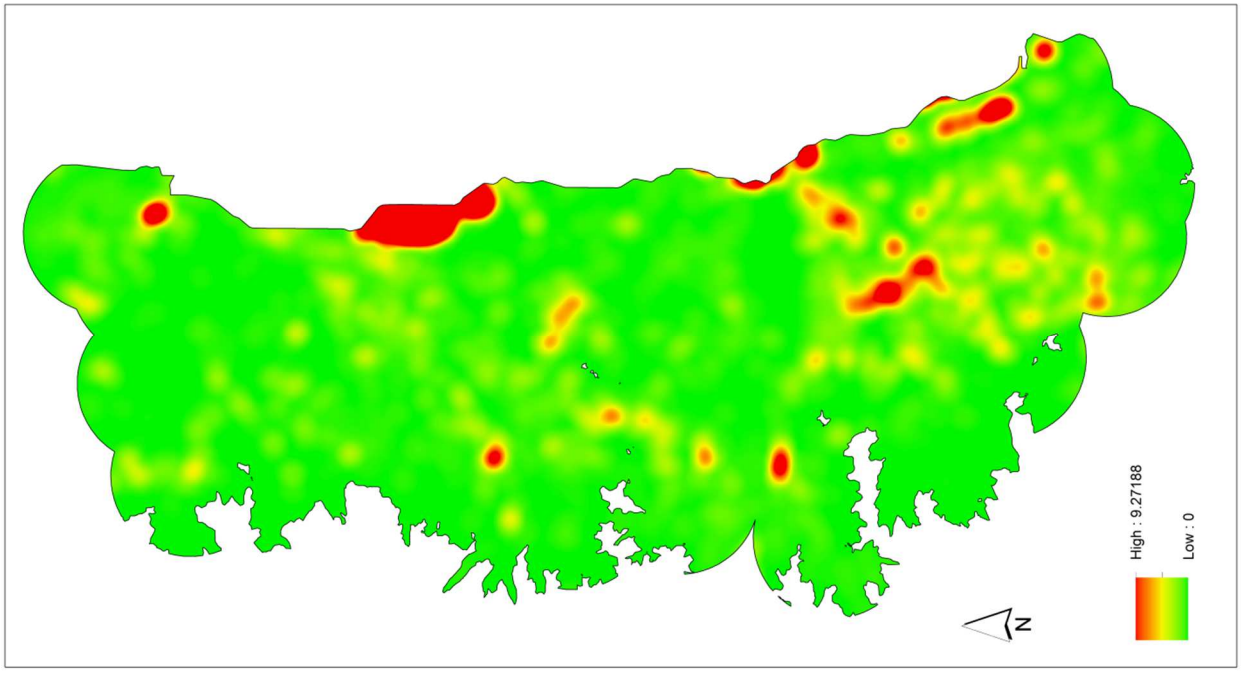

Figure A4.8. Structure kernel density map for a bandwidth of 1500 m (KD1500).

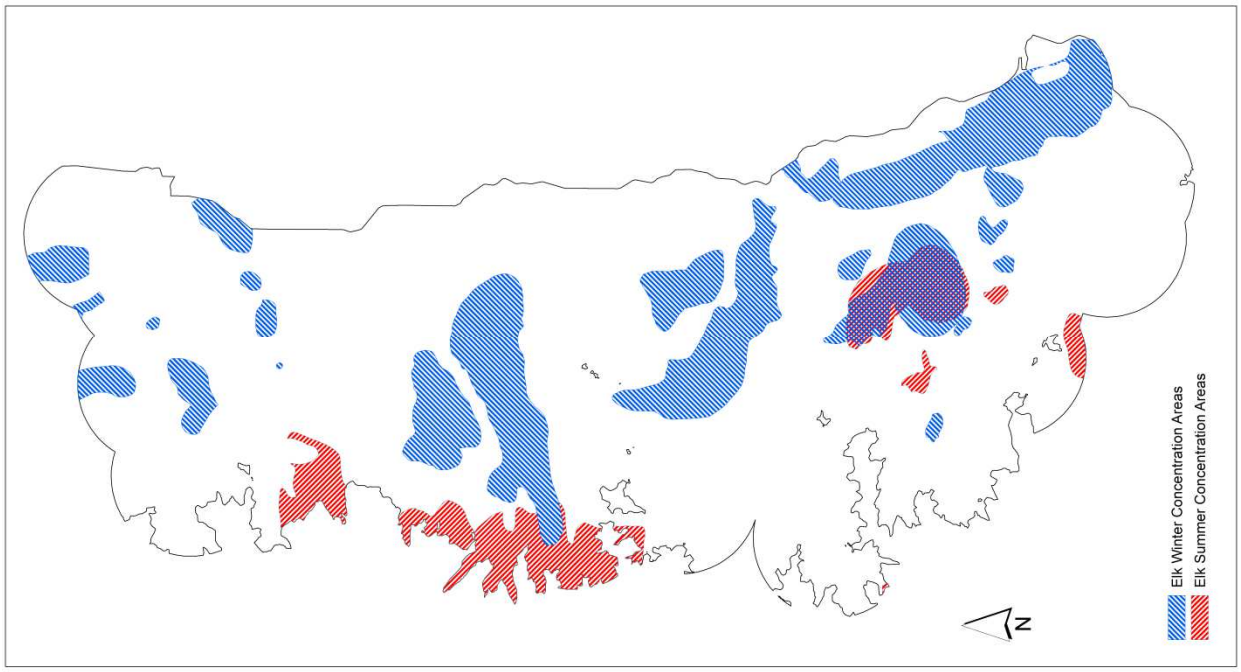

Figure A4.9. Colorado Parks and Wildlife's "Species Activity Maps" for winter (ELK_winconc) and summer (ELK_sumconc) concentration areas of elk.

LITERATURE CITED

Barrett, A. 2003. National Operational Hydrologic Remote Sensing Center SNOw Data Assimulation System (SNODAS) Products at NSIDC. National Snow and Ice Data Center. Boulder, CO, USA.

Clow, D. W., L. Nanus, K. L. Verdin, and J. Schmidt. 2012. Evaluation of SNODAS snow depth and snow water equivalent estimates for the Colorado Rocky Mountains, USA. Hydrological Processes 26:2583-2591.

Theobald, D. M. 2005. Landscape patterns of exurban growth in the USA from 1980 to 2020. Ecology and Society 25:999-1011.

APPENDIX 5: CAMERA TRAP UTILIZATION MODEL DIAGNOSTICS

This appendix gives model diagnostics of the compound-Poisson GLM used in Chapter 2.

Left panel: Normal Q-Q plots using the quantile residuals.

Right panel: Fitted (x-axis) vs. quantile residual plots (y-axis).

Mule Deer:

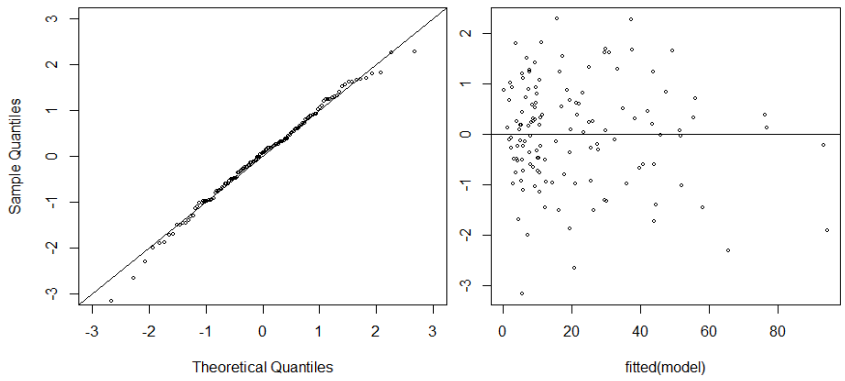

Raccoon:

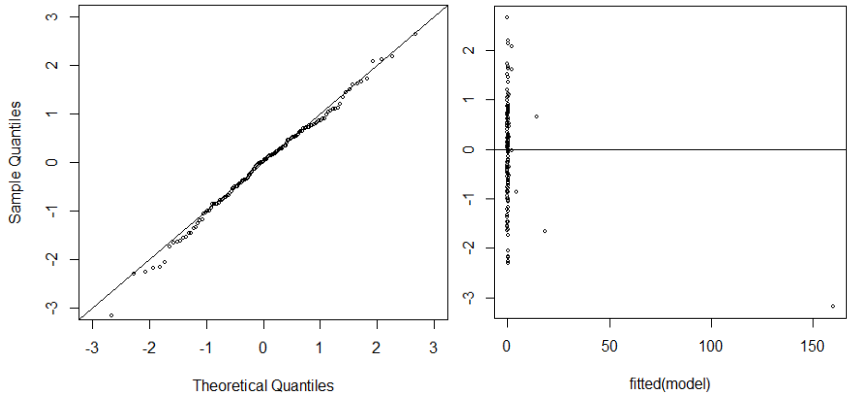

Elk:

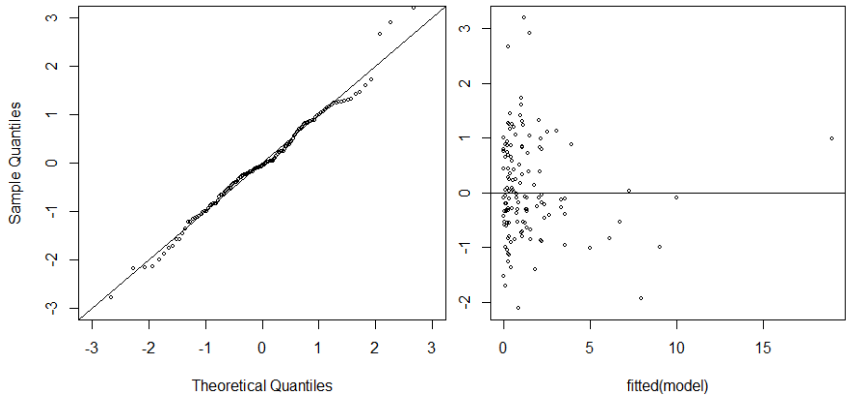

Red Fox:

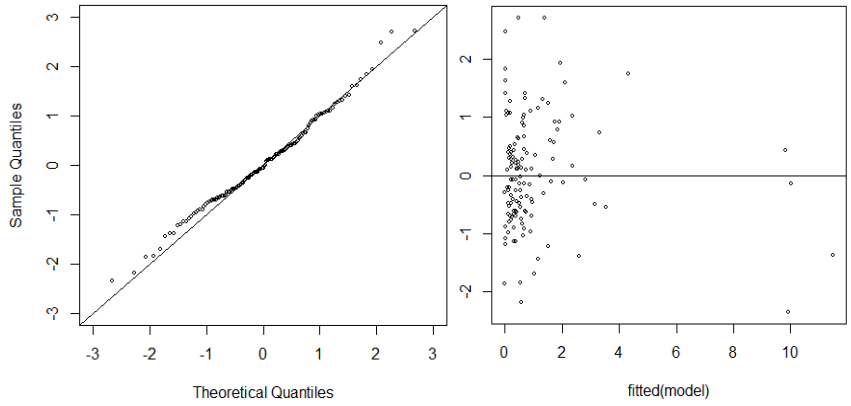

Domestic Cat:

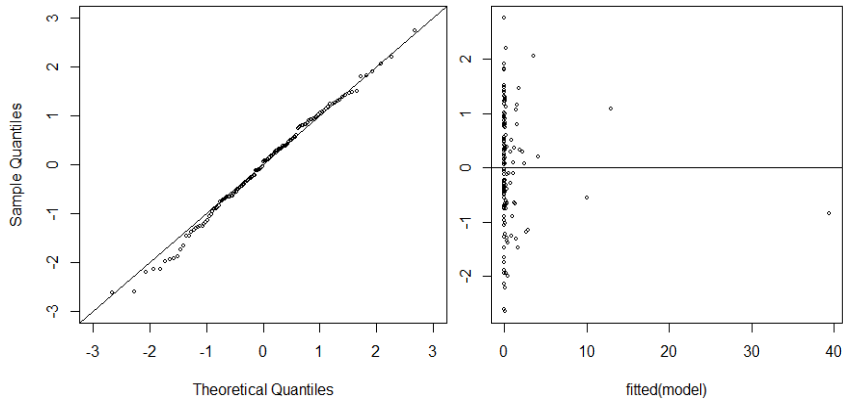

Coyote:

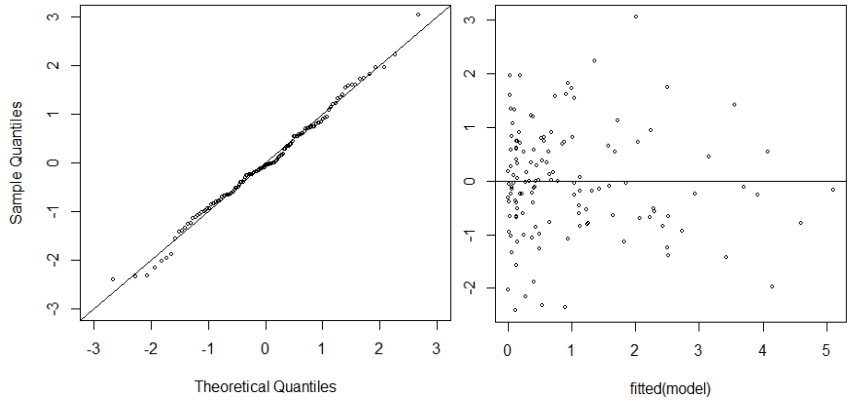

APPENDIX 6: UTILIZATION MODEL COEFFICIENT ESTIMATES

This appendix gives β estimates for the utilization models of Chapter 2. Bootstrap coefficient estimates, standard errors, and 95% confidence intervals for the best model rankings given in Table 2.5. Values are reflective of covariate values centered and standardized by one standard deviation. Power (p) and dispersion (ϕ) profile likelihood estimates are also provided.

Species	Ranking	Parameter	Estimate	Standard Error	Lower 95% C.L.	Upper 95% C.L.
Mule Deer	1	(Intercept)	-3.166	0.123	-3.387	-2.916
		ASP_NW	-0.304	0.086	-0.487	-0.139
		ELEV_12k	-0.728	0.113	-0.950	-0.501
		HDM250	0.889	0.317	0.315	1.569
		$HDM250^2$	-1.230	0.429	-2.411	-0.586
		UTM_Y	-0.216	0.090	-0.390	-0.040
		SHRUB	0.148	0.089	-0.020	0.334
		TPI_150	0.292	0.094	0.115	0.486
		Power	1.727			
		Dispersion	1.920			
	2	(Intercept)	-3.155	0.121	-3.381	-2.912
		ASP_NW	-0.328	0.087	-0.503	-0.170
		ELEV_12k	-0.793	0.097	-0.992	-0.608
		HDM250	0.817	0.298	0.253	1.456
		$HDM250^2$	-1.195	0.408	-2.340	-0.568
		UTM_Y	-0.230	0.090	-0.415	-0.059
		TPI_150	0.264	0.095	0.087	0.446
		Power	1.728			
		Dispersion	1.943			
	3	(Intercept)	-3.141	0.123	-3.359	-2.871
		ASP_NW	-0.313	0.091	-0.496	-0.141
		ELEV_12k	-0.636	0.107	-0.837	-0.406
		HDM250	0.971	0.305	0.439	1.679
		$HDM250^2$	-1.304	0.426	-2.555	-0.671
		SHRUB	0.173	0.096	0.000	0.380
		TPI_150	0.323	0.097	0.147	0.554
		Power	1.732			
		Dispersion	1.966			
	4	(Intercept)	-3.124	0.124	-3.349	-2.870
		ASP_NW	-0.344	0.088	-0.526	-0.183
		ELEV_12k	-0.705	0.091	-0.879	-0.523
		HDM250	0.896	0.287	0.369	1.506
		$HDM250^2$	-1.272	0.415	-2.517	-0.651
		TPI_150	0.289	0.099	0.113	0.508
		Power	1.735			
		Dispersion	1.997			
	5	(Intercept)	-3.125	0.122	-3.347	-2.872
		ASP_NW	-0.352	0.085	-0.530	-0.192
		ELEV_12k	-0.811	0.103	-1.022	-0.612
		HDM250	0.806	0.304	0.241	1.462
		$HDM250^2$	-1.183	0.415	-2.386	-0.563
		UTM_Y	-0.258	0.096	-0.451	-0.074
		Power	1.741			
		Dispersion	1.993			

…Continued

Continued from previous page

Species	Ranking	Parameter	Estimate	Standard Error	Lower 95% C.L.	Upper 95% C.L.
Raccoon	1	(Intercept)	-8.692	1.197	-10.930	-7.636
		HDM250	0.834	0.194	0.513	1.322
		STRUC	-3.025	2.145	-7.815	-0.958
		Power	1.360			
		Dispersion	2.651			
Elk	1	(Intercept)	-5.800	0.340	-6.334	-5.055
		ELEV	1.113	0.363	0.466	1.912
		ELK_conc	0.385	0.171	0.010	0.679
		FOREST3	-0.600	0.249	-1.144	-0.156
		SLOPE	-0.776	0.205	-1.161	-0.349
		KD1500	0.726	0.545	-0.166	2.015
		ELEV*KD1500	1.443	0.587	0.586	3.353
		Power	1.665			
		Dispersion	2.915			
	2	(Intercept)	-5.617	0.291	-6.136	-4.908
		ELEV	0.742	0.359	0.098	1.470
		ELK_conc	0.343	0.227	-0.052	0.674
		SLOPE	-0.820	0.201	-1.222	-0.418
		KD1500	0.675	0.515	-0.377	1.784
		ELEV*KD1500	1.445	0.561	0.541	3.062
		Power	1.670			
		Dispersion	3.055			
Red Fox	1	(Intercept)	-6.527	0.306	-6.865	-6.097
		ASP_E	0.277	0.136	0.018	0.544
		ELEV_12k	10.255	2.893	5.479	16.633
		$ELEV\_12k^2$	-10.386	2.893	-16.909	-5.619
		FOREDGE	0.174	0.163	-0.200	0.445
		HDM250	1.642	0.688	0.773	3.561
		$HDM250^2$	-1.351	2.021	-6.789	-0.310
		STRUC	-0.826	0.254	-1.428	-0.397
		FOREDGE*STRUC	-0.762	0.313	-1.623	-0.342
		Power	1.540			
		Dispersion	1.625			
	2	(Intercept)	-6.475	0.270	-6.846	-5.958
		ELEV_12k	10.356	2.734	6.093	17.164
		$ELEV\_12k^2$	-10.520	2.712	-17.282	-6.442
		FOREDGE	0.184	0.156	-0.129	0.475
		HDM250	1.620	0.667	0.787	3.645
		$HDM250^2$	-1.300	1.516	-7.664	-0.308
		STRUC	-0.837	0.269	-1.577	-0.419
		FOREDGE*STRUC	-0.792	0.301	-1.788	-0.386
		Power	1.548			
		Dispersion	1.703			

…Continued

Continued from previous page

Species	Ranking	Parameter	Estimate	Standard Error	Lower 95% C.L.	Upper 95% C.L.
Domestic Cat	1	(Intercept)	-14.267	7.723	-32.343	-10.232
		HDM250	0.449	0.156	0.209	0.860
		STRUC	-13.247	11.605	-42.437	-5.931
		Power	1.408			
		Dispersion	4.099			
	2	(Intercept)	-15.863	7.283	-31.240	-11.155
		SLOPE	-1.648	0.671	-3.310	-0.629
		STRUC	-15.134	10.876	-40.869	-7.126
		Power	1.412			
		Dispersion	4.177			
	3	(Intercept)	-9.355	4.967	-11.522	-8.044
		SLOPE	-2.088	0.654	-3.698	-1.042
		STRUC_yard	1.647	2.403	0.982	2.886
		Power	1.399			
		Dispersion	4.147			
Coyote	1	(Intercept)	-6.612	0.250	-7.000	-6.160
		CC_avg90	-0.423	0.199	-0.805	-0.016
		ELEV	0.280	0.150	-0.007	0.588
		FOREDGE	-0.164	0.155	-0.567	0.072
		HDM_pnt	-0.585	0.264	-1.238	-0.289
		SLOPE	-0.817	0.171	-1.187	-0.513
		TPI_50	-0.747	0.253	-1.358	-0.333
		TPI_50^2	-1.475	0.752	-4.300	-0.594
		CC_avg90*FOREDGE	-0.400	0.147	-0.812	-0.179
		Power	1.485			
		Dispersion	1.112			
	2	(Intercept)	-6.598	0.258	-6.996	-6.110
		CC_avg90	-0.241	0.179	-0.559	0.139
		FOREDGE	-0.188	0.160	-0.608	0.056
		HDM_pnt	-0.677	0.280	-1.409	-0.358
		SLOPE	-0.866	0.172	-1.247	-0.564
		TPI_50	-0.724	0.260	-1.301	-0.262
		TPI_50^2	-1.554	0.778	-4.398	-0.632
		CC_avg90*FOREDGE	-0.375	0.147	-0.817	-0.158
		Power	1.483			
		Dispersion	1.129			

APPENDIX 7: STUDY AREA PREDICTED UTILIZATION MAPS

This appendix gives the output utilization maps derived in Chapter 2, which are considered independent variables for the resource selection models of Chapter 3. Predicted utilization (30 second intervals used per square meter per day) is derived from the best or model averaged generalized linear model for mule deer (Figure A7.1), raccoon (Figure A7.2), elk (Figure A7.3), red fox (Figure A7.4), domestic cat (Figure A7.5), and coyote (Figure A7.6) over one year period (Chapter 2). The figures below can be compared visually to the underlying covariates (Appendix 4) and municipal boundaries (Figure 2.1).

Utilization values were mapped with a 30 m grain size. The range of utilization values predicted by the model is indicated on the gradient scale bar (legend). For variation to be visible across the mid-range of predicted values (rather than the extreme values), the color gradient was scaled linearly where the extremities are clipped (+/- 2.5 standard deviations from the minimum and maximum). Predictions were only allowed to occur in locations fitting the domain of landscape attributes sampled by the camera traps. Additionally, the location had to fall within 6.8 km of any camera, which is one half of the maximum nearest neighbor distance between pairs of cameras. For the western edge of the study area, this usually resulted in an elevation boundary of approximately 3100 m a.s.l, a geographic barrier of snow pack in the winter. The eastern border of the study area represented the transition zone between the mountains and plains, but was more precisely defined by U.S. highway 36, state highways 93 and C-470, and Broadway Avenue (Boulder City), which are major transportation routes thought to represent a geographic barrier to some animal movements. Water bodies (U.S.G.S. National Hydrological Dataset) were masked from predictions.

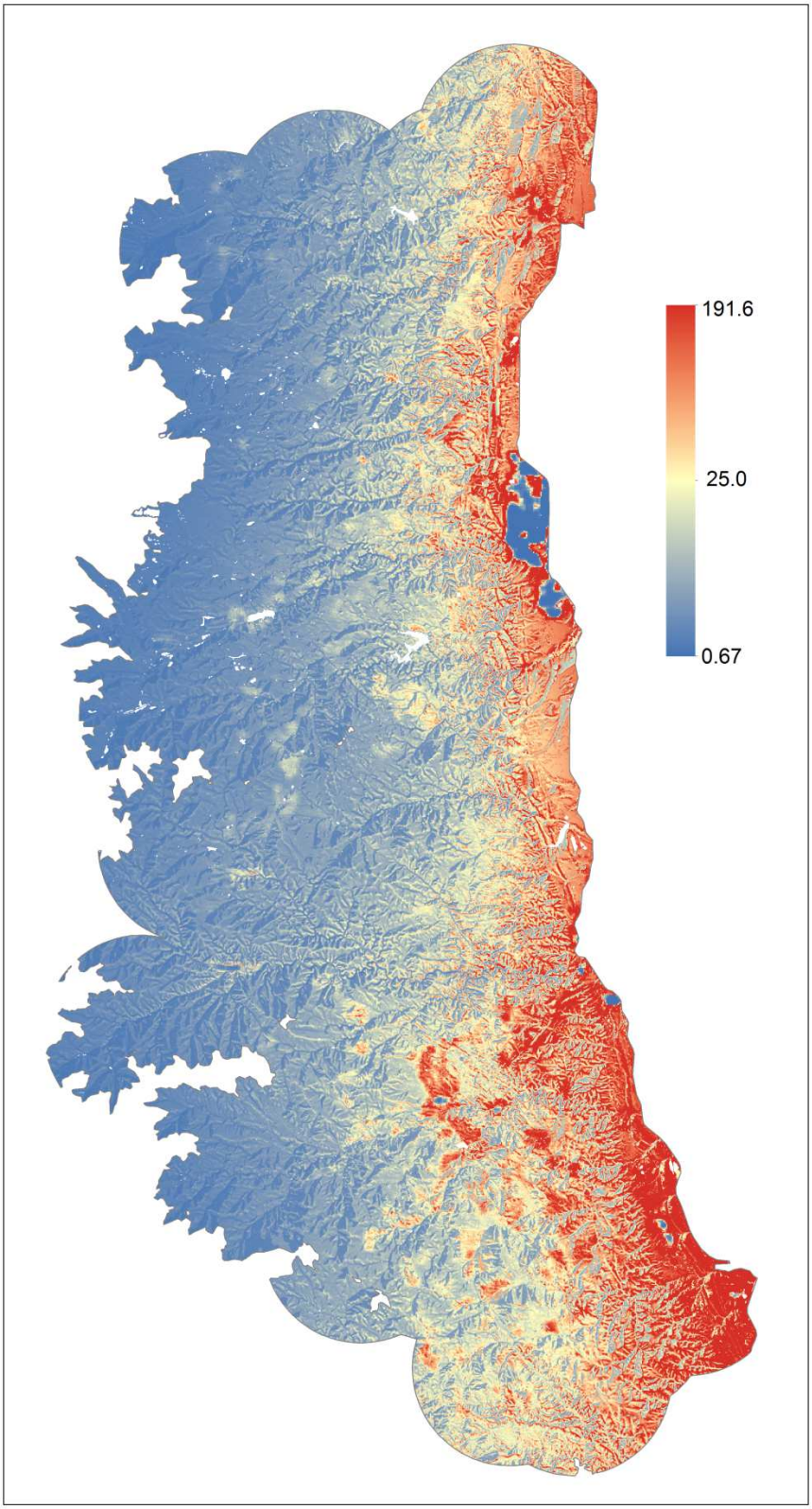

Figure A7.1. Mule deer utilization prediction map from model averaging.

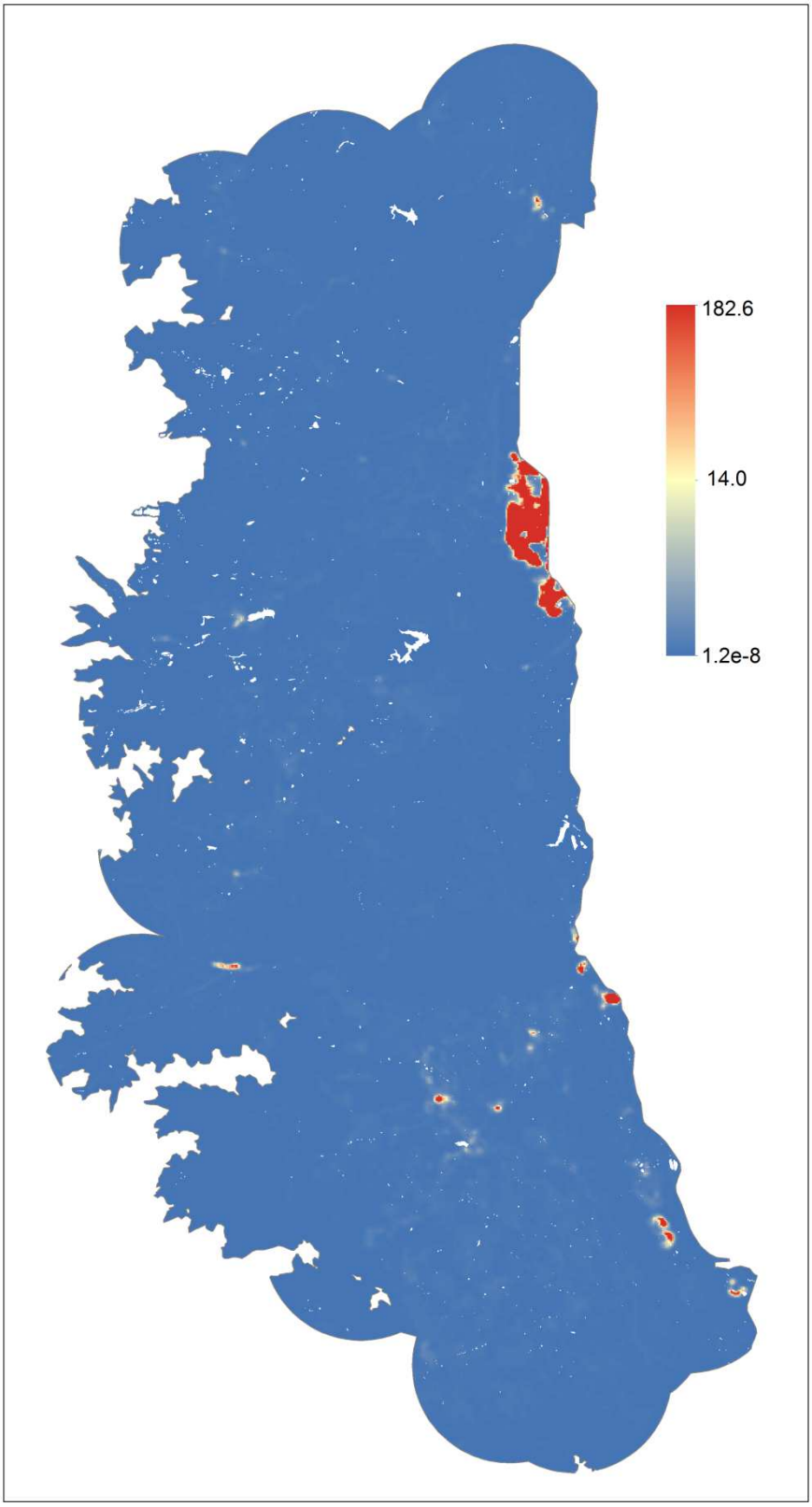

Figure A7.2. Raccoon utilization prediction map from the single best model.

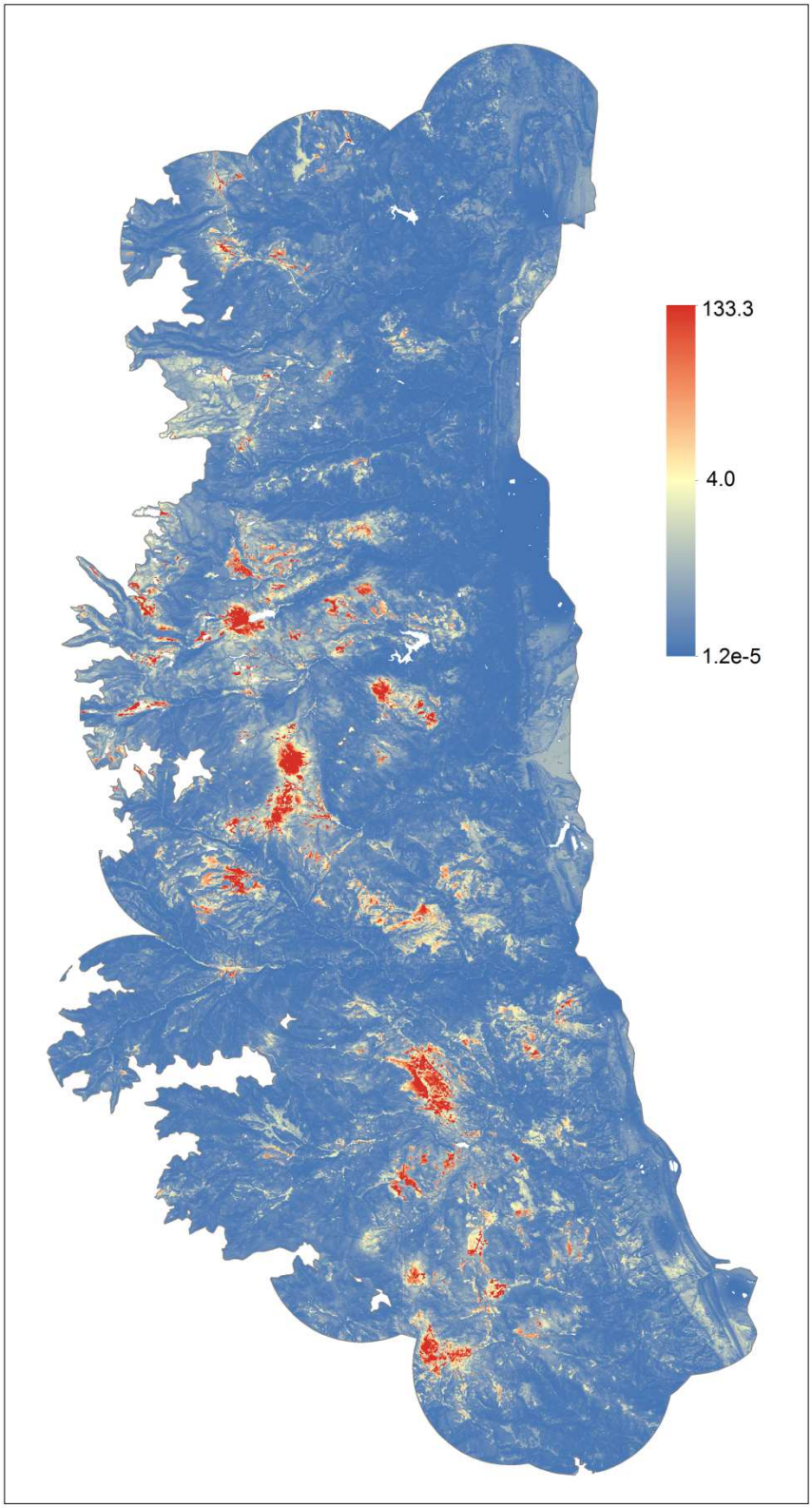

Figure A7.3. Elk utilization prediction map from model averaging.

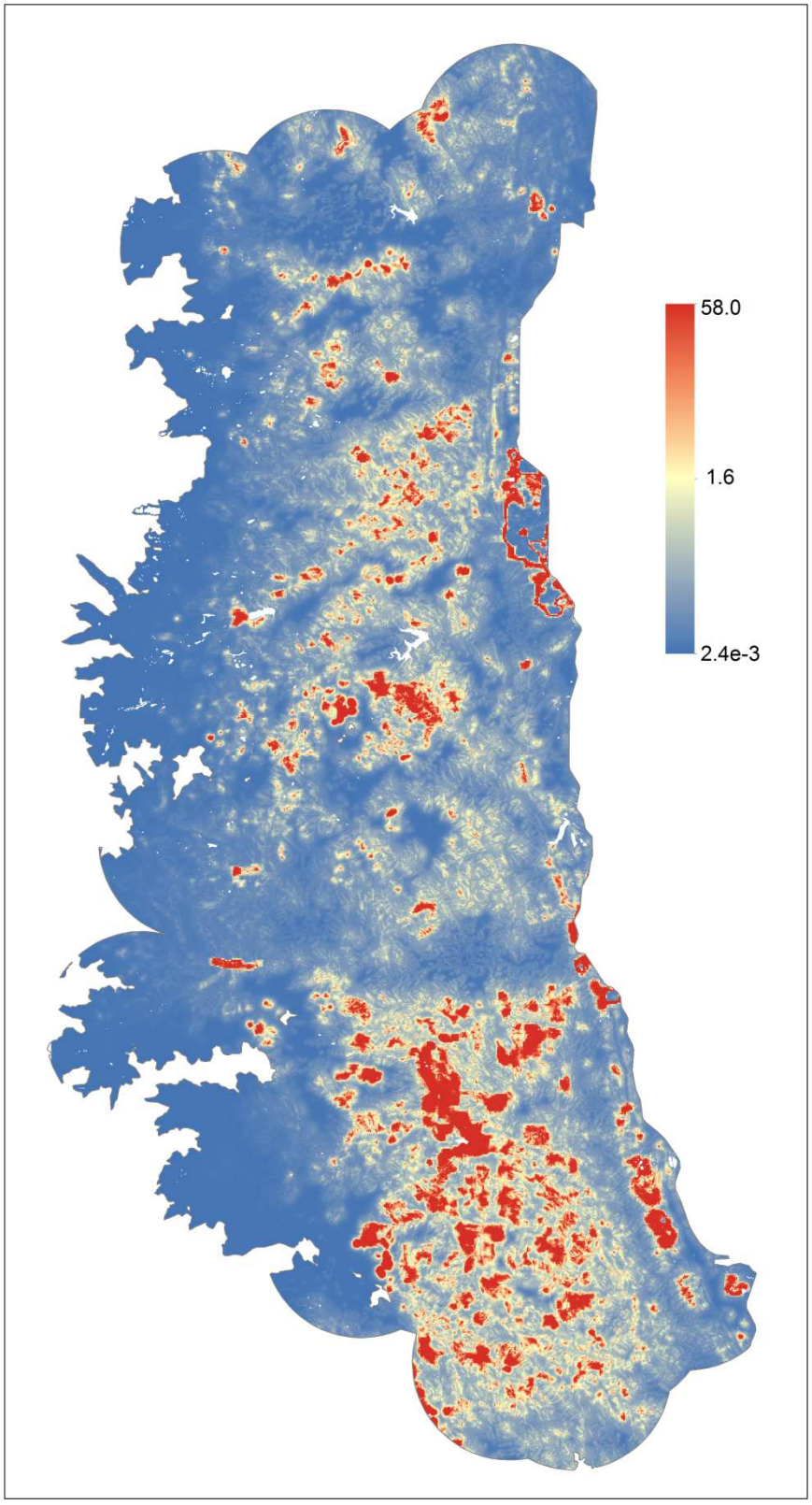

Figure A7.4. Red fox utilization prediction map from model averaging.

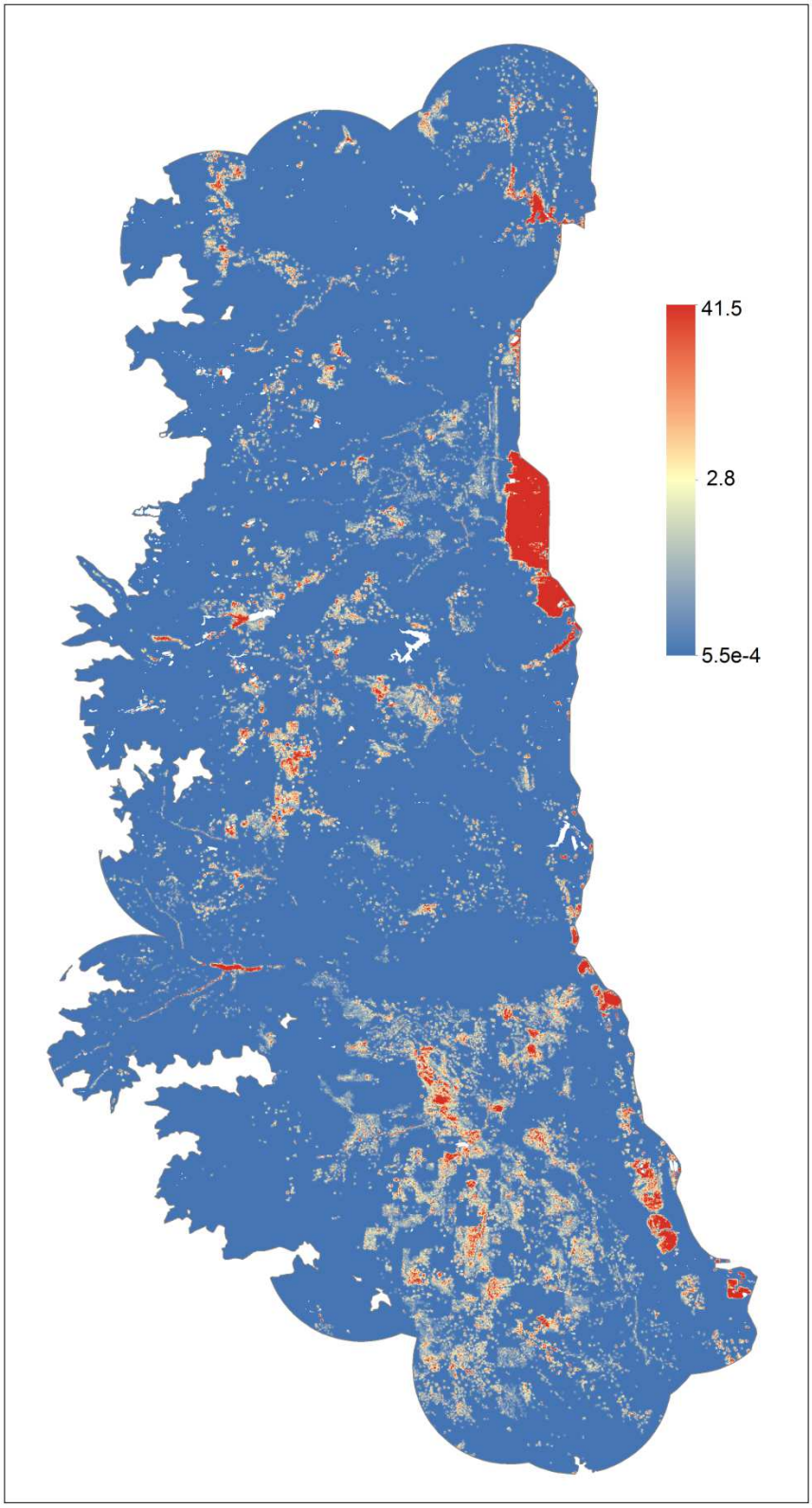

Figure A7.5. Domestic cat utilization prediction map from model averaging.

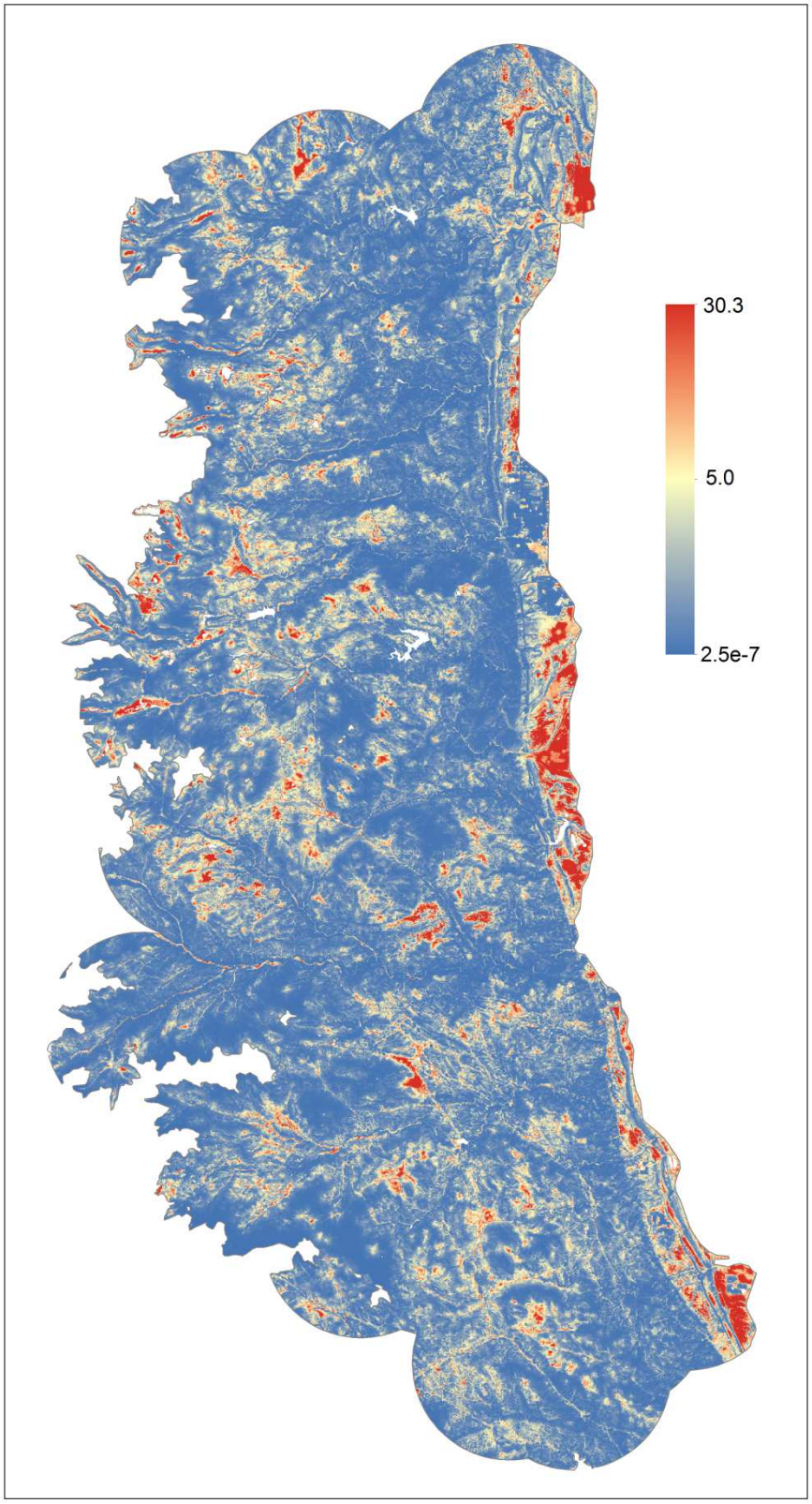

Figure A7.6. Coyote utilization prediction map from model averaging.

APPENDIX 8: GPS LOCATION ACQUISITION, CLUSTER IDENTIFICATION, AND KILL-SITE PREDICTION MODEL

This appendix provides detailed methodology for defining cougar kill and non-kill sites in Chapter 3. Cougar GPS collar data used in this study represent a portion of a larger parent project on cougar ecology led by Colorado Parks and Wildlife.

GPS Location Acquisition

Cougars were outfitted with one of three GPS collar models over the course of the study (Table A8.1). Collar data was retrieved via satellite uplink, UHF/VHF data transmission, or by flash-memory recovery. Each individual was monitored 2 to 57 months (median and mean - 14 and 18 months). Average monthly fix success rate of GPS collars (the percentage of scheduled fixes acquired) was 77.5% across animals.

Cluster Identification Algorithm

Unique clusters of GPS locations logged by the collars were identified using a customized algorithm (Alldredge et al. 2008) that utilizes spatial and temporal proximity characteristics to classify GPS locations into discrete clusters. For a given individual animal, GPS points containing a time stamp and UTM coordinates are chronologically synced with the predetermined GPS location acquisition schedule. Time steps correspond to the scheduled fix acquisition intervals (Table A8.1). Time step assignments reflect any missed GPS locations (i.e., time step 114 followed by 115 followed by time step 117, in which the 116^{th} scheduled acquisition was missed by the collar).

The algorithm classifies aggregations of two or more points within a specified distance and time interval. Placing all points into a matrix, an association measure A_{ij} was used to identify

unique pairings (points *i* and *j*) that were potentially considered a cluster based on distances in time t_{ij} (in time steps) and space d_{ij} (distance meters) simultaneously:

$$A_{ij} = \frac{1}{e^{d_{max}/d_{ij}}}\left(1 - \frac{t_{ij}}{t_{max}}\right)$$

The temporal and spatial window that a pairing could be considered a cluster was defined by t_{max} which was set at 28 time steps (4 days) and with a d_{max} of 200 m. The formulation weighted d_{ij} heavier than t_{ij} while ensuring that A_{ij} was negative for any locations outside the temporal window. Upon completion of the A_{ij} calculations for all matrix elements, the largest element value corresponded to the t_{ij} points that are spatially and temporally closest. If the t_{ij} of the pairing of points was within d_{max}, the mean of the point pairs' UTMs was calculated as a centroid seed. All other points were then compared to this seed with an association vector $\overrightarrow{A_c}$ using the A_{ij} formulation. The point within $\overrightarrow{A_c}$ with the highest nonnegative A_{ij} value, and within d_{max}, was then added to the cluster and a new centroid UTM was calculated. The procedure was reiterated until all points within t_{max} and d_{max} are exhausted. After a cluster was formed, the constituent points were removed from the next iteration of association matrix creation before proceeding. Points not a member of any *S1* cluster were then considered as *S2* cluster types, which are any two consecutively logged points within 500 m but separated temporally by one scheduled GPS fix, missed by the collar. Although the true proximity of the missing location to the temporally neighboring points was unknown, the expected probability of it being < 250 m would be relatively high given a straight-line path of travel.

The remaining points not considered as *S1* or *S2* (multi-point cluster types) were then classified as single-point "clusters". The observed proportion of feeding activities occurring at

single point clusters was only 0.03 – 0.06. Since predicting these rare events proved difficult (*unpublished data*), all single points were automatically classified as non-kill sites.

Ground-truthing Field Methods:

Algorithm processing was conducted in each of the 36 monthly intervals. While GPS locations were accumulating for a monthly interval, ground-truthing visits for the previous month were conducted. In the field, ground-truthing observers were directed to be unbiased within a monthly period with respect to cluster type, cougar, or habitat, unless inclement winter weather hindered access to a particular area. Observers were assigned to cougars and geographic sub-regions on a monthly rotation to account for differences in observer abilities. Novice observers were trained and accompanied by an experienced observer for 2-4 weeks prior to ground-truthing on their own to aid the development of a search image for prey remains and sign. Each sampled cluster site was exhaustively searched within a radius of 50 meters around each GPS location composing the cluster. Detailed searching commenced once prey remains were discovered. However, all spatially outlying GPS locations were eventually visited. Clusters were classified with a binary presence/absence indicator of a feeding event. In the case of feeding event presence; prey species, age, and sex were identified. It was assumed that all feeding events were actual kill events made by the cougar in question, even though in a few instances it was evident that the prey item was killed by a different cougar or from other sources.

Kill Prediction Model

GPS locations recorded within seven days of capture or locations spatially and temporally associated with a natal den were truncated. I used a generalized linear model (R Development Core Team 2013) with a logit link function to model the binary response of the presence (1) or absence (0) of feeding remains at a cluster using a suite of covariates hypothesized to influence

the probability of presence of prey remains. Covariates, as defined below, were grouped into three major classes: GPS spatio-temporal characteristics, activity sensor measures, and gound-truthing error attributes.

GPS spatio-temporal characteristics:

GPS location spatio-temporal characteristics of the cluster take advantage of the fact that cougars partake in particularly long handling times when feeding. However, cougars also exhibit movement behaviors to and away from clusters over the course of consumption. The number of GPS positions (POSCOUNT) collected at the cluster is a proxy for the amount of time potentially consuming the carcass. Most feeding activities take place during the night, while day-time resting activities often occur outside of the cluster defined spatial extent; thus the proportion of GPS positions within the cluster were collected during the night time (NIGHTPROP). An interaction between POSCOUNT and NIGHTPROP was included to help distinguish between repeat usage of day-bed sites and that of feeding sites. Spatial dispersion of GPS locations within a cluster (CENTR) was measured as the average distance from geometric center of each cluster to each constituent GPS position.

Activity sensor measures:

Additional bio-telemetry data is increasingly being incorporated with animal movement data for the remote identification of certain behaviors (Nams 2014). For cougars monitored with GPS PLUS collar models (Table A8.1), activity data logged by the collar's on-board activity sensor was used to derive metrics that may enhance the discrimination of feeding activities from non-resting and travelling activities. The sensor's X-axis measures the relative amount of forward-backward and head tilting movements, while the Y-axis measures the relative amount of side to side and head-rolling movements. ACCX was calculated as the mean of all 5 minute

activity intervals recorded on the x-axis within a 1.5 hr window of all locations constituting the cluster. This measure was recorded for the y-axis activity sensor as well (covariate: ACCY). ACCX and ACCY measures showed significant positive correlation (Pearson corr. coef. = 0.92). Despite this, I retained both measures and calculated the difference between the two (ACCXYDIFF), while never combining ACCX and ACCY main effects in any model. Specifically, ACCXYDIFF was the average difference within a 1.5 hr window; in which exploratory examination of the data seemed to indicate more positive vs. more negative values at confirmed feeding events. It is anticipated that a more positive ACCXYDIFF would indicate movements associated with feeding, while a more negative ACCXYDIFF would indicate movements not associated with feeding activities.

Ground-truthing error attributes:

Several covariates were included to assess the effect of false-absence sources while ground-truthing. The GPS fix acquisition success rate (FIXRATE) was calculated on a moving window for a 96 hr time period for each GPS location logged, which then was averaged among all GPS locations in the cluster. The proportion of positions downloaded successfully via satellite linkage (FIELDPROP) was calculated for each cluster, where lower FIELDPROP would be related to a lower probability of finding carcass remains, as observers had a higher potential to miss feeding remains caused by a slightly miss-focused investigation just outside the search radius. Because clusters were ground-truthed anywhere from 1-60 days post feeding, the search lag time (SEARCH) was used as a continuous variable to characterize an increasing false negative classification rate associated with carcass degradation over time. Tambling et al. (2010) found that the percentage of clusters ground-truthed containing kills declined within the first four weeks, but was constant within the following 16 weeks. Other studies were successful at locating

at least some prey remains with time lags of 6-12 months (Anderson and Lindzey 2003, Tambling et al. 2010). Therefore I tested transformations where a negative exponential decay function would be expected in addition to a simple linear term. The season (SEAS) (SUM: Jun 1 – Sep 30, NON-SUM: Oct 1 - May 31) was used as a proxy for general seasonal differences between carcass decay rates associated with summer temperatures. Smaller prey would be assumed to degrade and/or be displaced away from the feeding site quicker than larger prey.

Spatio-temporal covariates described above were chosen *a priori* based on results found in the other studies discussed, thus all combinations of the *a priori* chosen main effect covariates were used to create candidate models. All two-way interactions and quadratic terms were also specified, unless pairings of variables were not allowed to occur in the same model based on obvious co-linearity (Pearson corr. coef. > 0.6). Using AICc model selection (Burnham and Anderson 2002), the most parsimonious model held 29.7% of the AIC weight while the second and third (27.4% and 17% AIC weights respectively) were nested within the top model. Coefficient estimates and 95% confidence intervals for these estimates of the most parsimonious model are given in Table A8.2.

Performance of the best model was assessed by reapplying the model predictions back to the input dataset of clusters but by discretizing the predicted probabilities to a binary indicator for the presence or absence of feeding evidence by determining a probability cut-off value. If prediction is the goal, this cut-off value should be chosen to balance sensitivity (true-positive rate) and specificity (true-negative rate) (Hosmer and Lemeshow 2000, Knopff et al. 2009). Optimizing sensitivity and specificity resulted in a cut-off value of 0.372. Receiver Operator Characteristics (ROC) analysis (Sing et al. 2005) was carried out to calculate the area under the curve (AUC). An AUC of 0.893 was achieved, which indicates excellent discrimination. To

protect against potential over-fitting, the average AUC measure using K-fold cross validation with 20 hold out sets (k=20) was calculated (Boyce et al. 2002, Knopff et al. 2009). If this K-fold cross validation AUC measure exceeded the simple direct AUC measure then a simpler model structure may have been warranted. However, this resulted in a cross-validation measure of 0.886, which did not cause much concern.

Finally model predictions, along with appropriate feeding (kill event) vs. non-feeding (non-kill event) classification (based on the cut-off value) were applied to all clusters identified by the clustering algorithm (visited or not visited by an observer).

TABLES

Table A8.1. GPS collar models, acquisition schedules, fix acquisition scheduling, fix rates, and count of cougar subjects.

Date Range Monitored	GPS Collar Manufacturer	Model	Scheduled GPS Location Aquistion Times	GPS Location Acquisition Success	# of Cougar Subjects Monitored
Jan 1, 2008 - ca. Jan 1, 2009	Lotek Wireless, Inc, Newmarket, ON, CAN	4400s	00:00, 03:00, 06:00, 09:00, 12:00, 15:00, 18:00, 21:00	75.6%	15
ca. Jan 1, 2009 - ca. Jan 1, 2010	Northstar Science and Technology, LLC, King George, VA, USA	D-cell	00:00, 03:00, 06:00, 09:00, 12:00, 15:00, 18:00, 21:00	69.2%	17
ca. Jan 1, 2010 - Dec 31, 2012	Vectronics Aerospace, GmbH, Berlin, DE	GPS PLUS	02:00, 05:00, 8:00, 12:00, 16:00, 20:00, 23:00	79.9%	38

Table A8.2. Coefficient estimates for the most parsimonious model for predicting the occurrence of feeding events given a cluster location.

Covariate	Estimate	Std. Error	z - value	Pr(>|z|)	95% LCL	95% UCL
(Intercept)	-9.0745	1.87833	-4.83	<0.0001	-12.8092	-5.4512
ACCX	0.1483	0.02234	6.64	<0.0001	0.1054	0.1934
$ACCX^2$	-0.0007	0.00022	-3.28	0.0010	-0.0012	-0.0003
ACCXYDIFF	-0.0128	0.04572	-0.28	0.7787	-0.1013	0.0783
ACCXYDIFF*log(POSCOUNT)	0.1145	0.04427	2.59	0.0097	0.0289	0.2027
ACCXYDIFF*CENTRDIST	-0.0006	0.00017	-3.53	0.0004	-0.0010	-0.0003
log(POSCOUNT)	1.5205	0.43582	3.49	0.0005	0.6745	2.3866
NIGHT_PROP	-1.5152	0.85217	-1.78	0.0754	-3.1820	0.1661
log(POSCOUNT)*NIGHTPROP	2.1555	0.66515	3.24	0.0012	0.8693	3.4824
CENTRDIST	-0.0161	0.00814	-1.98	0.0478	-0.0319	0.0001
$CENTRDIST^2$	0.0001	0.00003	4.51	<0.0001	0.0001	0.0002
SEAS (base level: summer)	1.0210	0.21343	4.78	<0.0001	0.6063	1.4442
SEARCH	-0.0184	0.00812	-2.27	0.0235	-0.0345	-0.0026
FIELD_PROP	7.9887	4.66176	1.71	0.0866	-1.1515	17.1168
$FIELD\_PROP^2$	-4.6638	3.12911	-1.49	0.1361	-10.7860	1.4810

LITERATURE CITED

Alldredge, M. W., E. J. Bergman, C. Bishop, K. A. Logan, and D. J. Freddy. 2008. Pilot evaluation of predator-prey dynamics on the uncompahgre plateau. WP 3001: Wildlife Research Report, Mammals Program. Colorado Parks and Wildlife.

Anderson, C., R., and F. G. Lindzey. 2003. Estimating cougar predation rates from GPS location clusters. Journal of Wildlife Management 67:307-316.

Boyce, M. S., P. R. Vernier, S. E. Nielsen, and F. K. A. Schmiegelow. 2002. Evaluating resource selection functions. Ecological Modelling 157:281-300.

Burnham, K. P., and D. R. Anderson. 2002. Model selection and model inference: a practical information-theoretic approach. 2nd edition edition. Springer-Verlag, New York, NY, USA.

Hosmer, D. W., and S. Lemeshow. 2000. Applied Logistic Regression. Pages 392 *in* John Wiley and Sons, Inc., New York, NY, USA.

Knopff, K. H., A. A. Knopff, M. B. Warren, and M. S. Boyce. 2009. Evaluating Global Positioning System Telemetry Techniques for Estimating Cougar Predation Parameters. Journal of Wildlife Management 73:586-597.

Nams, V. O. 2014. Combining animal movements and behavioural data to detect behavioural states. Ecology Letters 17:1228-1237.

R Development Core Team. 2013. Vienna, Austria.

Sing, T., O. Sander, N. Berrenwinkel, and T. Lengauer. 2005. ROCR: visualizing classifier performance in R. Bioinformatics 21:7881 - 7882.

Tambling, C. J., E. Z. Cameron, J. T. Du Toit, and W. M. Getz. 2010. Methods for Locating African Lion Kills Using Global Positioning System Movement Data. Journal of Wildlife Management 74:549-556.

APPENDIX 9: STEP SELECTION FUNCTION ANALYSIS AND HUNTING SUCCESS MODELS

This appendix provides detailed methodologies for carrying out step-selection function (SSF) data processing and statistical model for inference on patch-selection and hunting success.

Assigning Matched Available Locations

For the step-selection function, movement steps were defined as the pairing of locations used by the cougar consecutively in time, which could be either a GPS location or a location cluster if multiple locations occurred within a temporal-spatial window of 200 m and 4 days (Appendix 8). For single GPS locations, time stamps and UTM x- and y-coordinates generated by the GPS collar were used. For clusters, the time stamp for the initial GPS location constituting the cluster and mean UTM x- and y-coordinates were used. For each cougar and step, the length and turning angle (angle relative to the previous step) was calculated.

For each cougar, the observed step lengths were fit to a set of candidate distributions (Poisson, Gaussian, normal, negative binomial, exponential, geometric, and log-normal), where the best fitting distribution of these step lengths was chosen using maximum likelihood (R package 'MASS') (R Development Core Team 2013). The log-normal distribution provided the best fit in all cougars. For each step, a new distribution of step lengths were generated, with a mean set to the observed length of the step in question, and standard deviation set by the fitted log-normal distribution (Figure A9.1). Other studies generate one global distribution from which new steps are drawn (Fortin et al. 2005). Generating a new distribution for each step allows the displacement of the generated available locations to correspond closer to the length of the actual step. However, the variance of the generated distribution increases with mean step length (Figure

A9.1). Because this inevitably results in some extreme step lengths being generated, a new random step distance was selected if it was greater than 10 km, as very few steps (if any for most animals) were observed to be greater than this distance. This resulted in fewer generated steps being projected outside the study area, especially on the east and west boundaries which are historically less suitable to cougar utilization. The observed turning angles for each cougar were fit to a wrapped normal distribution (R package 'circular') using maximum likelihood. This produced a concentration parameter ρ that was used, along with the observed turning angle, to generate a distribution of potential turning angles specific to that step (Figure A9.2).

For each step, 10 step lengths and turning angles were drawn from the generated log-normal and wrapped normal distributions, respectively, to project a set of matched locations for each step using standard trigonometric functions. These new locations were employed as available locations matched to the following observed GPS location (Figure 3.2). Thus, given the temporal interval of the steps, these available locations were ones that the cougar could have chosen at the end of the step, but simply did not (Thurfjell et al. 2014). Any matched point generated outside the study area was truncated (2.06% of the matched points being removed), which only causes an imbalance in the number of available locations per "use" location.

Like other studies, an arbitrary number (10) of matched locations were generated. Unfortunately, additional matched points significantly increased computational time given the model fitting procedures and statistical package utilized (as described below). Considering a large number of usage locations are collected with GPS collar studies, the influence of the number of locations is probably minimal (Thurfjell et al. 2014) as demonstrated by Northrup et al. (2013), but see Fortin et al. (2005) in the case of rare landscape features. Sensitivity of coefficient estimates, as given by the best model (described below), was assessed by comparing

the estimates when using all 10 matched locations to those derived with a random subset of fewer matched locations (1,…9). For most covariates, (i.e., MDEER), very little difference in coefficient estimates was found. For housing density (HDM), there was likely a positive bias associated with including fewer matched locations (Figure A9.3). However, this bias was most noticeable when only one matched location was implemented, and became progressively less discernable when more than four were implemented (Figure A9.3). Therefore, the 10 matched locations seemed like a reasonable compromise between bias and computation time.

Defining a Successful Hunt and Hunting Locations

After defining which clusters were highly probable kill events (Appendix 8), hunting locations were defined from all non-kill sites. Considering cougars are generally nocturnal hunters (Elbroch et al. 2013, Ruth et al. 2010, Sweanor et al. 2008), all day-time non-feeding clusters and day-time single GPS locations (and generated matched points) were removed. Results from the cluster prediction model used here (Appendix 8), and that of other studies (Ruth et al. 2010, Elbroch et al. 2013) indicate that an increasing percentage of day-time locations constituting a cluster significantly decreases the probability the cluster was a feeding event. Thus any cluster identified or single GPS location recorded completely during the daytime were likely day-bed locations. I also removed any GPS locations (or clusters) that coincided temporally with another cluster in which prey handling activities were already ongoing to avoid having the situation where travelling locations between kill-sites and resting sites were mistaken as hunting locations. Thus, the remaining locations predicted as non-feeding events (and generated matched points) were ones occurring entirely between the commencement of a feeding event and the start of another feeding event. It is assumed that these locations represented potential hunting events for the next prey item.

All kill locations are technically hunting locations, as they are the manifestation of a successful hunting location. Defining the kill and hunting locations separately allowed naturally defined "hunting sequences" when viewed chronologically (Figure 3.1). For the hunting success model, each hunting sequence was used as a strata level to be conditioned on when assessing which landscape factors contribute to the probability of a successful kill at a hunting location. In reality this probability is the joint probabilities of encountering an actual prey animal, launching an attack, and successfully subduing the prey. Decoupling all processes and decisions leading up to making a successful kill by a predator would be interesting (Hebblewhite et al. 2005, Hilborn et al. 2012, McPhee et al. 2012), but not practical given the data collected here. If kill events occurred back to back with no hunting points occurring in the inter-kill interval, then the second kill site was discarded for the hunting success model input.

Mixed Effect Conditional Logistic Regression Model

Inferences concerning patch choice can be classified as a third- or fourth-order resource selection problem (Johnson 1980). For the SSF analyses, a conditional logistic regression model (Manly et al. 2002, McDonald et al. 2006) can be harnessed to assess whether the probability of a free-ranging animal choosing a location over alternative available locations is determined by a certain landscape attribute $\mathbf{x}$ or set of certain landscape attributes (let $\mathbf{x}' = \mathbf{x}_1,\ldots\mathbf{x}_m$ landscape attributes). Considering the attributes of alternative available locations change as animal n (let $n = 1,\ldots,N$ for multiple animals) moves about the landscape, conditioning on a choice set, one can account for this changing availability. Let choice set t correspond to each multiple discrete movement event unique to animal n ($t_n = 1,\ldots T_n$) as wild animals would be unlikely to share the same choice set. Choice set t is composed of a j single location actually used, and the location or multiple locations available to be chosen from, i, (so let $j = 1$, and $i = 2,\ldots J$). J usually will equal

11 given that 10 available points were generated in the SSF processing, unless extreme outlying available locations were discarded. A starting point for understanding whether the choosing of location i_{tn} over location(s) j_{tn} is influenced by landscape covariates $\mathbf{x'}$ can be done by estimating a corresponding set of coefficients $\beta = \beta_1,\ldots \beta_m$, by acquire maximum likelihood estimates for β coefficients using:

$$L(\beta) = \prod_{t=1}^{T_n} \frac{\exp(\mathbf{x}'_{jtn}\beta)}{\sum_{i=1}^{J} \exp(\mathbf{x}'_{itn}\beta)} \qquad \text{eq. A9.1}$$

An intercept term does not exist given this conditioning on the strata. It is assumed that random errors are independent and identically distributed, all animals respond the same, and sampling intensity of j_{tn} is proportional to the animal's time spent in the population. To relax homogeneity in sampling intensity and in the response, random effect terms can be added (Gillies et al. 2006, Duchesne et al. 2010, Zeller et al. 2014, Merkle et al. 2015). I followed the conditional logistic mixed effect model given in Duchesne et al. (2010):

$$L(\beta,\theta) = \prod_{n=1}^{N} \int \prod_{t=1}^{T_n} \frac{\exp(\mathbf{x}'_{njt}\beta + \mathbf{z}'_{njt}\mathbf{b})}{\sum_{i=1}^{J} \exp(\mathbf{x}'_{nit}\beta + \mathbf{z}'_{nit}\mathbf{b})} f(\mathbf{b};\boldsymbol{\theta})\mathrm{d}\mathbf{b} \qquad \text{eq. A9.2}$$

where random effect $\mathbf{b}$ is independent and identically distributed $N(0,\sigma^2)$. $\boldsymbol{\theta}$ of the density $f(\mathbf{b};\boldsymbol{\theta})$ is a vector of unknown parameters to be estimated, which follow the categorical levels provided by animal identifiers ($\mathbf{b}_{\text{animal\_ID}}$) (corresponding to the N animals) or a segments of time (calendar month = $\mathbf{b}_{\text{Month}}$). These random effect terms were included as random regression coefficients as they allow the inter-individual responses to vary according to a set of covariates, $\mathbf{z'}$ which will often correspond with some or all of the covariates given in $\mathbf{x'}$.

Employing conditional logistic mixed effects models in step-selection function analysis is fairly recent (Thurfjell et al. 2014). The likelihood of the standard conditional logistic regression (eq. 1) is often fit with a Cox proportional hazards model with defined strata (Gail et al. 1981, Manly et al. 2002, McDonald et al. 2006) (all right censoring times set equal). The likelihood of the mixed effect conditional logistic regression (eq. 2) can be fit by extending either a Poisson log-linear, Poisson nonlinear, or a stratified proportional hazard model to incorporate random effects (Chen and Kuo 2001). Here, a mixed effect Cox-proportional hazard model, with strata terms indicating the choice set t_n, was used (R package 'coxme') (Therneau 2012, R Development Core Team 2013, Merkle et al. 2015). Estimated β coefficient values of the fixed effects on their linearized scale indicate the degree of selection, where more negative β coefficients or more positive β coefficients respectively infer increased selection against or selection toward an increasing value of some covariate **x** of interest. For purposes of this study, assessing which combination of covariates are most parsimonious (i.e., through model selection), for explaining the patch-selection process and the population level coefficient estimates β (on the linear scale), are of primary interest. Of secondary interest is the amount of variation, σ^2, explainable by the random effects $\mathbf{b}_{\mathbf{animal\_ID}}$ or $\mathbf{b}_{\mathbf{month}}$**.** The amount of heterogeneity imposed by **b** on $\beta_1,\ldots,\beta_m$ can be measured with a variance estimate σ^2 , obtained from the square root of the diagonal of the variance-covariance matrix of the estimated random effect parameters **(b;θ),** Actual estimates of **θ** are obtainable for a given random coefficient as conditional modes, but are not examined further given that the basic parameterizations available in the employed software is subject to a unit-sum constraint of zero (i.e., from **b** being $N(0,\sigma^2)$) when concerned with population level inference.

The mixed effect model presented here relaxes inter-animal autocorrelation, but does not account for within animal autocorrelation (Duchesne et al. 2010), which could inflate Type I errors. However, the processing steps discussed in the preceding section and in Appendix 8 related to defining clusters and removing likely non-hunting locations would reduce much of the spatial autocorrelation exhibited with raw GPS locations alone, especially considering the long handling times of the largest prey items (> 3 weeks).

Parameterization of the above model is focused on comparing the used and generated matched locations. However, it can also be extended to assessing the landscape variables attributing to hunting success in a similar manner. Again eq. A9.2 is used, but with $t_n = 1,\ldots T_n$ corresponding to the unique hunting sequence of animal *n.* All locations *J* then correspond to those actually visited by the animal (rather than generated available locations) where *j* corresponding to the kill location ($j = 1$), and *i* corresponding to 2,…,*J* hunting locations immediately preceding a kill location within that hunting sequence. Across cougars, *J* corresponded to a mean 8.87 locations per hunting sequence *t*.

Alternatively, a two-step estimation method was explored (Craiu et al. 2011) which fits separate ordinary conditional logistic regression models (under the cox proportional hazard approach) to each individual animal in an initial step. The second step combines the coefficient estimates from individual animals using restricted maximum likelihood implemented with an EM-algorithm (R package 'TwoStepCLogit') (Craiu et al. 2011;2014). Implementing this method with the SSF analysis produced similar results (not shown) in terms of direction and relative coefficient strengths (when comparing among variables in the same model). However, this software can't account for multiple sources of heterogeneity in the same model (i.e., nested random effects, random effects for both animal identifiers and temporal periods).

Model Parameterization Strategy

Several landscape variables may be important for determining the patch choice decisions revealed in the SSF or hunting success models. Four major classes of covariates were used: topographic, vegetation, anthropogenic, and prey availability. These covariates were drawn from a variety of prior radio telemetry studies devoted to understanding the habitat selection patterns of cougar (Table A9.1). To account for scale dependent habitat effects (Wilmers et al. 2013, Zeller et al. 2014), *a priori* selected covariates were measured at a range of spatial scales (Appendix 4). In other cases, two separate covariates could be used to measure similar phenomena (i.e., the presence of open habitat and forest habitat were inversely correlated). The anthropogenic class is of particular importance for this study to define potential risk to cougars. Finally, mule deer encounter rates (MDEER), as measured by the utilization of mule deer with camera traps (Chapter 2 and Appendix 7), was the single covariate comprising the prey availability class.

The model building strategy entailed choosing the fixed effect structure first (applying Eq. A9.1), followed by the random effects (applying Eq. A9.2). Candidate models were critiqued based on log-likelihood scores, delta AIC, and AIC weights (Burnham and Anderson 2002). Selecting a parsimonious model is a difficult task when a large candidate set (many possible combinations of landscape covariates) is available. Examining all combinations of $\beta_1,\ldots,\beta_m$ fixed effects and $\mathbf{b}_{\mathbf{animal}}$ and $\mathbf{b}_{\mathbf{month}}$ random slope terms was not computationally efficient given the software and hardware utilized. Extra care must also be taken to ensure separating any collinear covariate combinations (i.e., ELEV_3k and ELEV_9k or FOREST and CC_avg90). Collinearity of covariate pairings in the SSF and hunting success data were checked using Pearson's correlation coefficient (r), where collinearity was suspected if it lied outside the critical range of

-0.6 and 0.6. This was conducted at the scale of the overall dataset (all locations combined) and at the strata scale. At the overall-data scale, this was used *a priori* in model building steps to avoid having collinear variables appearing in the same candidate model. At the strata scale, *r* was calculated for each individual stratum (SSF stratum = 45,034 use locations, hunting success stratum = 4,312 hunting sequences) post-hoc for only the covariate pairings used in the final selected models to ease computation burden. These within-stratum *r*'s were summarized by their median and inner-quartile range, which was then examined against the critical range. It was found that a majority of the calculated within-strata *r*'s for any covariate pairing did lie inside the critical range (Figure A9.4).

Withholding any random effect terms in the model, the fixed effect structure for the SSF and hunting success models were chosen (using eq. A9.1). This was conducted by narrowing down the covariates to a parsimonious set for the topographic vegetation, and finally anthropogenic development and prey availability in a series of three steps. First, all combinations of topographical covariates (Appendix 4) were examined, retaining only the best (ΔAICc > 7) spatial scale or measurement method for a given covariate type (i.e. one elevation measure, one aspect measure, etc.). In the second step, vegetation covariate types were added to those retained in the topographic selection step, again running all combinations of covariates and retaining the best (ΔAICc < 7). Finally, covariates in the best fitting model of the vegetation step were retained for inclusion in a candidate set of models focusing on anthropogenic development (Appendix 2, Appendix 4) and prey availability, specific to mule deer (MDEER) (Appendix 7). For the final fixed effect candidate model set (topographic, vegetation, anthropogenic and prey availability combined), all models within 7 ΔAICc were kept as a top set for closer inspection.

This process was conducted for the SSF model (Table A9.2) and for the hunting success model (Table A9.3).

To help reduce spurious inferences within the top set, change of log-likelihood values were inspected of nested models that differed by the addition of a single covariate. An increase in log-likelihood of less than one or two may indicate that the covariate has a spurious effect, or is an uninformative "pretending" variable (Anderson 2008, Arnold 2010). Additional confirmation of a suspected pretender included assessing whether confidence intervals of the coefficient estimates overlapped zero (Anderson 2008). Models with uninformative variables were removed from consideration in order to simplify the model set (Arnold 2010).

Using the final SSF model with the best fitting fixed effect structure, a candidate set of mixed effect models were created (eq A9.2), each based on a single random slope term corresponding to one of the β coefficients of the model and either $\mathbf{b}_{\mathbf{animal\_ID}}$ or $\mathbf{b}_{\mathbf{month}}$ as levels (Table 3.2). It appeared that including any single random slope term would improve model fit. Other combinations of random effects, such as nesting Month inside animal_ID, would be interesting. But given the modeling package employed, adding multiple random slope terms greatly increased computation time. For the final model I limited the random slope terms where the HDM150 and MDEER coefficients were allowed to vary by animal_ID and where HDM150 was allowed to vary by Month (Table 3.1). Examining the coefficient estimates and corresponding confidence intervals of the final SSF mixed effect model, it was apparent that the coefficient corresponding to topographic slope (β_{SLOPE}) no longer contributed to improving model fit. Comparing the final model to a reduced version of the model (without the suspected coefficient) with a likelihood ratio test ($\chi^2 = 0.245$, df = 1, $P > 0.621$) supported this, and was thus removed from the model.

Using the final hunting success model with the most parsimonious fixed effect structure, a candidate set of mixed effect models were created; each based on a single random slope term corresponding to one of the β coefficients of the model and either $\mathbf{b}_{\mathbf{animal\_ID}}$ or $\mathbf{b}_{\mathbf{month}}$ to identify the levels. The four single random slope terms that contributed to a more parsimonious model and yielded σ^2 estimate > 0.01 (Table 3.3) were combined (non-nested) into a single final model (Table 3.1). This final model was used to draw the population level inferences of the influence of landscape covariates on hunting success.

TABLES AND FIGURES

Table A9.1. Landscape covariates of importance found in published cougar radio-telemetry studies categorized into topographic, vegetation, and anthropogenic classes. This is not an all-inclusive survey of studies nor is it an all-inclusive list of the variables found within a study. Various derivations and modifiers exist within each study.

Class	Covariate	Description	Logan & Irwin 1985	Pierce et al. 2004	Dickson et al. 2005, Dickson & Beier 2006	Holmes & Laundre 2006	Burdett et al. 2010	Kertson et al. 2011	Elbroch et al. 2012	Elbroch et al. 2013	Wilmers et al. 2013	Knopff et al. 2014
Topographic	ELEV	Elevation	X	X			X	X		X	X	
	TPI	Topographic position	X		X							X
	ASP	Solar aspect										X
	SLOPE	Slope						X		X	X	
Vegetation	OPEN	Open or grasslands		X	X	X	X		X		X	X
	SHRUB	Shrublands	X	X			X				X	X
	FOREST or CC	Forest or canopy cover	X		X	X	X	X	X		X	X
	FOREDGE	Euclidean distance to (Forest) edge				X		X		X		X
Anthropogenic	HDM	Housing density or other urbanized landcover					X	X			X	X
	RDS_euc	Road density			X							X
	STRUC	Structure proximity						X				X
	PROT.PUB	Protected public					X	X				

Table A9.2. Step Selection Function AIC model selection tables (fixed effect terms only) with the baseline topographic covariates alone, after adding the vegetation covariates, and after adding the anthropogenic and prey availability covariate (MDEER). Only the models, and constituent covariates, within the top seven delta AICc points are displayed.

SSF Models - Baseline Topographic Covariates:

ASP180	ELEV	SLOPE	TPI_100	df	logLik	ΔAICc	AICc weight
-0.1309	-0.1705	0.0615	-	3	-106340	0	0.73
-0.1309	-0.1705	0.0615	-0.0002	4	-106340	2.0	0.27

SSF Models - AddingVegetation Covariates:

ASP180	ELEV	SLOPE	FOREDGE	CC_avg90	FOREDGE * CC_avg90	df	logLik	ΔAICc	AICc weight
-0.157	-0.235	0.027	-0.190	0.192	0.031	6	-105626.1	0	1

SSF Models - Adding Anthropogenic & Prey Covariates

ASP180	ELEV	SLOPE	FOREDGE	CC_avg90	FOREDGE * CC_avg90	HDM150	MDEER	df	logLik	ΔAICc	AICc weight
-0.150	-0.264	0.014	-0.192	0.205	0.035	-0.107	0.069	8	-105462.1	0	0.883
-0.150	-0.266	-	-0.193	0.208	0.035	-0.111	0.068	7	-105465.1	4.04	0.117

Table A9.3. Hunting success AIC model selection tables for the baseline topographic covariates alone, after adding the vegetation covariates, and after adding the anthropogenic and prey availability covariate (MDEER). Only the models, and constituent covariates, within the top seven delta AICc points are displayed.

Kill-Success Model - Baseline Topographic Covariates:

ASP180	ASP45	ELEV	SLOPE	TPI_100	df	logLik	AICc	ΔAICc	AICc weight
-	-0.070	-0.281	-0.030	-0.363	4	-8111.8	16231.6	0.0	0.54
-	-0.073	-0.282	-	-0.363	3	-8113.18	16232.4	0.8	0.37
0.059	-	-0.280	-0.036	-0.364	4	-8114.05	16236.1	4.5	0.06
0.060	-	-0.282	-	-0.364	3	-8115.98	16238.0	6.4	0.02

Kill-Success Models - Adding Vegetation Covariates:

ASP45	ELEV	SLOPE	TPI_100	FOREDGE	CC_pnt	FOREST	SHRUB	SHRUB3	CC_pnt * FOREDGE	FOREDGE *FOREST	FOREDGE * SHRUB	FOREDGE * SHRUB3	df	logLik	ΔAICc	AICc weight
-0.074	-0.263	-0.028	-0.365	-0.012	-	0.009	-	-	-	-0.098	-	-	7	-8099.7	0.0	0.40
-0.077	-0.264	-	-0.365	-0.012	-	0.009	-	-	-	-0.098	-	-	6	-8100.9	0.4	0.34
-0.077	-0.249	-0.031	-0.363	-0.003	-	-	-	0.068	-	-	-	0.083	7	-8101.8	4.1	0.05
-0.068	-0.288	-0.036	-0.361	-0.026	0.060	-	-	-	-0.044	-	-	-	7	-8101.9	4.5	0.04
-0.075	-0.259	-0.029	-0.365	-0.003	-	-	0.030	-	-	-	0.098	-	7	-8102.0	4.5	0.04
-0.078	-0.260	-	-0.366	-0.004	-	-	0.029	-	-	-	0.099	-	6	-8103.2	5.0	0.03
-0.080	-0.251	-	-0.363	-0.004	-	-	-	0.066	-	-	-	0.084	6	-8103.2	5.0	0.03
-0.072	-0.288	-	-0.361	-0.027	0.056	-	-	-	-0.044	-	-	-	6	-8103.9	6.3	0.02

Kill-Success Models - Adding Anthropogenic & Prey Covariates:

ASP45	ELEV	SLOPE	TPI_100	FOREDGE	FOREST	FOREDGE * FOREST	HDM300	HDM350	HDM400	HDM450	HDM500	df	logLik	ΔAICc	AICc weight
-0.070	-0.198	-	-0.377	-0.004	0.003	-0.107	-	-	0.141	-	-	7	-8060.5	0.00	0.22
-0.070	-0.196	-	-0.378	-0.004	0.003	-0.106	-	-	-	-	0.145	7	-8060.8	0.53	0.17
-0.070	-0.199	-	-0.377	-0.004	0.003	-0.106	-	-	-	0.141	-	7	-8060.9	0.53	0.17
-0.070	-0.198	-0.001	-0.377	-0.004	0.003	-0.107	-	-	0.141	-	-	8	-8060.5	0.78	0.15
-0.070	-0.197	-0.001	-0.378	-0.004	0.003	-0.106	-	-	-	-	0.145	8	-8060.8	2.00	0.08
-0.070	-0.199	-0.001	-0.377	-0.004	0.003	-0.106	-	-	-	0.141	-	8	-8060.9	2.52	0.06
-0.070	-0.202	-	-0.377	-0.004	0.002	-0.106	-	0.136	-	-	-	7	-8062.0	2.78	0.05
-0.071	-0.201	-	-0.376	-0.004	0.002	-0.107	0.136	-	-	-	-	7	-8062.2	3.05	0.05
-0.070	-0.202	-0.002	-0.377	-0.004	0.002	-0.106	-	0.136	-	-	-	8	-8062.0	3.46	0.04
-0.071	-0.201	-0.001	-0.376	-0.004	0.002	-0.107	0.136	-	-	-	-	8	-8062.2	5.04	0.02

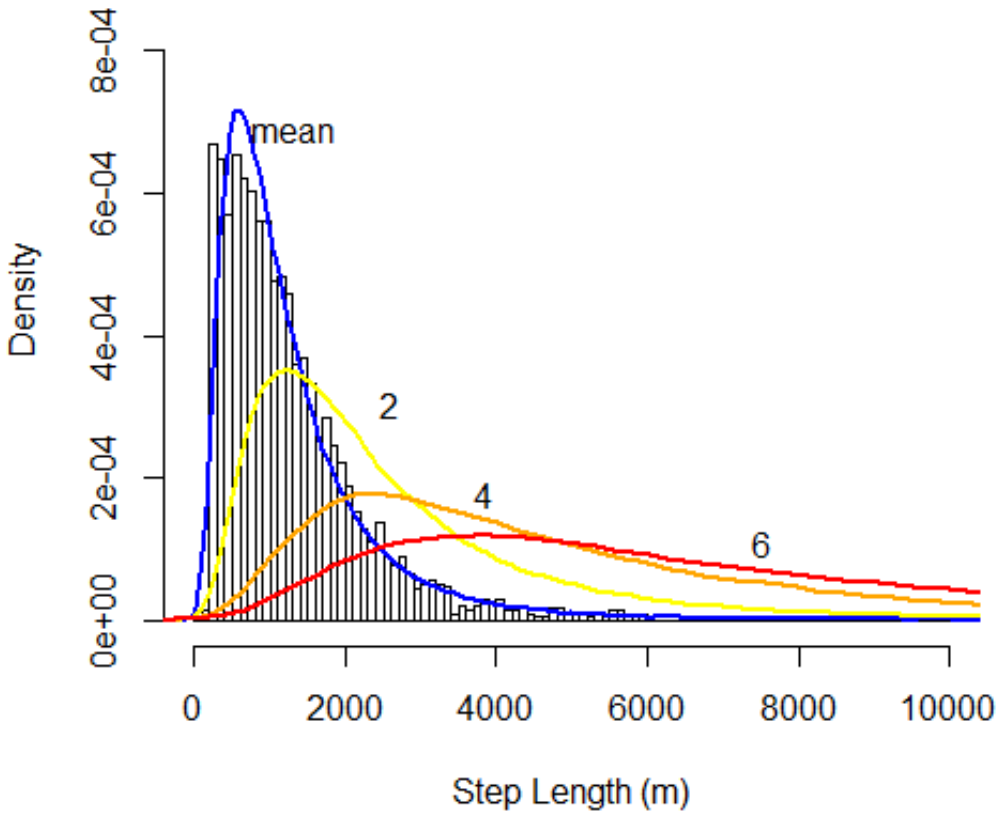

Figure A9.1. Observed distribution of step distances (bars) and the fitted log-normal step distance distribution set to a mean of the observed (blue), 2 km (yellow), 4 km (orange), and 6 km (red) for cougar individual "AF01".

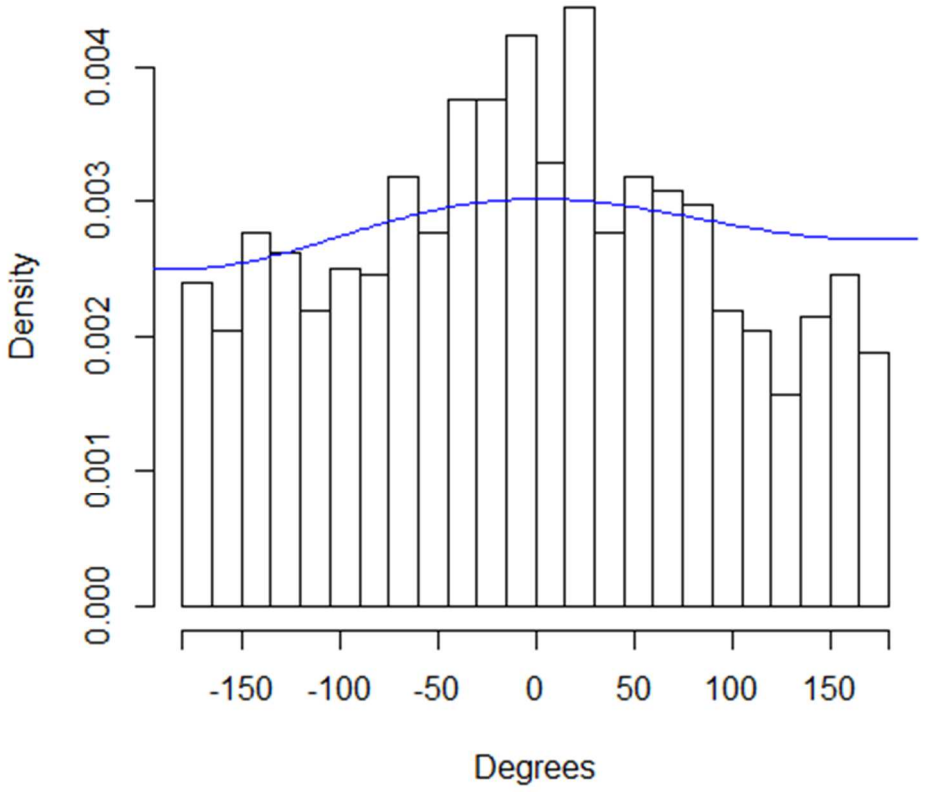

Figure A9.2. Observed distribution of turning angles for cougar individual "AF01".

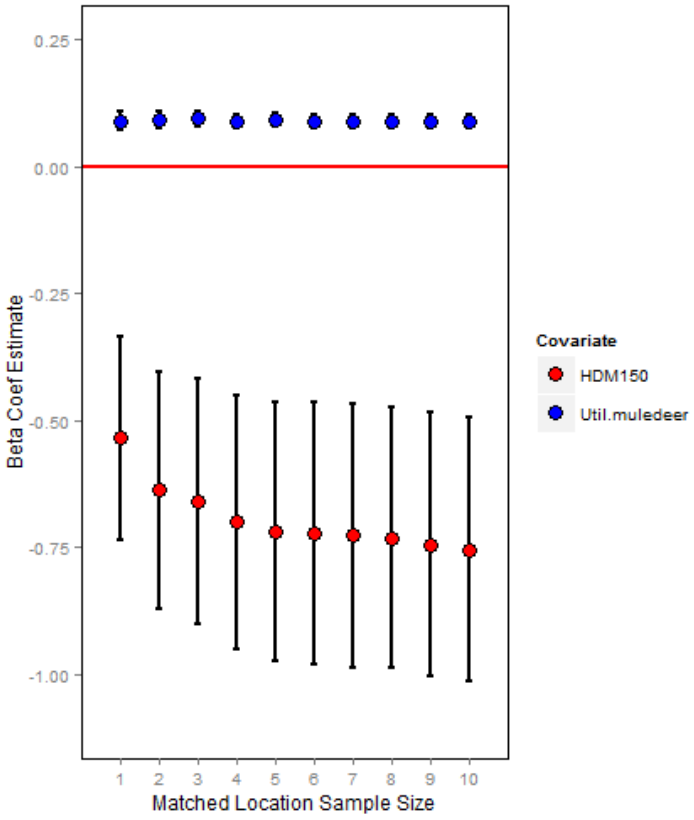

Figure A9.3. Selection coefficient estimates for housing density (βHDM) and prey availability (BMDEER) using the final step-selection function model with an incremental number of matched location (x-axis). Error bars indicate 95% confidence intervals.

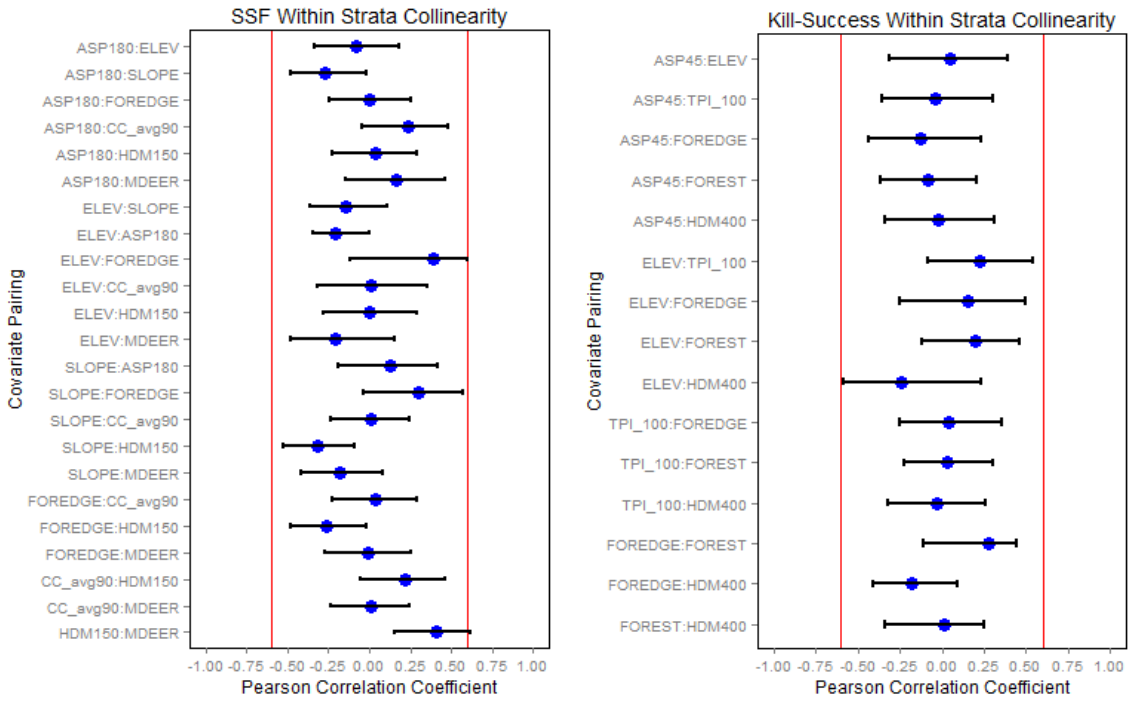

Figure A9.4. Pearson correlation coefficients, *r*, summarized for the "within strata" scale by each covariate pairing (covariates selected in final most parsimonious SSF and hunting success models) by the median and inner-quartile range (error bars). A majority of the observed *r's* for any covariate pairing lie within the critical range of -0.6 and 0.6 (red vertical lines).

LITERATURE CITED

Anderson, D. R. 2008. Model Based Inferences in the Life Sciences: A Primer on Evidence. Springer Science & Business Media, New York, NY, USA.

Arnold, T. W. 2010. Uninformative parameters and model selection using Akaike's Information Criterion. Journal of Wildlife Management 74:1175-1178.

Burdett, C. L., K. R. Crooks, D. M. Theobald, K. R. Wilson, E. E. Boydston, L. M. Lyren, R. N. Fisher, T. W. Vickers, S. A. Morrison, and W. M. Boyce. 2010. Interfacing models of wildlife habitat and human development to predict the future distribution of puma habitat. Ecosphere 1:art4.

Burnham, K. P., and D. R. Anderson. 2002. Model selection and model inference: a practical information-theoretic approach. 2nd edition edition. Springer-Verlag, New York, NY, USA.

Chen, Z., and L. Kuo. 2001. A note on the estimation of the multinomial logit model with random effects. The American Statistician 55:89-95.

Craiu, R. V., T. duchesne, D. Fortin, and S. Baillargeon. 2011. Conditional logistic regression with longitudinal follow-up and individual-level random coefficients: a stable and efficient two-step estimation method. Journal of Computational and Graphical Statistics 20:767-784.

_____. 2014. TwoStepCLogit: conditional logistic regression: A two-step estimation method. R package version 1.2.3.

Dickson, B. G., J. S. Jenness, and p. Beier. 2005. Influence of vegetation, topography, and roads on cougar movement in Southern California. Journal of Wildlife Management 69:264-276.

Duchesne, T., D. Fortin, and N. Courbin. 2010. Mixed conditional logistic regression for habitat selection studies. Journal of Animal Ecology 79:548-555.

Elbroch, L. M., P. E. Lendrum, J. Newby, H. Quigley, and D. Craighead. 2013. Seasonal foraging ecology of non-migratory cougars in a system with migrating prey. PLoS One 8:e83375.

Gail, M. H., J. H. Lubin, and L. V. Rubinstein. 1981. Likelihood calculations for matched case-control studies and survival studies with tied death times. Biometrika 68:703-707.

Gillies, C. S., M. Hebblewhite, S. E. Nielsen, M. A. Krawchuk, C. L. Aldridge, J. L. Frair, D. J. Saher, C. E. Stevens, and C. L. Jerde. 2006. Application of random effects to the study of resource selection by animals. Journal of Animal Ecology 75:887-898.

Hebblewhite, M., E. H. Merrill, and T. L. McDonald. 2005. Spatial decomposition of predation risk using resource selection functions: an example in a wolf-elk predator-prey system. Oikos 111:101-111.

Hilborn, A., N. Pettorelli, C. D. L. Orme, and S. M. Durant. 2012. Stalk and chase: how hunt stages affect hunting success in Serengeti cheetah. Animal Behaviour 84:701-706.

Johnson, D. H. 1980. The comparison of usage and availability measurements for evaluating resource preference. Ecology 61:65-71.

Kertson, B. N., R. D. Spencer, J. M. Marzluff, J. Hepinstall-Cymerman, and C. E. Grue. 2011. Cougar space use and movements in the wildland-urban landscape of western Washington. Ecological Applications 21:2866.

Knopff, A. A., K. H. Knopff, M. S. Boyce, and C. C. St. Clair. 2014. Flexible habitat selection by cougars in response to anthropogenic development. Biological Conservation 178:136-145.

Manly, B. F. J., L. L. McDonald, D. L. Thomas, T. L. McDonald, and W. P. Erickson. 2002. Resource Selection by Animals: Statistical Design and Analysis of Field Studies. Second edition. Kluwer Academic Publishers, Dordrecht, the Netherlands.

McDonald, T. L., B. F. J. Manly, R. M. Nielson, and L. V. Diller. 2006. Discrete-choice modeling in wildlife studies exemplified by northern spotted owl nighttime habitat selection. Journal of Wildlife Management 70:375-383.

McPhee, H. M., N. F. Webb, and E. H. Merrill. 2012. Hierarchical predation: wolf (*Canis lupus*) selection along hunt paths and at kill sites. Canadian Journal of Zoology 90:555-563.

Merkle, J. A., S. G. Cherry, and D. Fortin. 2015. Bison distribution under conflicting foraging strategies: site fidelity versus energy maximization. Ecology *in press*.

R Development Core Team. 2013. Vienna, Austria.

Ruth, T. K., P. C. Buotte, and H. B. Quigley. 2010. Comparing Ground Telemetry and Global Positioning System Methods to Determine Cougar Kill Rates. Journal of Wildlife Management 74:1122-1133.

Therneau, T. 2012. coxme: Mixed Effects Cox Models. R package version 2.2-3. R package version 2.2-3.

Thurfjell, H., S. Ciuti, and M. S. Boyce. 2014. Applications of step-selection functions in ecology and conservation. Movement Ecology 2:4.

Wilmers, C. C., Y. Wang, B. Nickel, P. Houghtaling, Y. Shakeri, M. L. Allen, J. Kermish-Wells, V. Yovovich, and T. Williams. 2013. Scale dependent behavioral responses to human development by a large predator, the puma. PLoS One 8:e60590.

Zeller, K. A., K. McGarigal, P. Beier, S. A. Cushman, T. W. Vickers, and W. M. Boyce. 2014. Sensitivity of landscape resistance estimates based on point selection functions to scale and behavioral state: pumas as a case study. Landscape Ecology 29:541-557.